Ca^{2+} - dependent conformational change in Synaptotagmin I

Leonora Frances Ciufo BSc
(University of Edinburgh)

Thesis for the degree of
Doctor of Philosophy

Department of Biochemistry
University of Edinburgh

September 1997

'Let me not to the marriage of true minds admit impediments.'

W. Shakespeare

Declaration

This study was carried out under the supervision of Dr. David K. Apps and Dr. Jeff Haywood in the Department of Biochemistry, University of Edinburgh between October 1993 and February 1997.

The experimental work carried out in this thesis, unless otherwise stated, is my own and this manuscript has been composed by myself.

Leonora Frances Ciufo

Department Of Biochemistry,
University of Edinburgh,
Hugh Robson Building,
George Square,
Edinburgh. EH8 9XD

August 1997

Abstract

Synaptotagmin (p65), a transmembrane glycoprotein of synaptic and endocrine secretory vesicles, is thought to be one of the proteins responsible for mediating Ca^{2+} control of regulated exocytosis. Extensive work has been carried out in neuronal tissue but the protein's role in endocrine cells is not clear. This thesis reports work on synaptotagmin I, the isoform that occurs in adrenal chromaffin granules.

Background work on synaptotagmin has been hindered to a certain extent by the difficulty in obtaining the protein in sufficient quantities and purity. This problem can be overcome by adopting molecular cloning and a bacterial expression system. DNA encoding the cytoplasmic domain of synaptotagmin I was amplified from a cDNA library and ligated to part of the *S.aureus* protein A gene in an *E.coli* expression vector so that the fused gene could be expressed as a chimaeric protein in bacterial cells. The protein A segment assisted purification and detection of the protein and has highly antigenic properties, enabling easy preparation of polyclonal antibodies. A thrombin cleavage site was incorporated into the design of the chimaeric protein so that digestion with thrombin released the isolated cytoplasmic domain of synaptotagmin.

The construct was characterised in terms of control of gene expression, solubility in the bacterial cytoplasm and optimal conditions for thrombin digestion. A simple purification strategy for the cytoplasmic domain of synaptotagmin was developed and the purified protein was then used for *in vitro* studies of both Ca^{2+}-dependent structural changes and interactions with other biological molecules.

The existence of a Ca^{2+}-dependent conformational change in synaptotagmin was initially established by analysing the change in sensitivity of the protein to proteolytic digestion with trypsin in the presence and absence of Ca^{2+}. An attempt was also made to investigate the Ca^{2+}-binding activity of the protein with the lanthanide terbium (Tb^{3+}), as a fluorescent probe for the Ca^{2+}-binding sites but this approach proved to be of limited use, due to protein aggregation. Interaction of

synaptotagmin with phospholipids was also found to be Ca^{2+}-dependent and the protein was found to show selectivity for certain phospholipids. The interaction of the protein with calmodulin was tested using *in vitro* binding to immobilised calmodulin and also to calmodulin modified with a fluorescent dansyl group to act as a reporter. Both types of measurement indicated a Ca^{2+}-dependent interaction between the proteins most probably due to affinity changes in calmodulin upon binding to Ca^{2+}.

Structural changes in synaptotagmin as a possible mechanism of action were investigated further using the biophysical techniques of circular dichroism (CD) and light scattering. Changes in quaternary structure from multimer to monomer were detected upon addition of Ca^{2+} alone whereas secondary structural changes were not detectable by CD unless phospholipid vesicles were also mixed with the protein. Gel exclusion chromatography and native gel electrophoresis were used to support the data and indicated changes in quaternary structure. These techniques also suggested that the native protein, isolated from chromaffin granules, exists as a multimeric form.

This study has demonstrated that synaptotagmin shows Ca^{2+}-dependent interactions with calmodulin and phospholipids and also that it undergoes measurable structural changes in the presence and absence of Ca^{2+}. This suggests that its action in exocytosis may be driven by a Ca^{2+}-triggered conformational change.

Acknowledgements

I would like to thank my two supervisors David Apps and Jeff Haywood for their contrasting styles of supervision and particularly David Apps for his extremely thorough reading of this thesis. Thanks also to all the members of the lab over the past four years: Shahida and Jan for emergency discussions when experiments didn't work out, the occasional loan of antibodies and reagents and for the general benefit of their collective experience, scientific and otherwise.

Thankyou to my friends both past and present - you have left a lasting impression and altered me by gradual degrees until I am now quite a reasonable person!

Thankyou Rose for always refusing to believe that I could be anything but an absolute success, you have provided balance against those who I constantly try, and fail, to please.

Finally, I think it would be curmudgeonly not to also thank my enemies who have taught me valuable lessons and provided a certain amount of cameraderie with my friends.

Abbreviations

DNA (cDNA)	deoxyribonucleic acid (complementary)
ATP	adenosine triphosphate
TTP	thymine triphosphate
CTP	cytosine triphosphate
GTP	guanidine triphosphate
dNTP	any of the above bases (deoxy form)
ddNTP	any of the above bases (dideoxy form)
NSF	N-ethyl maleimide sensitive factor
αSNAP	soluble NSF attachment protein
VAMP	vesicle associated membrane protein
SNAP-25	synaptosome associated protein - 25
SNARE	SNAP receptor
5-HT	5-hydroxytryptamine
NMR	nuclear magnetic resonance
ACTH	adrenocorticotrophic hormone
EC_{50}	The Ca^{2+} concentration at which there is 50% of the maximum bound
PCR	polymerase chain reaction
IPTG	isopropyl β-D-thiogalactopyrnoside
EDTA	ethylenediaminetetraacetic acid
OD_{600}	optical density at 600 nm
SDS	sodium dodecyl sulphate
TCA	trichloroacetic acid
IgG-HRP	immunoglobulin G conjugated to horse radish peroxidase
PMSF	phenyl methyl sulphonyl fluoride

PS/PC/PE/PI	phosphatidyl serine / choline / ethanolamine / inositol
SDS-PAGE	sodium dodecyl sulphate - polyacrylamide gel electrophoresis
NTA	nitrilotriacetic acid
PVDF	polyvinylidene difluoride
SytC(*sytc)*	the cytoplasmic domain ofsynaptotagmin upper case = protein, lower case italics = DNA
PrA(*pra)*	proteinA upper case = protein, lower case italics = DNA

Aminoacid abbreviations

Alanine	Ala	A	Cysteine	Cys	C
Glycine	Gly	G	Lysine	Lys	K
Leucine	Leu	L	Arginine	Arg	R
Valine	Val	V	Histidine	His	H
Isoleucine	Ileu	I	Asparagine	Asn	N
Proline	Pro	P	Glutamine	Gln	Q
Phenylalanine	Phe	F	Serine	Ser	S
Methionine	Met	M	Threonine	Thr	T
Tryptophan	Trp	W	Tyrosine	Tyr	Y
Aspartic acid	Asp	D	Glutamic acid	Glu	E

Contents

Chapter 2
Materials and Methods

Materials

Methods

Chapter 3
Production and purification of a Synaptotagmin-ProteinA fusion protein and a Synaptotagmin-His10 fusion protein

Appendix to chapter 3
Production of affinity purified polyclonal antibodies

Chapter 4
Biochemical analysis of Ca^{2+}-dependent conformational change, interaction with calmodulin and phospholipids of recombinant SytC

List of figures

List of tables

Chapter 1
Introduction

1.1 Introduction

Cells in multicellular organisms communicate by releasing chemical signals from secretory vesicles into the extracellular space which are subsequently detected and interpreted by other nearby cells. Synaptotagmin, the subject of this thesis, is a transmembrane protein of secretory vesicles and has been implicated in the process of regulated exocytosis which is a specialised form of secretion from cells controlled by intracellular levels of Ca^{2+}. In order to explain the possible role of synaptotagmin, the features of regulated exocytosis will be described briefly followed by a more detailed analysis of the theories and experimental work involving synaptotagmin which form the basis and context of the work carried out in this thesis.

1.2 Exocytosis

Eukaryotic cells deliver proteins to the cell membrane or the extracellular space by a sequence of vesicle-mediated transport steps beginning at the endoplasmic reticulum and passing through the Golgi complex until, from the *trans* Golgi network, vesicles finally arrive at the plasma membrane. Each step requires the formation of vesicles, their targeting to an acceptor membrane and subsequent fusion with that membrane. Fusion with the acceptor membrane results in incorporation of vesicle lipids and proteins into the membrane and in the case of the plasma membrane, release of the vesicle contents into the extracellular space. The process of fusion with the plasma membrane is known as exocytosis and may occur in a constitutive or regulated form. Constitutive exocytosis is the immediate fusion of vesicles from the *trans* Golgi network with the plasma membrane and is exhibited by many eukaryotic cell types. Regulated exocytosis involves the accumulation in the cytoplasm of vesicles which will only fuse with the plasma membrane when an appropriate signal is given (usually a rise in

intracellular Ca^{2+}). Although all cells carry out constitutive exocytosis, cells such as endocrine and neuronal cells will, in addition, carry out regulated exocytosis in large amounts.

The concept of a ubiquitous cellular membrane fusion mechanism for small vesicles involved in intracellular membrane traffic and in secretion has become more plausible in recent years. It seems likely that the same basic machinery is used in all cell types, with slight variations dependent on specific cell functions (O'Connor *et al.* 1994). This idea is supported by the discovery that NSF and α-SNAP, originally identified in studies of intracisternal vesicular traffic in the Golgi, can form a 20S complex containing the synaptic vesicle proteins VAMP (synaptobrevin) and synaptotagmin with syntaxin and SNAP-25 located in the synaptic plasma membrane (Sollner *et al.* 1993a). This has led to the formation of the so-called SNAP/SNARE hypothesis which describes binding between a vesicle SNARE (SNAP receptor) and the presynaptic membrane SNARE, mediated by the soluble factors NSF and SNAP (Sollner *et al.* 1993b). The authors propose that the interaction of synaptic vesicle protein synaptobrevin (v-SNARE)with plasma membrane proteins syntaxin and SNAP-25 (t-SNAREs) forms a docking complex which targets vesicles to release sites at the plasma membrane and that SNAPs and NSF subsequently bind to this complex and drive membrane fusion as a result of the ATPase activity of NSF (see figure 1.1)

The SNARE hypothesis can be applied to any vesicular transport step and has become a central theme of much work in this area. The importance for exocytosis of the proteins in this complex is supported by the fact that each of the SNARE proteins is a target for lethal clostridial toxins; tetanus

toxins which cause paralysis by blocking transmission in inhibitory neurons of the spinal cord and botulinum toxins which inhibit synaptic transmission at the neuromuscular junction (Goda 1997). However, some findings cast doubt on the model. The speed of exocytosis, especially in neurons is too fast to involve the slow ATPase activity of NSF (Morgan and Burgoyne 1995). In addition, exocytosis can be triggered by Ca^{2+} in chromaffin cells and mast cells in the absence of MgATP (Neher and Zucker 1993, Holz *et al.* 1989, Lindau and Gomperts 1991). Furthermore, evidence now favours a role for synaptobrevin in vesicle fusion rather than docking (Hunt *et al.* 1994).

This model marks the union of knowledge acquired from two sources: reconstitution of intracellular membrane traffic and synaptic membrane structural studies. Although some of the details may be inaccurate, the prospects are good for the general applicability of this mechanism to all cell types and cell locations particularly since homologues of syntaxin and synaptobrevin are found throughout the yeast secretory pathway and in vertebrate and invertebrate tissues and mutations of these homologues cause disruption of vesicle fusion (Bennet *et al.* 1993). It is particularly interesting to note that the similarities between the homologues becomes more striking if they are functionally located toward the plasma membrane suggesting that neuronal secretion is an evolutionary modification of an existing exocytotic system.

Although it now appears that the same proteins are involved in the targeting, docking and fusion of vesicles in both constitutive and regulated exocytosis, there are a number of differences in the process. Apart from the obvious sensitivity to Ca^{2+} found in cells undergoing regulated

exocytosis compared to constitutive, there are also differences in the kinetics of regulated secretion among different cell types, which may point to the involvement of some unique proteins or perhaps the differential regulation of the same exocytotic machinery according to the requirements of each particular tissue.

1.2.1 Dense granules and synaptic vesicles

Two different types of secretory vesicle are involved in Ca^{2+}-triggered exocytosis (Morgan and Burgoyne 1997). Large dense-core vesicles or granules (LDCV) are the main type of vesicle in endocrine cells and are thought to be produced by the budding and fusion of immature granules from the *trans* Golgi network (Bauerfeind and Huttner 1993). A proportion of these granules undergo exocytosis when the cytosolic Ca^{2+} concentration increases and some evidence suggests that the granule membrane is recycled by endocytosis and transported back to the *trans* Golgi network (Patzak and Winkler 1986). Small synaptic-like vesicles (SSLV) are also present in endocrine cells but in much smaller quantities and resemble synaptic secretory vesicles.

Synaptic vesicles are the main type of vesicle present in neurons and are thought to be created from constitutive secretory vesicles which are recycled from the plasma membrane to a specialised endosome (Calakos and Scheller 1996) which sorts synaptic vesicle membrane proteins and contents into the vesicles. These vesicles also undergo exocytosis upon a rise in cytosolic Ca^{2+} and are thought to be recycled via the same endosome. Some evidence suggests these vesicles are also able to fuse briefly with the plasma membrane to allow discharge of their contents before reforming by pinching off and reloading with small molecule

neurotransmitters (but not peptide neurotransmitters) without returning to the endosome (Fesce *et al.* 1994).

1.2.2 Stages of exocytosis

Secretion is intrinsically a multi-stage process because it involves the passage of substances formed deep within the cell through various membrane compartments finally to the cell surface. Evidence is now accumulating that the final process of membrane fusion in regulated exocytosis is in itself a complex, multi-step process. Capacitance increases in neuronal cells are used as a highly sensitive and rapid measurement of membrane expansion due to exocytosis and have been very useful for the study of the process. Using this type of measurement, it has been shown that cells upon stimulation exhibit a rapid exocytotic burst which presumably corresponds to the exocytosis of vesicles already competent for fusion (Parsons *et al.* 1995) followed by a slower component which may correspond to fusion of vesicles which have to be first prepared in some way before undergoing exocytosis. If stimulation is continued, the exocytotic response has a further late component due to recruitment of vesicles to the plasma membrane during the stimulation (Gillis *et al.* 1996). Figure 1.3 shows a schematic representation of the typical changes in capacitance measured from secreting chromaffin cells and the time scale of events including an illustration of capacitance change in the first second after stimulation. Chromaffin cells were loaded with a caged calcium compound and patch-clamp capacitance measurements were made after inducing secretion by release of the calcium (Neher and Zucker 1993). The authors reported exceptionally fast exocytosis responses to $[Ca^{2+}]$ in the range of 50-200μM when the Ca^{2+} spike lasted for more than a few ms (arrow no. 1). It is possible that the fast response represents release from

a pool of secretory vesicles which are immediately ready for release and the necessity for a long Ca^{2+} signal may be due to the fact that vesicles are relatively distant from the membrane and must move toward it before fusing. The capacitance continues to increase at a slower rate after the fast response in the absence of a further Ca^{2+} stimulus and continues to do so after another Ca^{2+} stimulus (arrow no. 2). The slower exocytotic response visualised with this technique may represent release from vesicles which have to be first prepared for fusion with the membrane and hence the secretory response is slower. The further action of Ca^{2+} in the later phase of the release could indicate Ca^{2+}-dependent steps, apart from fusion itself, required to mobilise other pools of vesicles.

1.2.3 The releasable pool of vesicles

Secretory granules in endocrine cells such as chromaffin cells are not docked at the plasma membrane but are held distant by a cytoskeletal actin network (Trifaro and Vitale 1993). This work illustrated that disassembly of the cortical cytoskeleton allowed the movement of granules to the membrane at discrete sites where their contents was released and that this process involved the Ca^{2+}-dependent actin-severing protein scinderin. In addition to this, a protein kinase C substrate is implicated because phorbol esters cause disassembly of the cytoskeleton. Cytoskeletal disassembly alone however is not sufficient for exocytosis to occur so it is apparent that fusion of vesicles is yet another Ca^{2+}-dependent step.

In neuronal cells, synaptic vesicles are not directly bound to actin. A small proportion are docked at release sites on the plasma membrane while others are cross-linked to actin through the vesicle protein synapsin I

(Trifaro and Vitale 1993, Valtorta *et al.* 1992). The docked vesicles undergo exocytosis within 200 μs in response to high Ca^{2+} concentrations at the membrane. Diffusion of Ca^{2+} creates lower Ca^{2+} concentrations a short distance away from the membrane. This activates Ca^{2+} /calmodulin dependent protein kinase II which phosphorylates synapsin I allowing release of more vesicles to the membrane.

1.2.4 Kinetics of exocytosis

Fusion of synaptic vesicles can occur within 200 μs of a stimulus which is ten times faster than granule exocytosis in neuroendocrine cells where the fastest fusion events measured are between 2-50 ms after the release of caged Ca^{2+} (Burgoyne and Morgan 1995). The faster kinetics in neurons is probably due to the fact that most vesicles are already physically docked at the membrane whereas in chromaffin cells all but a few granules are held in the actin network. Even the granules which are free and closer to the membrane have rarely been seen actually docked except by electron microscopy of frozen cells (Parsons et al. 1995). It is also a possibility that the higher degree of surface tension associated with the high curvature of synaptic vesicles simply makes membrane fusion more energetically favourable.

1.2.5 Ca^{2+} requirements of exocytosis

There is a large difference in the Ca^{2+} concentrations required for exocytosis in neurons and chromaffin cells. Flash photolysis studies of caged Ca^{2+} showed that exocytosis was half-maximal in adrenal chromaffin cells at 10-20 μM Ca^{2+} but at 190 μM in retinal neurons (Heinemann *et al.* 1994, Heidelberger *et al.* 1994). Intracellular dialysis of Ca^{2+} via a patch pipette indicated that the threshold for activation of exocytosis was 0.3 μM

in adrenal chromaffin cells and 20-50 μM in neurons (Augustine and Neher 1992, Burgoyne 1991). The great difference in Ca^{2+} sensitivities of the two cell types implies that a different Ca^{2+}-binding proteins may be involved in granule and synaptic vesicle exocytosis.

As well as regulating exocytosis, Ca^{2+} regulates secretory granule recruitment (von Ruden and Neher 1993) and priming for exocytosis. Priming is the phenomenon whereby exposure to MgATP increases the extent of subsequent exocytosis (Bittner and Holz 1992) and is discussed below. The requirement for Ca^{2+} for priming in chromaffin cells is consistent with the existence of a high-affinity Ca^{2+} sensor implied by the Ca^{2+} affinities measured in other experiments.

1.2.6 Vesicle recruitment

ATP seems to be required for vesicle recruitment before docking as well as for some ATP- dependent priming which occurs after docking. Studies in permeabilised adrenal chromaffin cells show that only 4% of vesicles undergo Ca^{2+}-activated exocytosis in the absence of ATP whereas a much larger fraction undergo exocytosis in the presence of ATP (Holz *et al.* 1989). Capacitance measurements showed that 4% of vesicles, corresponding to those morphologically docked, could undergo exocytosis when cells were depleted of ATP (Parsons *et al.* 1995) suggesting that ATP-dependent steps had already occurred just before or immediately after docking. Since it has been shown that vesicles in chromaffin cells must be mobilised by release from an actin cortex (Roth and Burgoyne 1995, Vitale *et al.* 1995) it is possible that the ATP requirement for recruitment involves an ATP-dependent motor such as myosin II or protein kinases such as Ca^{2+}-regulated myosin light chain kinase. After vesicles are recruited, they

must dock with the plasma membrane. The SNAP/SNARE hypothesis suggests that docking of vesicles is mediated by interactions between vesicle and membrane proteins but this has been questioned because clostridial neurotoxin treatment which destroys these proteins results in more morphologically docked vesicles than before (Broadie *et al.* 1995). It therefore seems that, although these proteins are probably important for targeting vesicles and certainly for their eventual fusion with the membrane, the interactions which specifically drive or maintain docking have yet to be dissected.

1.2.7 Priming

ATP-dependent reactions also occur after vesicle docking but before fusion (Banerjee *et al.* 1996). ATP was found to be important as a substrate for two lipid kinases that act sequentially in phospholipid phosphorylation (Hay *et al.* 1995, Wiedemann *et al.* 1996). Production of phosphatidylinositol 4,5-bisphosphate by these kinases seems to be important because destruction of this compound inhibits Ca^{2+}-triggered fusion although its mechanism of involvement is not yet known.
ATP also serves as a substrate for the ATPase NSF the importance of which in regulated fusion is undisputed since the original characterisation of the SNAP/SNARE complex. Originally, it was shown that NSF catalysed the ATP-dependent dissociation of the SNARE complex and this was thought to occur after docking to drive membrane fusion. However, NSF has recently been shown to have a role in constitutive fusion before docking (Mayer *et al.* 1996) and more evidence is now accumulating from studies of cells undergoing regulated exocytosis that NSF is involved in a priming reaction prior to, or at the same time as, docking (Burgoyne *et al.* 1996). This study shows that α-SNAP, identified as one of the soluble factors

important in the assembly of the vesicle docking complex along with NSF, stimulates ATP-dependent but not ATP-independent secretion. A previous study had already illustrated that α-SNAP acts at an early Mg-ATP-requiring stage of exocytosis rather than the late Ca^{2+}-triggered steps immediately prior to membrane fusion (Chamberlain *et al* 1995). In addition, the reported presence of NSF on free synaptic vesicles in complex with SNARE proteins suggests that it has a role before docking (Walch-Solmena *et al* 1995).

1.2.8 Fusion, the final Ca^{2+}-triggered step of regulated exocytosis

Many proteins have been identified as being involved in constitutive and regulated membrane traffic. There are so many potential actors on the stage that the exocytosis plot is becoming amazingly complicated. Table 1.1 summarises the proteins identified, grouped in broad categories of possible function although many of the proteins listed are not discussed further.

The final stage of exocytosis, fusion of the secretory vesicle with the plasma membrane, is likely to be the point at which regulated exocytosis diverges from constitutive secretion and where regulated secretory cells differ from each other since this is the point at which sensitivity to Ca^{2+} becomes important. The ubiquitous SNARE proteins have been found to be essential for this stage since neurotoxin action on these proteins abolishes Ca^{2+}-activated fusion. In addition the ATP-dependent action of NSF in assembling the complex of proteins is also found to be necessary.

Table 1.1 Proteins involved in regulated exocytosis

Proteins implicated in recruitment of vesicles or mobilisation from cytoskeletal anchorage.

kinesin, 14-3-3, myosin II, myosin light chain kinase, scinderin, synapsin, calmodulin dependent protein kinase II, rab3, rabphilin, actin

Proteins with uncharacterised roles

synaptophysin, synaptoporin, SV2, synaptogyrin, SCAMP, $pp60^{src}$, cysteine string proteins, calmodulin

Proteins with unknown sites of action

Rab3, rabphilin, RabGDI, MSS4, Doc-2, complexin, Hrs-2, unc-41p, unc-18p (munc18, Sec1, rop), unc-13p, aex-3p,rSec6, rSec8, annexin, GAP-43, neurexin, VAP-33

Proteins required for ATP-dependent priming

phosphatidyl inositol transfer protein (PEP 3), phosphatidyl inositol 4-kinase, phosphatidyl inositol 4 phosphate 5-kinase (PEP1), NSF, $\alpha/\beta/\gamma$ -SNAP

Proteins required for late stages proximal to fusion

synaptobrevin, syntaxin, SNAP-25, synaptotagmin, CAP

adapted from Martin 1997

Figure 1.1 Model of the fusion complex assembly

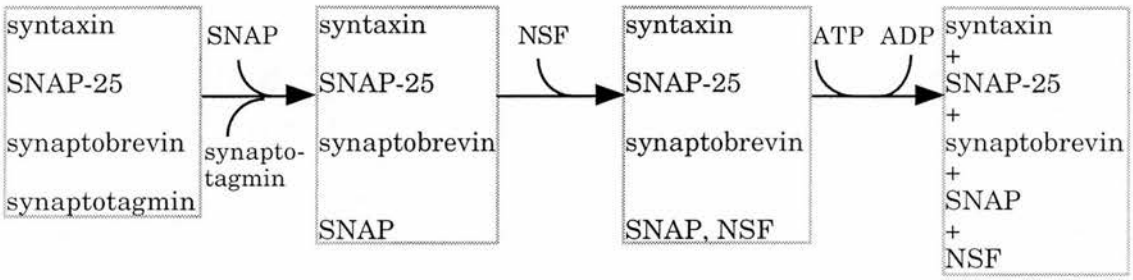

Sollner *et al* 1993b

Figure 1.2 Schematic representation of the structural features of synaptotagmin

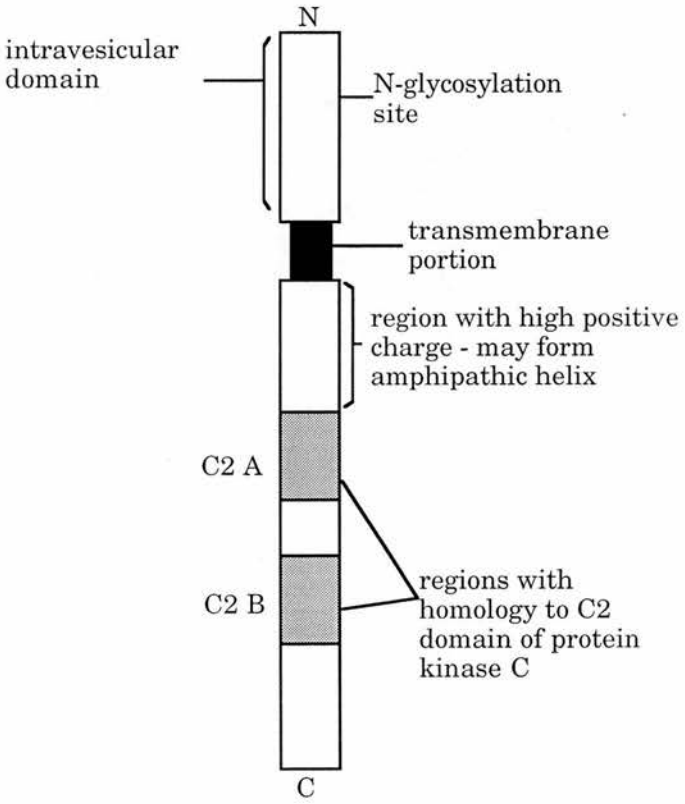

Figure 1.3 The stages of exocytosis measured by capacitance change in single cells

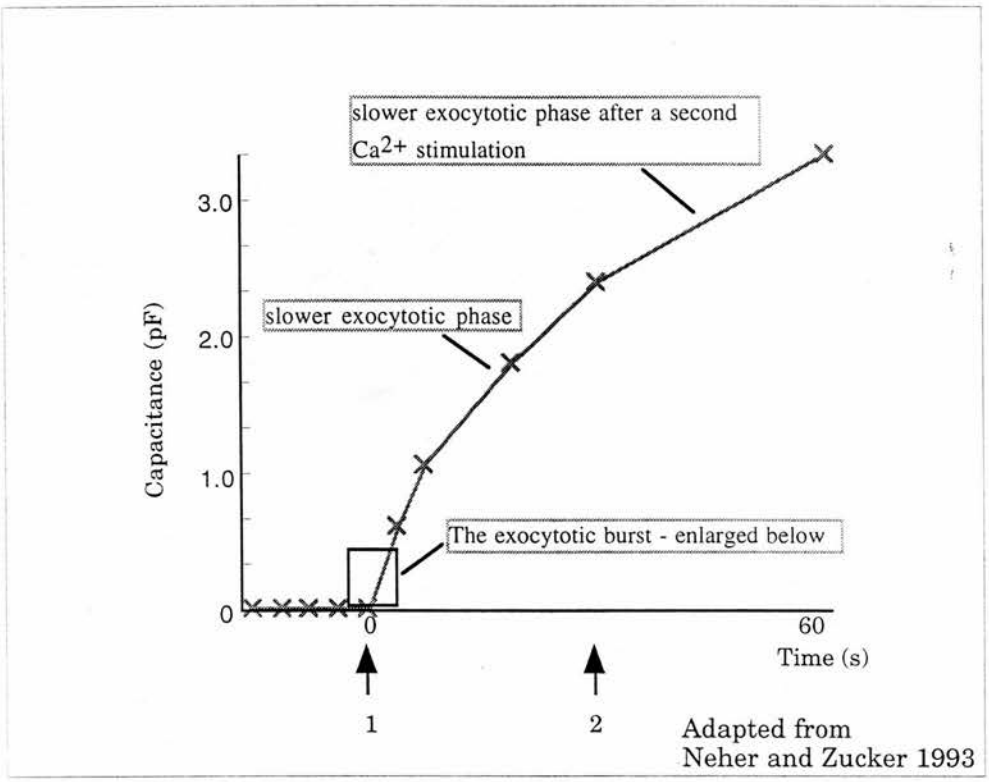

The exocytotic burst within 1 s of a Ca^{2+} stimulus

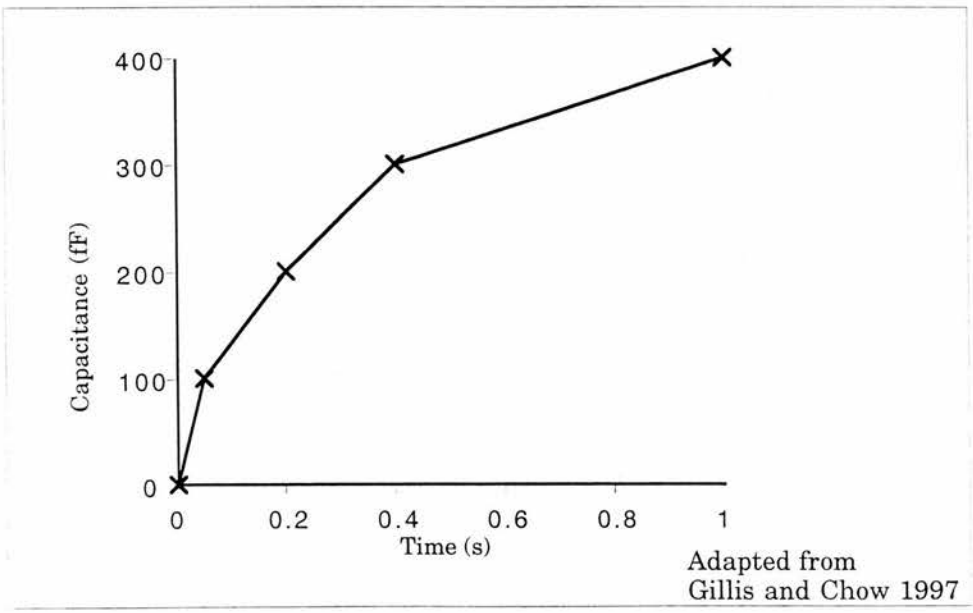

1.3 Specialisation for regulated exocytosis

There are some proteins which seem to be present only in cells which carry out regulated exocytosis and as such are probably involved in the Ca^{2+}-dependent stages of the process. Synaptotagmin is a candidate for the mediator in the control of Ca^{2+}-regulated exocytosis. Theories about its role suggest it is either directly responsible for Ca^{2+}-dependent fusion or that it behaves as a Ca^{2+}-sensitive 'clamp' which prevents the normal course of constitutive fusion until the signal is given for fusion to occur. The protein has been studied extensively using both *in vitro* and *in vivo* techniques.

1.4 *In vitro* studies of synaptotagmin function

1.4.1 Structure and structural modifications

Synaptotagmin was first identified as a component of synaptic vesicles (Matthew *et al.* 1981) and antibodies against it were found to precipitate chromaffin granules (Lowe *et al.* 1988). Later it was shown that synaptotagmin was the same as the 65 kDa calmodulin-binding protein identified in granule membranes (Fournier and Trifaro 1988a and b, Fournier *et al.* 1989). The amino acid sequence was deduced by sequencing a cDNA clone (Perin *et al.* 1990) and suggested a single transmembrane span with a small intravesicular N-terminal domain including a putative N-glycosylation site. The larger cytoplasmic domain contained two repeated sequences similar to the C2 regulatory domain of protein kinase C and are therefore referred to as the C2 domains.

The predicted transmembrane topography of the protein in chromaffin granules was further supported by work using monoclonal antibodies, protease and endoglycosidase treatments (Tugal *et al.* 1991) and by the use

of proteolytic cleavage, sucrose density gradients and antibodies to various epitopes of the protein (Perin *et al.* 1991a). The latter work also suggested that the protein forms a higher molecular weight complex with synaptotagmin dimers as a basic unit. The authors suggest that a region of the protein between the transmembrane portion and the first C2 domain may form an amphipathic α helix and cause stable dimerization. The structural features of the protein are summarised in figure 1.2. Some other work has also suggested that the protein may form a homotetramer (Brose *et al.* 1992).

Synaptotagmin was shown to be structurally and functionally conserved from *Drosophila* to humans (Perin, *et al.* 1991b). Rat and human synaptotagmins show 97% identity whereas rat and *Drosophila* are only 57% identical but conservation in the C2 domains is particularly significant at 78% between all three species. The two C2 repeats are only slightly more homologous to each other than to protein kinase C but the differences in the two C2 domains are conserved suggesting they are important differences and that the two domains may not be functionally equivalent.

This particular study also showed that recombinant cytoplasmic domains of human and *Drosophila* synaptotagmins bound specifically to phosphatidylserine as does the rat protein. These proteins also caused agglutination of erythrocytes which was inhibited by negatively-charged phospholipids. It has been proposed that the C2 domains confer Ca^{2+}- and phospholipid-binding properties to synaptotagmin and evidence is accumulating to suggest this is the case. Ca^{2+} and phospholipid binding appear to be interdependent and together cause conformational change when measured using partial proteolysis (Davletov and Südhof 1994)

whereas crystallographic measurements of the first C2 domain showed only a small structural change when Ca^{2+} alone was introduced into the protein crystal (Sutton *et al.* 1995).

In brain homogenates, synaptotagmin was shown to be a major substrate for casein kinase II, which phosphorylates a single conserved threonine (Davletov *et al.* 1993a). The phosphorylation was dependent on a lysine-rich sequence in the protein which, if removed, made the phosphorylation dependent on exogenous polylysine. Furthermore, several presynaptic proteins including synaptotagmin have been found to be substrates for Ca^{2+}/calmodulin-dependent protein kinase II (CaMKII) *in vitro* (Popoli 1993). Although the significance of this phosphorylation has not been investigated, phosphorylation by an endogenous kinase suggests that it may also occur *in vivo* and implies a possible modulatory role for synaptotagmin in synaptic function. It was recently shown that if 5-HT reuptake is blocked, for example by the use of some antidepressant drugs, CaMKII activity and auto-phosphorylation is increased, resulting in a 2-3 fold increase specifically in the phosphorylation of synaptotagmin (Popoli *et al.* 1997). This establishes a link between synaptotagmin phosphorylation and levels of neurotransmitter release and is of possible functional relevance.

Synaptotagmin has been shown to be palmitoylated at a cysteine-rich region adjacent to the transmembrane region (Chapman *et al.* 1996a). Acylation of soluble proteins could have the function of anchoring the protein to the membrane but it is not clear why a transmembrane protein should need this modification. Palmitoylation has been shown to regulate the rate of internalisation of other proteins such as the transferrin receptor

(Alvarez *et al.* 1996) so it is possible that the phosphorylation of synaptotagmin may similarly regulate endocytotic vesicle membrane traffic. This idea has some support from the findings that synaptotagmin binds AP-2 (Zhang *et al.* 1994) and that synaptotagmin-deficient *C.elegans* seems to have endocytosis defects (Jorgensen *et al.* 1995).

1.4.2 Distribution and regulation of expression

Synaptotagmin has been found in neural and endocrine tissue of many vertebrate and invertebrate species but no homologue is present in yeast. Study of neurogenesis in *Drosophila* embryos has shown that it is very quickly localised to the synapse during axonogenesis and accumulates at synaptic contact sites, suggesting a general role in synapse function (Littleton *et al.* 1993a). In the rat nervous system synaptotagmin I (one of the more currently-studied isoforms of the protein) was found principally in adrenergic and sensory neurons and was absent from motoneurons (Li *et al.* 1994). It has also been detected at the neuromuscular junctions of crayfish (Cooper *et al.* 1995). The protein was initially detected in bovine chromaffin granules (Lowe *et al.* 1988) but has also been found in bovine posterior pituitary (Egger *et al.* 1994) in the large dense core granules although its presence in anterior pituitary is more variable, being positively identified in only a limited number of adenohypophyseal endocrine cells (Redecker 1995). All the variations in the distribution of the protein may reflect differential requirements for synaptotagmin in these cell types but in light of the number of novel isoforms of the protein now uncovered, it is also possible that the cells apparently lacking synaptotagmin I contain other isoforms which were not detected by the antibodies used.

1.4.3 Isoforms of synaptotagmin

A second isoform (synaptotagmin II) was discovered in 1991 (Geppert *et al.* 1991). This protein is highly homologous to the first isoform especially in the C2 repeats where they show 88% sequence identity. The two isoforms show complementary patterns of expression in brain, with synaptotagmin I present in rostral regions and synaptotagmin II in caudal regions. Synaptotagmin II has been shown to be incorporated into the axon plasma membrane after exocytosis (Angaut-Petit *et al.* 1995) indicating its involvement in the membrane fusion process. Since the discovery of the second isoform, it has been found that mammalian brain expresses at least eight isoforms of the protein (Li *et al.* 1995), all of which show similar AP-2 binding properties (suggesting a role in endocytosis) but show different Ca^{2+}-dependent interactions within each C2 domain, with phospholipids and syntaxins, also consistent with a general role in exocytosis. Three of the isoforms (VI, VII and VIII) are widely expressed in non-neural tissues whereas isoforms I, II and III are exclusively neural.

The synaptotagmins divide into three classes (Li *et al.* 1995) depending on their Ca^{2+}-dependent interactions. Isoforms IV, VI and VIII are not affected by Ca^{2+}, III and VII bind phospholipids and syntaxin at low Ca^{2+} concentrations and synaptotagmins I, II and V bind phospholipids at low $[Ca^{2+}]$ and syntaxin at high $[Ca^{2+}]$ (see table 2). The Ca^{2+}-dependent syntaxin-binding of synaptotagmins II and V is the same as the Ca^{2+} dependence of synaptic vesicle exocytosis (Heidelberger *et al.* 1994) and suggests that these synaptotagmins are involved in the fast neurotransmitter release that is brought about by high Ca^{2+} concentrations. This is consistent with the phenotype of mice lacking

Table 1.2 Differential properties of synaptotagmins

Isoform	Tissue distribution	Ca^{2+}-dependent binding of phospholipids (μM)		Ca^{2+}-dependent binding of syntaxin (μM)		Ca^{2+}-independent binding of AP-2 (μM)
		C2-A	C2-A/B	C2-A	C2-A/B	C2-A/B
I	Rostral brain	3-6	3-6	200-400	200-400	0.1-1.0
II	Caudal brain	3-6	ND	300-500	ND	ND
III	Brain	3-6	ND	<10	ND	0.1-1.0
IV	Brain (ubiquitous)	no binding	ND	no binding	ND	0.1-1.0
V	Brain	3-6	ND	300-500	ND	0.1-1.0
VI	Ubiquitous	no binding	ND	no binding	Ca^{2+}-independent	0.1-1.0
VII	Ubiquitous	3-6	ND	<10	<10	0.1-1.0
VIII	Ubiquitous	no binding	ND	no binding	ND	0.1-1.0

ND not determined

Li *et al* 1995

synaptotagmin I which show a defect in fast neurotransmitter release (Geppert *at al* 1994). An analogous role for other synaptotagmins in other membrane fusion reactions is suggested by the fact that they are able to bind to non-neural forms of syntaxins.

The expression of the various isoforms of synaptotagmin in brain is confusing and seems not to be governed by any common principle (Ullrich and Südhof 1995). Isoforms I, II and VI are expressed highly differentially whereas II, IV and VII are relatively uniformly expressed. This suggests that, in some cases, the different isoforms may perform separate functions in the same cell, a conclusion which is supported by the finding that cells with synaptotagmin I mutations are defective in fast neurotransmitter release even though other isoforms are present in the same cell (Ullrich *et al.* 1994). Clearly, therefore, the other isoforms cannot replace the function of synaptotagmin I.

No specific functions have been assigned to the different synaptotagmin isoforms and work on them is at an early stage. Indeed, even the role of synaptotagmin I is not well understood and although a large body of work and information on the protein is available, its precise role in exocytosis is elusive. Recent work has suggested that synaptotagmin IV may be involved in modulation and adaptation of synaptic structure and function in response to neural activity because expression of the gene is induced by depolarisation and sustained exocytotic activity in PC12 cells, brought about by such methods as potential depolarisation, Ca^{2+} ionophore, ATP and forskolin as well as kainic acid-induced seizures in rat brain (Vician *et al.* 1995, Tocco *et al.* 1996). In contrast, growth factors, which might affect the level of expression due to cell growth, and phorbol 12-myristate 13

acetate, which would affect exocytosis via protein kinase C (Bittner and Holz 1990) do not affect expression of the synaptotagmin IV gene. Since this isoform does not appear to bind Ca^{2+} and phospholipids yet still binds to AP-2 (table 2) , it may be that the modulatory role of the protein involves rapid endocytotic reuptake of vesicle material to compensate for increased exocytotic activity.

1.4.4 Nature and structure of C2 domains

Protein kinase C has four highly conserved regions known as C1-C4. Whilst C3 and C4 contain catalytic activity, the C1 and C2 domains are regulatory (Newton 1995). The two regulatory domains are of great interest particularly because they appear in many other apparently unrelated proteins (Newton 1997). The C2 domain, present in phospholipase Aδ, phospholipase Cγ, the GTPase activating protein GAP, rabphilin 3A, Doc2 and synaptotagmin, has been extensively studied because it is known to confer phospholipid- and Ca^{2+}-binding activity on protein kinase C, and this implies a role for synaptotagmin in Ca^{2+}-regulated membrane fusion. Elucidation of the structure of the C2 domains from synaptotagmin (Sutton *et al.* 1995) and phospholipase C (Grobler *et al.* 1996, Essen *et al.* 1996) revealed a β-sheet rich domain with a novel Ca^{2+}-binding pocket consisting of two loops formed by the amino and carboxyl termini of the C2 core sequence, which come together to form an aspartate-lined mouth which coordinates Ca^{2+}. NMR spectroscopy has shown that this pocket coordinates two metal ions (Shao *et al.* 1996).

Synaptotagmin has two C2 domains in its structure termed C2A (amino terminal) and C2B (carboxyl terminal). In general experimental investigations, the C2 domains of synaptotagmin have been shown to bind

phospholipids in a Ca^{2+}-dependent manner. It is now emerging that the two C2 domains may have distinct activities. The C2A domain appears to exhibit Ca^{2+}-dependent binding of phospholipids and syntaxin (Sugita *et al.* 1996) whereas the C2B domain is inactive in similar assays but binds the interacting molecules in a Ca^{2+}-independent manner. The C2B domain, however, seems to cause Ca^{2+}-dependent self-association, which can also be stimulated by Sr^{2+} or Ba^{2+}. Some work has shown that the protein forms a dimer at an EC_{50} of 3-10 μM Ca^{2+} (Damer and Creutz 1996, Chapman *et al.* 1996b) and then exhibits Ca^{2+}-dependent syntaxin binding at higher Ca^{2+} concentrations (EC_{50} = 100 μM Ca^{2+}) suggesting that this reflects a two-step Ca^{2+}-dependent process, involving synaptotagmin, in exocytosis.

Studies of exocytosis from giant squid axons using antibodies directed against C2A or C2B domains of synaptotagmin suggest that the C2A domain is directly related to the fusion of synaptic vesicles (Mikoshiba *et al.* 1995) and the C2B domain may be involved in vesicle recycling (Fukuda *et al.* 1995a). Similar work with antibodies in permeabilised chromaffin cells seems to confirm the direct involvement of C2A in Ca^{2+}-triggered vesicular fusion but suggests a more subtle role for C2B. Antibodies against the second C2 domain have no effect on Ca^{2+}-triggered exocytosis but do increase the spontaneous Ca^{2+}-independent release which is also seen in regulated cells. Inositol polyphosphates bind to the C2B domain and inhibit both Ca^{2+}-dependent and Ca^{2+}-independent release in a dose-dependent manner, but this could be totally reversed by the addition of the antibody and substantially reversed by high concentrations of Ca^{2+} (50 μM). This suggests that the interaction of inositol polyphosphates with C2B might have a role in the prevention of spontaneous fusion of docked or primed

vesicles until the binding of Ca^{2+} to C2A releases the suppression allowing fusion to proceed. Similar experiments were also carried out in cultured rat sympathetic neurons (Mochida *et al.* 1997) and the same conclusions drawn.

1.4.5 Phospholipid and inositol high polyphosphate binding

a. Phospholipids

Synaptotagmin I was found to cause aggregation of erythrocytes (Perin *et al.* 1990) and so the phospholipid-binding properties of the protein were investigated by a haemagglutination assay. The cytoplasmic domain alone of native synaptotagmin was found to bind acidic phospholipids and sphingolipids with high affinity and specificity resembling that of protein kinase C. Similar experiments with recombinant whole synaptotagmin show that it also demonstrates specificity for negative charges on lipid headgroups and also that it only binds phospholipids with two acyl chains rather than one. It is suggested that this implies that the protein makes contact with the hydrophobic portion of the phospholipid, perhaps inserting partially into the bilayer.

Subsequent work concentrated on recombinant single C2 domains of the protein and showed that the first C2 domain of synaptotagmin I (C2A) was able to bind Ca^{2+} and phospholipids alone with high affinity (half maximal at 4-6 μM free Ca^{2+}) and displayed positive cooperativity in binding the ion and specificity for charged phospholipids (Davletov and Südhof 1993). The C2A domain also showed similar binding to other divalent cations (Sr^{2+} and Ba^{2+}) known to stimulate exocytosis, but had much lower affinity for Mg^{2+} which does not stimulate vesicle release. Further evidence to support this

was found using a proteolytic fragment of synaptotagmin I containing both C2 domains, which was able to bind to various natural membranes in a Ca^{2+}-dependent manner (EC_{50} = 30 μM Ca^{2+}). The binding was insensitive to proteolysis of the membranes suggesting the interaction was with lipids (Chapman and Jahn 1994). A recombinant protein containing the two C2 domains also exhibited the same effect and the interaction was located to the C2A domain. Mutational analysis further narrowed the functional region to a highly-conserved motif of nine aminoacids, disruption of which was sufficient to abolish the Ca^{2+}-dependent lipid binding of the domain. Other work using aggregation of proteinase-treated chromaffin granules as a lipid-binding assay suggested that both domains were needed for binding granule membranes, although each separate C2 domain did bind artificial PS/PC vesicles containing 10-40% PS. The C2A domain showed Ca^{2+}-dependent binding to vesicles whilst the second C2 domain (C2B) bound vesicles independently of Ca^{2+}. The two domains together, however, bound vesicles in much larger amounts than either of the two individual domains, suggesting synergistic action of the two domains (Damer and Creutz 1994).

Other isoforms of synaptotagmin (II-VI) have also been found to bind negatively-charged phospholipids in a Ca^{2+}- dependent manner with positive cooperativity (Fukuda *et al.* 1996). Synaptotagmin IV showed two EC_{50} values of 5 and 120 μM free Ca^{2+} and a Hill coefficient of 2 whereas all the other isoforms showed high affinity binding (EC_{50} 0.3-1.0 μM) and a Hill coefficient of 3-3.5. Synaptotagmin IV was also unique in that binding to negatively charged phospholipids was inhibited by PC or PE. This effect of lipid composition was found to be due to the substitution of the amino acid aspartate for serine at position 244. When the whole cytoplasmic domain of synaptotagmin IV was tested it also showed this unique lipid

binding but the Ca^{2+}-dependence and cooperativity measurements became the same as the other isoforms. Recently, synaptotagmin III has also been found to have unusual properties in that it shows a Mg^{2+}-dependent interaction with PS comparable to that of Sr^{2+} or Ba^{2+} (Fukuda *et al.* 1997). This property is specific to synaptotagmin III and is also not found in other C2-containing proteins such as rabphilin 3A, Doc2α/β or $Gap1^{m}$. This suggests that synaptotagmin may be involved in different presynaptic functions.

b. Inositol polyphosphate

Preinjection of inositol 3,4,5, tetrakisphosphate, inositol 1,3,4,5,6, pentakisphosphate or 1,2,3,4,5,6, hexakisphosphate into squid giant synapse blocked synaptic transmission (Llinas *et al.* 1994). Inositol 1,4,5 trisphosphate did not produce this effect. Both Ca^{2+}-stimulated (evoked) and spontaneous transmitter release were blocked although the inward Ca^{2+} current was not affected. Repeated stimulation of the axon showed that there was a gradual reduction in the postsynaptic response demonstrating that vesicular fusion was being prevented. Synaptotagmin III was found to bind these compounds via the C2B domain which had previously been found to bind phospholipids independently of Ca^{2+}. Scatchard analysis of the binding indicated a single binding site with a K_d of 30 nM (Niinobe *et al.* 1994). Thirty amino acids at the centre of the C2B domain and specifically three lysine residues which are not conserved in the C2A domain were found to be essential for inositol polyphosphate binding (Fukuda *et al.* 1995b). This binding is not found in rabphilin 3A, another protein with C2 domains implicated in regulated exocytosis. The effect of inositol polyphosphates on synaptic transmission coupled with the binding to synaptotagmin III suggests that these two elements are directly

involved in the process of fusion of vesicles with the plasmalemma.

Recently, the C2B domain of synaptotagmin I has been shown to bind phosphatidyl inositol 4,5-bisphosphate, its isomer inositol 3,4-bisphosphate and phosphatidyl inositol 3,4,5-trisphosphate (Schiavo *et al.* 1996). Ca^{2+} ions switch the specificity of binding from trisphosphate at low Ca^{2+} concentrations (< 30 μM), to 4,5-bisphosphate at the higher Ca^{2+} concentrations required for transmitter release (20-1000 μM). Inositol polyphosphates inhibit this binding and this could be one possible cause for their inhibitory effect on neurotransmitter release. The authors of this paper propose a scheme in which a rise in Ca^{2+} levels switches synaptotagmin I from a resting conformation (bound to phosphatidyl inositol trisphosphate) to a fusion-competent conformation (bound to phosphatidyl inositol 4,5- bisphosphate). This is also supported by the finding that phosphatidyl inositol 4-kinase, phosphatidyl inositol-specific transfer protein and phosphatidyl inositol 4-phosphate 5-kinase are all needed for fusion to be triggered by Ca^{2+} (Hay *et al.* 1995, Wiedemann *et al.* 1996) since these proteins would be required to maintain the pool of phosphatidyl inositol bisphosphate needed to bind the C2B domain in the fusion-competent conformation.

1.4.6 Ca^{2+} binding

The Ca^{2+} binding properties of synaptotagmin I were first demonstrated using equilibrium dialysis techniques (Brose *et al.* 1992). The binding was shown to be dependent on the presence of phospholipids and was half-maximal at 10^{-5} M Ca^{2+}. Mg^{2+}, Ba^{2+} or Sr^{2+} did not produce the same effect. Increasing concentration of acidic phospholipids shifted the Ca^{2+} sensitivity to lower concentrations giving a response within the range

expected at the synapse during exocytosis. The total Ca^{2+} binding reached 4 moles/mole synaptotagmin at a free Ca^{2+} concentration of 10^{-4} M indicating more than one Ca^{2+}-binding site per molecule or perhaps cooperative binding of a synaptotagmin multimer. Most of the other synaptotagmin isoforms also show affinity for Ca^{2+} in a lipid-dependent manner as shown in table 2 (Li *et al.* 1995) and so are all potential candidates for involvement in Ca^{2+}-dependent exocytosis.

Most other work has not focused on the direct binding of Ca^{2+} to the protein but has looked at the Ca^{2+}-dependent interactions of the protein and its effect on exocytosis in various cell systems. The methodology used to investigate this generally involves the use of biochemical assays, analysis of genetic mutants and transfected cell lines as well as the introduction of peptides and antibodies into cells. Such studies have uncovered numerous interactions associated with synaptotagmin and *in vivo* work has generally implicated synaptotagmin in Ca^{2+}-dependent exocytosis although there have also been contradictory findings.

1.4.7 Interactions with other proteins

Synaptotagmin was originally discovered as a calmodulin-binding protein (Fournier and Trifaro 1988) and has since been found to bind at least eight other proteins as well as forming an oligomer itself. Synaptotagmin was shown to co-purify with the Ca^{2+}-dependent α-latrotroxin receptor (neurexin) on immobilised α-latrotroxin (Petrenko *et al.* 1991). α-latrotoxin causes massive spontaneous synaptic vesicle exocytosis in the presence or absence of Ca^{2+} so neurexin, its putative target protein, is implicated in the process. No other synaptic protein was found to interact with neurexin (a plasma membrane protein) in this way and the interaction seemed to be

through the cytoplasmic region of synaptotagmin. Neurexin also inhibited phosphorylation of synaptotagmin I in a dose-dependent manner and so it is suggested that an interaction between the two proteins along with the modulation of synaptotagmin phosphorylation plays a role in vesicle fusion. Interaction between these two proteins was corroborated by evidence from PC12 mutant cells lacking synaptotagmin I and synaptotagmin II (Shoji-Kasai *et al.* 1994). These cells do not exhibit Ca^{2+}-dependent release of neurotransmitter induced by α-latrotoxin which implies that the mechanism of action of the toxin is through disruption of the synaptotagmin/neurexin complex rather than through neurexin alone. The site of interaction of the two proteins was located to the cytoplasmic domain of neurexin (Hata *et al.* 1993) and was found to be Ca^{2+}-independent. A highly conserved 40 amino acid sequence which makes up most of the cytoplasmic tail of neurexin was found to be essential for the binding. This evidence was taken to imply a vesicle-docking or targeting role for the two proteins. the interaction has been further dissected and found to rely on as little as 34 amino acids from the carboxyl terminal of synaptotagmin (Perin 1994). The other synaptotagmin isoforms (except III and VIII) and rabphilin 3A which shows conservation in this region, displayed the interaction (Perin 1996). Deletion analysis of the sequence led the author to submit that the mirror image motif Leu-X-His-Trp-X_{13}-Trp-His-X-Leu was responsible for the binding and that this sequence also mediated in the interaction of synaptotagmin with calmodulin. The importance of the synaptotagmin interaction with neurexin has been called into question by the discovery that neurexin is not the only α-latrotoxin receptor. An additional α-latrotoxin receptor which binds the toxin in a Ca^{2+}-independent manner has been isolated (Davletov *et al.* 1996) which appears to be a G-protein-coupled receptor found in brain tissue

(Krasnoperov *et al.* 1997). Since neurexin only binds the toxin in the presence of Ca^{2+}, it cannot be responsible for the stimulation of exocytosis caused by the toxin in calcium-free medium and so may not have such a central role in maintaining a docked complex or triggering exocytosis as was previously imagined. However, the interaction of neurexin with synaptotagmin may still be significant especially in the light of further protein interactions discovered involving these two proteins with other proteins thought to be involved in exocytosis as discussed below.

Up to this point, only synaptotagmin and neurexin had been found to co-purify on immobilised α-latrotoxin. One group, however, found that syntaxin also co-purified in this system (O'Connor *et al.* 1993). In addition, it was shown that α-latrotoxin was immunoprecipitated with anti-syntaxin antibodies and that the same antibodies as well as antibodies against neurexin also immunoprecipitated ω-conotoxin-binding proteins (Ca^{2+} channels). This work has led to the theory of an exocytosis-organising complex made of these proteins and perhaps additional factors which together would be known as the 'synaptosecretosome'. The interaction of synaptotagmin with Ca^{2+} channels was supported by the discovery that synaptotagmin was a specific auto-antigen associated with N-type Ca^{2+} channels in Lambert-Eaton Myasthenic Syndrome (El Far *et al.* 1993) a disease which causes muscle weakness, autonomic dysfunction and decreased Ca^{2+} currents in motor nerve terminals (Smith *et al.* 1995) through down-regulation of Ca^{2+} channels. In addition, repeated injection of a peptide consisting of residues 20-58 of synaptotagmin has been found to produce a model of the disease in rats (Takamori *et al.* 1994) but its presence as an antigen in the disease has also been disputed (Hajela and Atchison 1995).

Similar methodology of immunoprecipitation and binding to immobilised proteins was used to further investigate the interaction between synaptotagmin and syntaxin (Chapman *et al.* 1995). Ca^{2+} was found to increase the affinity of this interaction by two orders of magnitude. The Ca^{2+}-dependence had two components with EC_{50} values of 0.7 and 180 μM Ca^{2+} and the binding could also be stimulated by Ba^{2+} or Sr^{2+} but not by Mg^{2+}. The interaction was mediated by the carboxyl terminal region of syntaxin and was not abolished by mutations in the Ca^{2+}-dependent lipid binding site of synaptotagmin I (in the C2A domain) although this is not conclusive because the C2A domain has also been found to be responsible for the interaction in other work (Li *et al.* 1995, Kee and Scheller 1996). The two components of the interaction with different Ca^{2+}-affinities have been suggested to represent a conformational change in one or both proteins and since the lower-affinity component (EC_{50} = 180 μM) corresponds to the dependence of transmitter release reported in neurons (Heidelberger *et al.* 1994) it is possible that the putative conformational change functions in the late steps of exocytosis. Recently, NMR analysis and site-directed mutagenesis of the C2A domain of synaptotagmin (Shao *et al.* 1997) showed that the interaction is mediated by the cooperative action of basic residues surrounding the Ca^{2+}-binding region. The binding of Ca^{2+} causes the electrostatic potential of the domain to change and so the authors propose a mechanism in which synaptotagmin acts as an electrostatic switch, promoting a structural rearrangement in the fusion machinery through its interaction with syntaxin.

Many other interactions are proposed for synaptotagmin and have some experimental work to support them. Synaptotagmin was placed in the correct context for a Ca^{2+} sensor in exocytosis when it was shown to

associate with the cytosolic region of N-type Ca^{2+} channels (Leveque *et al.* 1992, Wiser *et al.* 1997) and also to restore the kinetic properties of the channel in a Ca^{2+}-dependent manner when the channel kinetics were modified by its association with syntaxin. Synaptotagmin has also been found to associate with the synaptic vesicle protein SV2 via the C2B domain (Schivell *et al.* 1996). The binding was inhibited by Ca^{2+} with an EC_{50} value of 10 μM. In addition, synaptotagmin I has been identified as the target for clostridial botulinum B neurotoxin (Nishiki *et al.* 1994, Nishiki *et al.* 1996) in association with gangliosides G_{T1b}/G_{D1a}. The neurotoxin is a potent inhibitor of exocytosis through proteolysis of synaptobrevin 2; this finding implicates synaptotagmin as necessary for the entry of toxin into susceptible cells. Exocytosis is often followed by the rapid assembly of clathrin-coated pits and this is preceded by the binding of the heterooligomeric complex, clathrin/AP-2 to the inside surface of the plasma membrane (Anderson 1993). It has been suggested that one of the functions of synaptotagmin is as a membrane recycling protein after the discovery that AP-2 interacts with the C2B domain of synaptotagmin.

One further molecular interaction of synaptotagmin has raised much interest recently. The SNAP/SNARE hypothesis already outlined emphasises the role of SNAP-25 (a plasma membrane protein) as a key constituent of the vesicle docking complex. Experiments with a cell-free system which relies on exocytosis occurring from docked and primed vesicles, show that blocking SNAP-25 with antibodies prevents Ca^{2+}-triggered exocytosis from the membranes (Mehta *et al.* 1996) suggesting that SNAP-25 is involved at a very late stage of exocytosis. It was therefore quite an interesting indication of the importance of synaptotagmin to find that it binds to SNAP-25 in the absence of Ca^{2+}

although the binding was promoted slightly by addition of Ca^{2+} (Schiavo *et al.* 1997). This work also showed that although synaptotagmin binds syntaxin in a Ca^{2+}-dependent manner, it was able to do so in the absence of Ca^{2+} if SNAP-25 was present. This suggests that the docking complex may actually be promoted by SNAP-25 and synaptotagmin at resting Ca^{2+} concentrations. Thus in effect, SNAP-25 and synaptotagmin are respectively an additional t-SNARE and v-SNARE.

1.4.8 Interaction with calmodulin

The role of calmodulin in exocytosis has long been a mystery and has not been studied to the same extent as other proteins implicated in exocytosis. Recent work has shown that antibodies to calmodulin and calmodulin antagonists decreased Ca^{2+}-induced noradrenalin release from permeabilized synaptosomes, although exogenous calmodulin had no effect (Hens *et al.* 1996). In adrenal chromaffin cells, calmodulin was found to have an effect on rapid endocytosis after release but not on exocytosis itself (Artalejo *et al.* 1996). However, other work using patch-clamp measurements of chromaffin cells dialysed with calmodulin indicated that calmodulin regulated late steps in Ca^{2+}-dependent exocytosis, because the introduction of the protein into cells increased initial rates of exocytosis two-fold (Kibble and Burgoyne 1996). Calmodulin was shown to bind adrenal chromaffin membranes via a polypeptide complex (Hikita *et al.* 1984) and so was implicated in stimulus-secretion coupling. When the granule-binding sites for calmodulin were investigated further they were found to be of high affinity, displaying Ca^{2+}-dependent binding at 10^{-4} M free Ca^{2+} and due to a 65 kDa protein (Bader *et al.* 1985).

The 65 kDa protein recognised as a calmodulin-binding protein in

chromaffin cells was identified as synaptotagmin which was, at the same time, described as a granule membrane protein (Fournier and Trifaro 1988a and b). The protein in granules also appeared to bind calmodulin since the subcellular distribution of calmodulin, measured by density gradients, resembled that of granules when Ca^{2+} was present but became diffuse in the absence of Ca^{2+}. Although there is quite a lot of evidence to show binding between synaptotagmin and calmodulin, it has not been the subject of many studies and is regarded by some as an artifact which, considering the number of other synaptotagmin interactions considered significant, is somewhat illogical. However, since the importance of calmodulin in exocytosis has become more apparent it is likely that the interaction will be investigated more thoroughly in the future.

The number of interactions described for synaptotagmin and the importance ascribed to them all should be a matter for debate and further experiment. It has become increasingly clear that synaptotagmin is what is euphemistically known as a 'sticky' protein and it is possible that some of the interactions are actually misleading artifacts that do not occur under physiological conditions. It is particularly important to note that the same methodology has nearly always been used to uncover these interactions and so a method that originally claimed to show only one protein interacting with synaptotagmin has now revealed many others. It is comforting to believe that amidst so many reported interactions, some at least are significant and of course it is not impossible that synaptotagmin is a multi functional protein. Finding new interactions is useful for maintaining a flow of fresh hypotheses but the secrets of a complicated process such as exocytosis are unlikely to be revealed by one more synaptotagmin-binding partnership yet to be discovered. One should perhaps be wary of placing

too much emphasis on binding studies until the hypothesis is supported by more functional studies which test the protein in a cellular context.

1.5 *In vivo* studies of synaptotagmin function

Since the number of potential roles proposed for synaptotagmin, based on *in vitro* work, is large, it has also become a subject for *in vivo* studies of function. The techniques adopted for this area of work fall into three categories; genetic manipulations of whole organisms, transfection of cell lines and injection or introduction of antibodies and synaptotagmin peptides into cells which exhibit regulated exocytosis.

1.6 Genetic manipulations

1.6.1 Rat

Genetic manipulation in rat cells has exclusively involved the use of the phaeochromocytoma-derived cell line PC12. Uninduced PC12 cells from a line selected to be deficient in synaptotagmin I and synaptotagmin II were still able to release dopamine and ATP (Shoji-Kasai *et al.* 1992) and so it seemed the protein has no essential role in these cells. However, these cells were later discovered to produce synaptotagmin III in abundance (Mizuta *et al.* 1994) and this has been suggested to compensate for the lack of other isoforms. This deficient cell line was further studied and although secretion from secretory granules was unaffected as found previously, the acetylcholine release from synaptic-like vesicles was no longer Ca^{2+}-dependent (Bauerfeind *et al.* 1995). The results have been taken to indicate the possibility of two exocytosis mechanisms for small vesicles, one of which is Ca^{2+}-dependent and is no longer viable without synaptotagmins I and II.

More direct evidence that synaptotagmin plays an important role in neurotransmission comes from genetic disruptions of the synaptotagmin gene (*syt* locus) in *Drosophila*, *C.elegans* and mouse.

1.6.2 *Drosophila*

Only one isoform of synaptotagmin has so far been identified in *Drosophila*. Most embryos that lacked synaptotagmin I failed to hatch at all (Littleton *et al.* 1993b) and displayed very reduced, uncoordinated muscle contractions. Measurements from larvae with partial lack of function were possible and showed that they exhibited almost no evoked exocytotic response at 0.4 mM Ca^{2+} and a very reduced response at 1 mM Ca^{2+}. The spontaneous vesicle fusion rate had increased. These experiments showed the importance of synaptotagmin activation of exocytosis by Ca^{2+} and the authors conclude that there must also be separate pathways for evoked and spontaneous exocytosis since they were differentially affected by the mutation. However, it is possible that the differential effect on the two types of exocytosis was simply the two sides of one pivotal control point. Spontaneous fusion may be a manifestation of an event which is energetically favourable, particularly in a subset of vesicles already competent for fusion, but mostly held in check by a control protein in cells which exhibit regulated exocytosis. Thus spontaneous fusion might be due to 'escapee' vesicles. A protein (or group of proteins) responsible for restraining vesicles from fusion must also be able to detect Ca^{2+} in order to release them at the appropriate signal. Such a 'fusion clamp' would have a role in Ca^{2+}-stimulated fusion through its ability to detect $[Ca^{2+}]$. It is therefore consistent with the data that synaptotagmin prevents fusion. The mutant *Drosophila* cells show a reduced Ca^{2+} response because there is no Ca^{2+} sensor to control exocytotic events and consequently, without

such control, spontaneous fusion increases. Further electrophysiological studies by this group (Littleton *et al.* 1994) showed that defects in fly embryos were consistent with the idea that synaptotagmin acts as a barrier to vesicle fusion but that its activity was not entirely due to this. In addition, this work supported the idea that synaptotagmin functions as a Ca^{2+} sensor in an oligomeric complex.

Many *syt* mutations are found to be lethal in *Drosophila,* but one group isolated homozygotes for an apparent null allele which did hatch (DiAntonio *et al.* 1993). Electrophysiological recordings in embryonic cultures showed that synaptic transmission persisted even in null mutants showing that synaptotagmin is not absolutely required for the process. There were however some interesting deficiencies in the synaptic transmission of the null mutants assayed at the neuromuscular synapse. Evoked vesicle release was reduced by a factor of 10 and the fidelity of excitation-secretion coupling was impaired so that any given stimulus gave a variable release (Broadie *et al.* 1994). Spontaneous vesicle fusion had increased by a factor of 5 but contrary to the previous work, the Ca^{2+}-dependence of the residual evoked exocytosis was similar to that in normal embryos. This work suggests that synaptotagmin is not the sole Ca^{2+} sensor for exocytosis but that the protein plays an important role in increasing the efficiency of synaptic transmission and regulating spontaneous fusion.

1.6.3 *C.elegans*

Similar mutational analysis of nematodes has been carried out (Nonet *et al.* 1993). Mutants defective in the gene *snt-1* exhibit behavioural abnormalities that are characteristic of deficiencies in synaptic function such as problems with locomotion, feeding and defaecation. The worms

also accumulate acetylcholine, showing an impairment in exocytosis, but are still capable of coordinated motor movements showing that there is not a complete blockade of neurotransmitter release. It was proposed from this that synaptotagmin either controls one of several independent pathways to vesicle release or that it controls endocytosis. The latter point was supported by the finding that synaptic vesicles are depleted in these mutants (Jorgensen *et al.* 1995) and the depletion was due to defects in vesicle recycling rather than vesicle transport or an increase in vesicle release.

1.6.4 Mice

Mutations in *syt1* were produced in mice (Geppert *et al.* 1994). At birth, there was no phenotypic difference between homozygous and heterozygous mutants. Homozygous pups were capable of breathing, responding to tactile stimuli and showing pain avoidance reflexes. However, after a few hours, the homozygotes show weakness, have not suckled and are often neglected by their mothers and die within 48 hours of birth. Heterozygotes show no abnormalities. Autopsies of dead mice reveal no major congenital malformations. Cultured hippocampal neurons from homozygous mice revealed that the synchronous, fast component of Ca^{2+}-dependent neurotransmitter release is decreased whereas asynchronous release such as spontaneous vesicle fusion and the release triggered by hypertonic solution or α-latrotoxin were unaffected. A study by Goda and Stevens (1994) described two components of transmitter release; a fast component mediated by an efficient, low-affinity Ca^{2+} receptor, and a slower component with a less efficient, higher-affinity receptor. The work on mouse mutations has been interpreted in the light of this study and this would mean that synaptotagmin is the low-affinity receptor for fast

transmitter release. This interpretation would explain the data well and may also explain why measurements in mutant non-neuronal cells (which have an overall much slower exocytotic response) are more variable as they can perhaps accommodate a mutation in the putative fast Ca^{2+} sensor to a greater degree.

1.7 Cell transfections

CHO fibroblast cells which have taken up acetylcholine by endocytosis show spontaneous quantal and Ca^{2+}-evoked acetylcholine release. Cells transfected with synaptotagmin I show the formation of actin-rich filopodal processes (Feany and Buckley 1993), a reduced spontaneous release and an enhanced evoked release of acetylcholine compared to control markers (Morimoto *et al.* 1995). The endocytotic function of these cells was normal, as assessed by the use of a separate marker for endocytosis. Either of the popular theories for synaptotagmin function would be consistent with this work, namely, that synaptotagmin is a 'fusion clamp' that inhibits exocytosis at resting intracellular Ca^{2+} concentrations or alternatively that synaptotagmin is a positive effector of exocytosis

1.8 Introduction of antibodies and peptides into cells

Antibodies to synaptotagmin were injected into PC12 cells and found to decrease the Ca^{2+}/K^{+} - mediated dopamine β hydroxylase surface staining which was used as a measure of secretion (Elferink *et al.* 1993). Injection of peptides from corresponding to the C2 domains of synaptotagmin I into the squid giant axons resulted in a rapid and reversible inhibition of neurotransmitter release (Bommert *et al.* 1993). Introduction of peptides into cells which already contain the endogenous protein is a technique which assumes the peptides will bind to sites in competition with the native

protein and thus have an inhibitory effect. Reversal of the effect of the peptides in the squid axon was slower if more peptide was added which is consistent with a competitive mechanism of inhibition in which the peptide's action would depend on diffusion to and away from binding sites. The inhibition of Ca^{2+}-evoked release suggests that Ca^{2+} probably initiates exocytosis by regulating the interaction of synaptotagmin with an acceptor protein.

The introduction of either of the C2 domains or the whole cytoplasmic domain of synaptotagmin into AtT-20 mouse pituitary cells albeit by transfection (Wendland and Scheller 1994) relies on the same principle of competitive effect. In this experiment, the transfected cells showed no effect. Vesicle targeting, regulated ACTH secretion, constitutive secretion and endocytosis, monitored by the uptake of transferrin, all seemed to be normal. The authors suggest that there is redundancy in the process of exocytosis with several pathways possible to the same endpoint so that dysfunctional synaptotagmin is simply bypassed by alternatives. It is also possible that exocytosis in endocrine cells is under slightly different control even though the same protein machinery is present since the kinetics of the process in these cells is quite different from that in neurons (Morgan and Burgoyne 1997). Furthermore, the introduction of smaller peptides (as in the first experiment described) may be more efficient at producing an effect because a particular binding site may be fully exposed. A whole domain of a protein, as used in AtT-20 cells, may have binding sites concealed within its structure and depend on more complex interactions to allow them to be exposed or alternatively may not be correctly folded. Either way, it is possible that competitive interactions from such introduced proteins will not actually occur.

Exocytosis is a complex process involving many proteins, some of which have probably not yet been identified. Synaptotagmin is a major candidate for the Ca^{2+}-sensor in the process and, as such, has been the subject of a phenomenal amount of work in the last four years. For some time, the role of synaptotagmin was disputed because of contradictory results, confusing differences between cell types and because the protein has never actually been shown to be essential for exocytosis. This probably says more about the flexibility of exocytosis than about the protein itself and has been a useful lesson in that it has forced us to think in terms of redundant pathways, alternative and interchangeable Ca^{2+}-sensors and multifunctional proteins rather than one protein, one function, one mechanism. It is now becoming accepted that synaptotagmin is a low-affinity Ca^{2+}-receptor, involved in modulating the fast step of exocytosis and that it controls the spontaneous fusion of vesicles by virtue of the fact that it only allows fusion to proceed when a critical Ca^{2+} concentration is achieved. There is also some evidence that it has a secondary role in the recycling of vesicle material in endocytosis. Clearly, there must be additional factors responsible for Ca^{2+} threshold and kinetic variations in different cell types but it is in the fast fusion process, which occurs in all these cells, that synaptotagmin is implicated. The most interesting area still to be explored in more depth is the role of synaptotagmin isoforms with unusual Ca^{2+} affinities or binding properties and especially the isoforms being discovered in non-neural cells. Perhaps the neuronal isoform is a modification of a fusion-control protein existing in most cells and even constitutive fusion has more of an element of control than its basic description implies.

1.9 The aims of the project

Most of the information on synaptotagmin presented was not available at the beginning of this project and a few subjects of this study were published by other groups whilst my experiments were being carried out. The main direction of enquiry, however, is one that has only recently become more popular. It was originally suggested that ATP hydrolysis by NSF could drive membrane fusion (Rothman 1994, Sollner *et al.* 1993a and b) but the speed of exocytosis, especially in neurons is too fast to involve the slow ATPase activity of NSF (Morgan and Burgoyne 1995). In addition, exocytosis can be triggered by Ca^{2+} in chromaffin cells in the absence of MgATP (Neher and Zucker 1993). Fusion is far more likely to involve a conformational change of a protein or proteins. Synaptotagmin is ideally placed to promote fusion by undergoing a Ca^{2+}-dependent conformational change and all the evidence suggesting it is involved in the final fast fusion step give weight to this argument. The possibility of a conformational change in synaptotagmin was therefore studied by various biochemical techniques as were the factors which may affect it such as binding to Ca^{2+}, phospholipid and calmodulin.

Chapter 2

Materials and Methods

Materials

2.1 Chemicals and biochemicals

All general chemicals were obtained from Sigma Chemical Co., BDH Chemicals, Fisher Ltd, Calbiochem or Boehringer Mannheim. α- [^{35}S] - dATP was obtained from Amersham International plc. Media components were from Difco Laboratories. Enhanced chemiluminescence (ECL) kit and Hyperfilm - MP for western blotting was obtained from Amersham International. IgG Sepharose (Fast Flow) was from Pharmacia LKB. Calmodulin-agarose was from Sigma Chemical Co. Ni-NTA agarose and kits for plasmid DNA preparation and purification of DNA from agarose gels were from Qiagen Ltd. 0.02μm nylon filters for molecular dynamics sample treatment were obtained from Millipore.

2.2 Enzymes, proteins and antibodies

Calmodulin, lysozyme, trypsin and thrombin were all obtained from Sigma Chemical Co. All DNA modification enzymes were from BRL or NEB. *Taq* polymerase was from Promega and high fidelity DNA polymerase was from Boehringer Mannheim Biochemicals. Monoclonal antibody cgm67 was obtained from Dr Bülent Tugal, previously a postgraduate student in this laboratory, and other antibodies not raised in this study were from Sigma Chemical Co. and the Scottish Antibody Production Unit.

2.3 Bacterial strains and plasmids

The strains of *E. coli* used in this study are listed in Appendix 1. Transformants are denoted by listing the strain, followed by the plasmid with which it has been transformed in parenthesis. All plasmids that were used in this study are described in Table A2a (Appendix 2).

2.4 Media

Bacterial cultures were grown in complete medium (Luria broth; L-broth) containing 1% (w/v) Bacto tryptone, 0.5% (w/v) Bacto yeast extract and 0.5% (w/v) NaCl. Bacto agar was added to the above to 1.5% (w/v) when solid medium was required. Liquid and solid media were supplemented where necessary with ampicillin to 100 μg/ml or kanamycin to 50 μg/ml. Solid medium for blue/white selection also contained 0.015% Xgal (w/v) and 100 μM IPTG.

In order to maintain the F' plasmid, the bacterial strain NM522 was stored on M9 minimal plates which contain 2% agar, 0.4% glucose, M9 salts (0.7% (w/v) sodium phosphate (dibasic), 0.3% (w/v) potassium phosphate (monobasic), 0.05% (w/v) sodium chloride, 0.1% (w/v) ammonium chloride), 0.1 mM calcium chloride, 2 mM magnesium sulphate and 2 μg/ml vitamin B1.

2.5 DNA manipulations

General DNA manipulation techniques including PCR amplification, ligation, extraction with phenol, precipitation with ethanol, and restriction endonuclease cleavage were performed as described by Sambrook *et al* (1989).

Plasmid DNA was isolated from bacterial cells using the method described by Birnboim & Doly (1979). When extremely pure plasmid DNA was required for DNA sequence analysis, a purification kit supplied by Qiagen Ltd was used and the manufacturer's instructions followed. Purification of DNA from agarose gels was also carried out with a kit from Qiagen Ltd and the manufacturer's method used.

Initial cloning of PCR products involved the use of the commercial vector pGEM-T obtained from Promega. Ligation was carried out as suggested in the manufacturer's product instructions. Gel electrophoresis, for the separation and visualisation of DNA fragments, was routinely carried out using agarose gels of 0.8% (w/v) agarose; the size of fragments of DNA was estimated by comparing their mobility through an agarose gel with that of fragments of known size present in a commercially available product (1 kbp DNA ladder - Gibco-BRL).

2.6 Transformation of bacterial cells

Bacterial cells which had been treated with $CaCl_2$ were transformed with DNA as described by Sambrook *et al* (1989).

2.7 Stock preservation

All bacterial cultures were preserved in 15% (v/v) glycerol and stored at -70°C.

2.8 DNA sequence analysis

DNA sequences were analysed using double stranded plasmid DNA (produced in DH5α *E.coli* cells) and the USB Sequenase version 2.0 DNA sequencing kit. The dideoxy chain termination method of Sanger *et al* (1977) was employed in the presence of α–[^{35}S] - dATP. A sequencing reaction was prepared as follows:

5 µl plasmid DNA (1 µg/µl)
1 µl primer (10 ng/µl)
1 µl 1M NaOH

These were mixed and incubated at 37°C for 10 min to allow the DNA to denature. 1 µl 1M HCl and 2 µl 5x Sequenase reaction buffer (200mM Tris.HCl pH 7.5, 100 mM $MgCl_2$, 250 mM NaCl) was then added and the primer allowed to anneal for 5 min at 37°C.

The polymerisation reaction was initiated by adding in order

1 µl 0.1 M DTT
2 µl labelling mixture (containing 1.5 mM dGTP, 1.5 mM dCTP, 1.5 mM dTTP) diluted five fold with distilled water
0.5 µl α -[^{35}S] - dATP (Bq)
2 µl Sequenase diluted eight fold with enzyme dilution buffer (10 mM Tris.HCl pH 7.5, 5 mM DTT, 0.5 mg/ml BSA.

After incubation at room temperature for 5 min, 3.5 µl of the reaction was transferred to each of 4 pre-warmed tubes containing 2.5 µl of one of the dideoxynucleotide mixtures (80 µM dNTP and 8 µM ddNTP). This was incubated at 37°C for 5 min before adding 4 µl of stop solution (95% formamide, 20 mM EDTA, 0.5% bromophenol blue and 0.05% Xylene Cyanol FF)

The sequencing reactions were analysed by electrophoresis on 6 - 8% acrylamide wedge gels containing 8 M urea.

2.9 Production of hybrid proteins from *E.coli*

2.9a Induction of expression from the *lac* promoter

A culture of bacteria harbouring a plasmid containing a gene under the control of the lac promoter (eg pKpra) was grown in selective medium at 37°C to an OD_{600} of 0.8. Expression was then induced by adding IPTG to a final concentration of 0.1 mM and the culture was grown for a further 3 h.

2.9b Fractionation of a bacterial culture by differential centrifugation

Cells were harvested by centrifugation for 10 min at 10000 rpm in a Beckman JA14 rotor. The cells were then washed by resuspension and centrifugation and then finally resuspended in one twentieth of the original culture volume of 100 mM Tris.HCl pH 7.4. Lysozyme was added to a final concentration of 1 mg/ml and a protease inhibitor mixture added (1 µg/ml each of aprotinin, leupeptin, pepstatin, antipain, 1 mM benzamidine, 1 mM PMSF) and the mixture left on ice for 20 min. The cells were then sonicated on ice (five bursts of 30 s with 2 min cooling intervals) and the

lysate clarified by centrifugation at 3000 rpm for 5 min in a Beckman JA20 rotor. The pellet P3 was retained and the supernatant centrifuged again in the same rotor at 20000rpm for 20 min to yield the soluble S20 and the insoluble P20 fractions. The P3 and P20 fractions were then resuspended in one twentieth of the original culture volume of 100 mM Tris.HCl pH 7.4 to facilitate comparison of protein composition of each fraction. The fractions were then analysed by SDS-PAGE.

2.9c Use of IgG-Sepharose in the purification of protein A fusion proteins

A 10 ml soluble fraction from a 1 l bacterial culture containing a protein A fusion protein (chapter 3) was prepared in TST buffer (50 mM Tris.HCl pH 7.4, 150 mM NaCl, 0.05% Tween - 20) and was incubated overnight at 4°C on a Denley Spiramix with 2 ml IgG-Sepharose which had been previously equilibrated by resuspension in TST buffer followed by brief centrifugation and removal of the used buffer. After overnight incubation, the Sepharose was pelleted by centrifugation at 1000 rpm for 30 s in a MSE bench-top centrifuge and the soluble extract removed. The IgG-Sepharose was washed twelve times in 20 ml TST buffer and five times in 20 ml ammonium acetate pH 5.0. The Sepharose was then resuspended in 4 ml 0.2 M glycine.HCl pH 2.8. The bound material was eluted by gentle mixing at 4°C for 20 min. The eluate was removed by pelleting the Sepharose as previously described and removing the buffer. A second elution was performed for a further 10 min and the two eluates pooled. The eluates were neutralised immediately by addition of an equal volume of 0.2 M Tris,HCl pH 8.0. The IgG-Sepharose was then reequilibrated by washing with TST until the pH reached 7.4 and was then stored in 20% ethanol in TST at 4°C.

2.9d Use of Ni-NTA agarose in the purification of oligohistidine fusion proteins

A 10 ml soluble fraction from a 1 l bacterial culture containing a oligohistidine fusion protein (Chapter 3) was prepared in phosphate buffer A (50 mM NaH_2PO_4 pH 8.0, 300 mM NaCl) and incubated overnight at 4°C on a rotating mixer with 1 ml Ni-agarose which had been equilibrated with the same buffer. The soluble fraction was removed after centrifugation at 1000 rpm for 1 min in a MSE benchtop centrifuge and the agarose washed in 10 ml buffer A by resuspension and centrifugation until the used buffer had an A_{280} of 0.01. The washing was then repeated with buffer B (50 mM NaH_2PO_4 pH 6.0, 300 mM NaCl, 10% (v/v) glycerol). The Ni-agarose was then washed in buffer B containing 50 mM imidazole until the A_{280} was 0.01 and final elution of bound material was achieved by resuspending in 3 ml buffer B containing 250 mM imidazole and mixing gently for 10 min at 4°C. This elution was repeated twice more and the eluates pooled. The Ni-agarose was reequilibrated in buffer A with 0.1% (w/v) NaN_3 and stored at 4°C

2.10 Electrophoretic separation and detection of proteins

Electrophoretic separation of proteins was performed using SDS polyacrylamide gels following the basic procedures described by Laemmli (1970) using the solutions detailed below.

Separating gel buffer 1.5 M Tris.HCl pH 8.8, 0.4% SDS

Stacking gel buffer 0.5 M Tris.HCl pH 6.5, 0.4% SDS

Acrylamide stock solution 30% (w/v) acrylamide, 0.8% (w/v) N,N'

methylene bisacrylamide

Electrophoresis buffer 0.125 M Tris, 0.2 M glycine, 0.1% (w/v) SDS (gives pH 8.3 without adjustment)

SDS sample buffer 50 mM Tris.HCl pH 6.5, 5% (w/v) SDS, 10% (v/v) glycerol, 10 mM DTT, 50 μg/ml bromophenol blue

Routinely, separating gels of 10% (w/v), 12% (w/v) or 13% (w/v) acrylamide with a 5% (w/v) stacking gel were used to achieve separation of proteins.

2.10a Coomassie Blue R staining

Following electrophoretic separation, protein bands were visualised by staining with Coomassie Blue: the gel was covered with a solution of 0.25% (w/v) Coomassie Brilliant Blue R dissolved in 50% (v/v) methanol, 7% (v/v) acetic acid for 10 - 15 minutes. The stain was then poured off and destaining of the gel was achieved by gently agitating the gel in 10% (v/v) methanol, 7% (v/v) acetic acid.

2.10b Silver staining

Silver staining was carried out as outlined in Wray (1981). Gels were soaked in 50% (v/v) methanol overnight. The stain solution was made fresh as follows: 0.8 g of $AgNO_3$ was dissolved in 4 ml distilled water (solution 1); 21 ml of 0.36% NaOH was added to 1.4 ml of 14.8 M NH_3 (solution 2). Solution 1 was added dropwise to solution 2 with constant stirring and the final volume was made up to 100 ml with distilled water.

The gel was soaked in the stain solution for 15 min with gentle agitation.

The stain was then poured off and the gel washed in distilled water for a minimum of 5 min after which the gel was covered with freshly-made developer solution (0.005% (w/v) citric acid, 0.019% (v/v) formaldehyde). When bands had appeared on the gel, the development was stopped by washing the gel with distilled water and then placing it in 50% (v/v) methanol, 10% (v/v) acetic acid.

2.11 Transfer of proteins onto nitrocellulose

2.11a Semi-dry blotting

Proteins were transferred from gels, after electrophoresis, onto nitrocellulose filter by a semi-dry blotting procedure using an LKB semi-dry blotting apparatus and the following buffers:

Anode buffer 1	0.3 M Tris, 20% (v/v) methanol, 0.1% SDS (pH 10.4 without adjustment)
Anode buffer 2	25 mM Tris, 20% (v/v) methanol (pH 10.4 without adjustment)
Cathode buffer	25 mM Tris, 20% (v/v) methanol, 0.1% SDS, 40mM 6-amino-N-hexanoic acid (pH 9.4 without adjustment)

Six pieces of Whatman 3MM paper and one piece of nitrocellulose membrane were cut to the same size as the gel to be blotted. Two pieces of Whatman 3MM were soaked in anode buffer 1 and placed on the anode plate. Another piece of 3MM paper, soaked in anode buffer 2, was placed on top of this , followed by the nitrocellulose which had been soaked in water and the gel, soaked in cathode buffer. The remaining three pieces of 3MM were soaked in cathode buffer and layered on top of the gel. The

cathode plate was secured on top of the gel sandwich and a current of 0.8 mA/cm^2 gel area was applied for 1 h.

2.11b Wet blotting

Some proteins, especially those of high molecular weight do not transfer well in 1 h. For this, it was necessary to use a wet blotting procedure which allows transfer for long periods of time. The gel was placed next to a sheet of nitrocellulose which had been soaked in blotting buffer (20 mM Na_2HPO_4, 0.02% (w/v) SDS,20% (v/v) methanol) and sandwiched on either side by three sheets of 3MM and a pad of Scotchbrite sponge also soaked in blotting buffer. The assembly was then encased in a cassette and slotted into a tank so that it was completely submerged in blotting buffer and the nitrocellulose was closest to the anode. A current of 0.5 A was then applied for up to 12 h.

2.11c Ponceau S staining

The presence of proteins on nitrocellulose filters was detected using Ponceau S. The nitrocellulose was immersed in 0.2% (w/v) Ponceau S dissolved in 3% (w/v) TCA, 3% (w/v) 5-sulphosalicylic acid for 10-15 min. The stain was then poured away and destaining achieved by washing the nitrocellulose repeatedly with distilled water until bands appeared.

2.12 Immunoblot analysis

After transfer of proteins onto nitrocellulose membrane, the unfilled binding sites on the filter were filled by gentle agitation for 1 h in blocking buffer (5% (w/v) non-fat dried milk, 1% Tween-20 in TBS; 10 mM Tris.HCl pH 7.4, 150 mM NaCl). The filter was then exposed to primary antibody for 2 h with gentle agitation. Antibodies were diluted in TBS containing 5

mg/ml BSA, 5% new born calf serum and 0.5% Tween-20 as described in the text. Following exposure to primary antibody, the filter was washed five times for 5 min with washing buffer (0.5% (v/v) Tween-20 in TBS). If necessary, the filter was then exposed to a secondary antibody; an anti-mouse IgM-HRP (μ chain specific) conjugate was used at a dilution of 1:4000 in wash buffer for 1 h when the monoclonal antibody cgm67 was used as a primary antibody, anti-rabbit IgG-HRP was used in the same way when polyclonal antibodies were used as the primary antibody. The filter was then washed as before and developed using enhanced chemiluminescence (ECL) with ECL reagent in accordance with the manufacturer's instructions or by immersing in a developer solution containing 12.5 mM luminol, 4.5 mM *p*-coumaric acid, 0.15% H_2O_2 in 0.1 M Tris.HCl pH 8.5.

2.13 Production of polyclonal antibodies from rabbits

2.13a Immunisation and serum collection

For immunisation with the protein A fusion protein, 100 μg of the protein (in a 250 μl volume) was emulsified with an equal volume of Freund's complete adjuvant. This was then administered to New Zealand White rabbits by subcutaneous injection. Twelve weeks after the initial injection, a booster of the same amount of the protein was administered in Freund's incomplete adjuvant. A second boost was given in this way, six weeks after the first and 5 ml of blood was collected from the animal ten days later. The blood was allowed to stand at room temperature for 1 h and then at 4°C for 24 h. The serum was then separated from clotted material by centrifugation for 10 min at 10000 rpm in a Beckman JA-20 rotor and finally filtered through a 0.22 μm Millipore membrane. The serum was

tested for the desired antibodies by checking for recognition of the oligohistidine fusion protein and for recognition of the protein in chromaffin granule membranes. The animal was then sacrificed (not more than fourteen days after the last boost) and serum prepared from the blood. The serum was stored in 1 ml aliquots at -20°C with 0.1% (w/v) sodium azide.

2.13b Affinity purification of antibodies using purified protein.

Purified SytC protein (200 μg) was subjected to electrophoretic separation on an acrylamide gel with a single well across the top. This was then transferred to nitrocellulose and stained briefly with Ponceau-S. The large band of protein was cut out and the antigen bearing face of the strip was marked. The membrane was then washed in TBS to remove the Ponceau-S and incubated in blocking buffer (previously described) for 90 min. The strip was then placed on a piece of parafilm and the rabbit serum applied so that as much serum is used as will stay on the strip by surface tension. The serum was then left for 2 h before removing and washing the nitrocellulose three times for 5 min in TBS. Antibodies bound to the antigen strip were then recovered by applying 0.2 M glycine pH 2.8 in the same way as the serum. After 20 min, the glycine was removed and neutralised by adding an equal volume of 0.2 M Tris.HCl pH 8.5. The affinity purified antibody was was stored at 4°C with the addition of 0.5% (w/v) NaN_3 and was used for immunoblot analysis at a dilution of 1:100.

2.14 Hybridoma culture - production of monoclonal antibody

In order to use the monoclonal antibody to synaptotagmin (cgm67), it was necessary to culture secreting hybridoma cells from a frozen stock culture. The medium used for hybridoma culture was made as follows:

RPM I - 1640 (with 25 mM Hepes.NaOH pH 7.2)	500 ml
Foetal calf serum	100 ml
50x HT supplement (hypoxathine,thymidine)	10 ml
50 mM mercaptoethanol 0.5 ml	
100x glutamine	5 ml
Penicillin/streptomycin (5 mg/ml)	10 ml
Amphotericin B (1.25 mg/ml)	1 ml

Cells were cultured at 37°C in a sterile incubator containing 5% (v/v) CO_2, 100% humidity.

A 0.5 ml aliquot of frozen hybridoma culture (preserved in liquid N_2) was thawed and added to 5 ml medium (pre-warmed to 37°C) and left to grow for several days at 37°C. When the cells were growing strongly, most of the medium was poured off and kept. The cells were shaken off the flask in 2 ml of the used medium and transferred to a larger flask containing 30 ml of fresh medium and incubated again for two to three days. The cells were allowed to establish exponential growth and then divided into two flasks containing 30 ml fresh medium, grown and again moved to larger flasks containing 150 ml fresh medium. Each time the cells had grown, the used medium was kept, filtered through a 0.45 μm filter, neutralised with a few drops of 2 M Tris and stored at 4°C with 0.1% (w/v) NaN_3 added. The medium was tested for cgm67 activity by using it as a primary antibody (at a 1:5 dilution) with a western blot of chromaffin granule membranes and purified cytoplasmic domain of synaptotagmin.

2.15 Protein purification

2.15a Gel exclusion chromatography

Gel exclusion chromatography was carried out as the second step in the purification of the cytoplasmic domain of synaptotagmin after the initial step involving affinity chromatography with IgG-Sepharose.

Biogel P100 (exclusion limit 100,000 Da) was equilibrated in distilled water at room temperature for 24 h and was then resuspended in fresh water and allowed to settle several times to allow aspiration of the fine particulate material which may otherwise distort the flow in the column. The 50% water/gel mixture was degassed under vacuum for 15 min. The Biogel slurry was then used to pack a 40 ml column (1 m in length and 0.75 cm diameter) as follows: the column was clamped in an upright position and a few ml of distilled water poured into the column; with the bottom tap closed, a few ml of slurry was gently poured in and when the gel could be seen settling to a few centimetres depth, the column was filled completely with the gel; once the gel had settled again, the bottom outlet was opened and the water allowed to drain a little whilst topping up the gel to the desired level.

The packed column was kept and used at 4°C. Before use, the column was equilibrated in the buffer to be used (normally 50 mM Tris.HCl pH 7.6, 100 mM NaCl supplemented with either 1 mM $CaCl_2$ or 1 mM EGTA) and run with a hydrostatic pressure giving a flow rate of 2.5 ml/h. The protein was applied to the column in a volume not more than 0.5 ml by removing excess buffer and gently layering on top of the gel. When the protein solution had run into the gel, buffer was applied again and the column

allowed to run for 20 h. The flow-through was collected in 0.5 ml fractions. Protein content in the fractions was estimated by reading the A_{280} and the protein composition of the fractions was analysed by gel electrophoresis.

2.15b Concentration of protein sample

Freeze drying

Freeze drying was used for large volumes of protein. The protein solution was placed in a round bottom Quickfit flask and rapidly frozen by swirling in a -40°C bath. The flask was then attached with a 24/29 Quickfit adaptor to a Edwards Modulyo freeze-dryer and dried at -70°C, 10^{-2} atmospheres for 6-8 h. Once the protein had been freeze-dried, it was resuspended in distilled water or 20 mM Tris.HCl pH 7.4 depending on the buffer and salt content of the dialysed protein solution.

Spin columns

Amicon spin columns with cutoff 12,000 Da were used for concentration of smaller volumes following the manufacturer's instructions

Precipitation with ammonium sulphate

Precipitation was achieved by adding 0.516 mg/ml $(NH_4)_2SO_4$ gradually to the protein solution on ice, stirring constantly, whilst measuring and maintaining the pH of the solution throughout by titration with HCl. When all the salt had been added, the solution was stirred on ice for a further 15 min to allow complete equilibration and then centrifuged at 20000 rpm for 20 min in a Beckman JA20 rotor. The resultant pellet was resuspended in a small volume (less than 0.5 ml) of 20mM Tris.HCl pH 7.4.

2.15c Desalting

Two techniques were employed to desalt protein solutions. Dialysis tubing with a 12,000 Da cutoff (previously boiled in distilled water/EDTA for 1 h and stored in 50% (v/v) ethanol at 4°C) was clipped at one end, filled with protein solution, sealed and submerged in 2 l of buffer or water depending on the final solvent required for the protein solution. This was then placed at 4°C and and stirred for at least 2 h. The external buffer was replaced a further three times. The protein solution was then removed from the membrane and freeze-dried as previously described.

Desalting was also achieved by using Biogel P6DG. A column was prepared on a small scale using an Eppendorf tube. A hole was pierced in the top and bottom of the tube and a small amount of glass wool pushed into the bottom. Biogel P6DG, equilibrated in distilled water, was pipetted into the tube and allowed to settle to three quarters of the way up the tube. Several ml of the final required buffer was allowed to drip through the mini column which was suspended in a conical glass tube and the residual buffer removed by centrifugation at 1500 rpm for 1 min in a MSE bench-top centrifuge. The column was then transferred to a fresh glass tube and the protein solution applied (200-400 µl per column containing 1 ml Biogel) and allowed to soak into the gel for 2 min. The protein solution was then recovered by centrifugation as before.

2.16 Estimation of protein concentration

Protein was routinely detected using the value for absorbance at 280 nm. The concentration of protein used in *in vitro* interaction studies was measured using a combination of spectrophotometric and densitometric techniques. The spectrophotometric method used was Peterson's

simplification of the method by Lowry *et al* (1951) and is outlined below.

Stock solutions

Copper tartrate carbonate (CTC) was made by adding 45 ml solution A (20% (w/v) sodium carbonate) dropwise to 45 ml solution B (0.4% (w/v) potassium sodium tartrate, 0.2% (w/v) copper sulphate pentahydrate) and the final volume made up to 100 ml with distilled water. BSA (1mg/ml), 10% (w/v) sodium deoxycholate and Folin-Ciocalteau reagent (available commercially) were also kept as stock solutions. Working solutions were made from stocks as follows:

reagent A	equal volumes of CTC, NaOH, SDS and distilled water
reagent B	one volume of Folin Ciocalteau with five volumes of distilled water

Precipitation of protein

The protein sample to be measured (containing between 10 and 60 µg protein) was brought to a volume of 400 µl with distilled water. 40 µl of 0.15% deoxycholate was added and the protein allowed to stand at room temperature for 10 min and a further 40 µl of 72% (w/v) TCA was then added and again incubated at room temperature for 5 min. The sample was then centrifuged at 6000 rpm for 10 min in a MSE MicroCentaur, the supernatant discarded and the pellet used for the next step.

2.16c Spectrophotometry

Distilled water (400 µl) was added to the TCA pellet along with 400 µl of reagent A was then added and left for 10 min at room temperature. Reagent B (200 µl) was added and the absorbance at 700 nm was read

after 30 min. In order to calibrate the spectrophotometric response of the assay, duplicates containing 0 μg, 10 μg, 25 μg, 40 μg, 60 μg BSA were used and treated similarly.

This protein assay was often supplemented by running and staining a SDS PAGE gel of the protein sample along with known quantities of BSA and then scanning the resultant protein bands using a Joyce-Loebl densitometer following manufacturer's instructions. The intensities for the bands of BSA were then used to create a calibration curve for stain intensity which could be used to quantify the unknown protein.

For more accurate protein measurement, freeze-dried samples of the protein were subjected to acid hydrolysis and total amino acid analysis at the facility at Department of Molecular and Cell Biology, Marischal College, The University of Aberdeen.

2.17 Preparation of chromaffin granule membranes

Chromaffin granule membranes were prepared using bovine adrenal tissue by first dissecting the medulla from the cortex of twenty whole glands. This was placed in 0.3 M sucrose, 10 mM Hepes.NaOH, 2 mM EDTA pH 7.0 at 4°C, passed through a steel mincer and then homogenised with a loose fitting pestle at speed 5-6 in an automatic homogeniser. The homogenate was diluted to 750 ml with the same buffered sucrose and centrifuged at 4,000 rpm for 5 min in a Beckman JA14 rotor. The pellet was discarded and the supernatant centrifuged at 14000 rpm for 30 min in the same rotor. The resultant supernatant was discarded and the upper mitochondrial pellet washed away with buffered sucrose. The lower pink pellet was then resuspended by gentle homogenisation and centrifuged for

20 min at 15000 rpm in a Beckman JA20 rotor. The supernatant was discarded, the upper mitochondria removed again and the lower pellet resuspended in 50 - 80 ml of buffered sucrose.

To purify the granules further, 20 ml portions of the resuspended pellet were overlaid on 50 ml of 1.6 M sucrose, 10 mM Hepes.NaOH pH 7.0 and centrifuged at 45000 rpm for 60 min in a Beckman Ti45 rotor. The pellet of purified granules was resuspended by gentle homogenisation in 0.3 M sucrose, 10 mM Hepes.NaOH pH 7.0 and stored in 2 ml aliquots at -20°C.

2.18 Fractionation of membrane proteins with Triton X-114

Triton X-114, pre-condensed by the method of Bordier (1981), was made up as a 10% (w/v) solution for this procedure. Its concentration was assayed by the method of Garewal (1973). Chromaffin granule membranes were resuspended in TBS with 2% (w/v) cold Triton X-114 at 0°C to a protein concentration of 4 mg/ml and incubated on ice for a further 5 min. The solubilised membranes were then centrifuged at 100000 rpm for 15 min at 2°C in a Beckman TL-100.3 rotor to remove the precipitate formed by insoluble proteins. The pellet (P1) was washed twice at 0°C by resuspension to the original volume in TBS, 2% (w/v) Triton X-114 and stored in one fifth the original volume TBS.

The supernatant was layered over 1 ml cushions of 0.25 M sucrose containing TBS and 0.06% (w/v) Triton X-114 in conical glass tubes and incubated at 30°C for 5 min to separate the detergent and aqueous phases. These were then centrifuged at 4000 rpm for 5 min in a MSE bench-top centrifuge. The aqueous phase was removed from above the sucrose cushion, the sucrose cushion discarded and the detergent-rich phase taken

up in ice cold TBS to its original volume. This process was repeated twice more with the individual phases. The detergent phase was then stored in one fifth the original volume of TBS.

Residual detergent was removed from the aqueous phase by dialysis against TBS containing 1% (w/v) Amberlite XAD-2, 0.2 mM PMSF, 1mM benzamidine at 4 °C for five days. The dialysed fraction was then diluted with three volumes of TBS and centrifuged at 100000 rpm in a Beckman TL100.3 rotor for 15 min at 2°C. The pellet, which is rich in glycoproteins, was resuspended in one fifth the original volume 10 mM Hepes.NaOH pH 7.2 with 0.1% (w/v) Triton X-114. All fractions were stored at -70°C.

2.19 Preparation of synaptosomes

Synaptosomes were prepared following the method of Krueger *et al* (1979). Whole brains were dissected from rats and placed in 50 mM NaCl at 4°C. The brains were then weighed and made to 10% (w/v) with 25 mM Hepes.KOH pH 7.0, 0.32 M sucrose. The brain tissue was homogenised and then centrifuged at 6000 rpm for 10 min in a Beckman JA20 rotor. The supernatant was layered onto equal volumes of 1.2 M sucrose (buffered as before) and centrifuged at 31000 rpm for 15 min in a Beckman SW41 rotor. The interface material from this step was collected in as small a volume as possible, diluted with two volumes of buffered 0.32 M sucrose and layered onto equal volumes of buffered 0.8 M sucrose. These were then centrifuged at 31000 rpm for 15 min in a Beckman SW41 rotor. The synaptosomal pellet was finally resuspended by gentle homogenisation in 25 mM Hepes.KOH pH 7.0 containing 125 mM potassium acetate, 25 mM magnesium acetate, 1 mg/ml glucose and 0.1 mM EGTA.

2.20 Preparation of phospholipid vesicles

To prepare phospholipid vesicles of volume V ml, 2V/3 ml of settled Calbiosorb resin was equilibrated in the buffer required (usually 25 mM Hepes.NaOH pH 7.4 for this study). Phospholipid solutions of 20 mg/ml in 2:1 (v/v) chloroform / methanol were measured to the correct concentration and percentage weight composition for each lipid in the final vesicle preparation. The lipids were then dried under a gentle stream of nitrogen gas and redispersed in the buffer used containing 2% (w/v) octylglucoside by constant stirring for approximately 15 min.

The equilibration buffer was removed from the Calbiosorb and the dispersed lipids added. After 5 min at 4°C, the solution became turbid due to vesicle formation and the whole mixture was pipetted into an Eppendorf tube which had been pierced at the top and bottom and plugged with glass wool. The Eppendorf tube was placed in a conical glass tube and centrifuged for 30 s at 1000 rpm in a MSE bench-top centrifuge.

2.21 Phospholipid vesicle binding assay

Phospholipid vesicles were prepared at a concentration of 10 mg/ml total lipid content. The vesicles always contained 20% (w/v) cholesterol and either 80% (w/v) of a single phospholipid or 40% (w/v) each of two phospholipids (all possible combinations of PS, PI, PC and PE were used)

The purified recombinant cytoplasmic domain of synaptotagmin (15 μg) was mixed with 400 μg of phospholipid vesicles in a 100 μl volume of 50 mM Hepes.NaOH pH 7.2 , 100 mM NaCl supplemented with either 2 mM EGTA or 100 μM Ca^{2+} . This was incubated at room temperature for 15 min and centrifuged at 100,000 rpm for 30 min in a Beckman TL -100.2

rotor. The pellets were resuspended directly in 50 µl of SDS-PAGE sample buffer. The protein in the supernatants was precipitated by adding 10 µl of 0.15% (w/v) sodium deoxycholate and 10 µl of 72% (w/v) TCA and incubating overnight at 4°C. The precipitates were centrifuged for 10 min at 13000 rpm in a MSE MicroCentaur and resuspended in 50 µl of SDS-PAGE sample buffer.

The protein compositions of the lipid and aqueous fractions were analysed by gel electrophoresis followed by Western blotting using the synaptotagmin-specific antibody cgm67.

2.22 Binding to immobilised calmodulin

Recombinant synaptotagmin was dialysed extensively (3 changes of 1000-volumes 10 mM Hepes.NaOH pH 7.2) to remove salts and Ca^{2+}. This was then lyophilised and resuspended in one twentieth of the original volume 10 mM Hepes.NaOH pH 7.2) and then treated with Chelex resin, equilibrated in the same buffer, following manufacturer's instructions, to remove any further Ca^{2+}. The protein was clarified by centrifugation for 10 min at 13000 rpm in a MSE MicroCentaur. 20 µl packed volume of calmodulin-agarose was washed 3 times by pelleting (600 rpm in MSE MicroCentaur for 30 sec) and resuspension in Eppendorf tubes. After the final wash the calmodulin-agarose was mixed with 800 µl protein samples of 0.4 mg/ml. The following experimental conditions were used:

100 µM Ca^{2+};
100 µM Ca^{2+} and 5 mM EGTA.NaOH pH 7.2;
100 µM Ca^{2+} and anti-synaptotagmin antibody (protein preincubated with antibody for 30 min at room temperature prior to mixing with calmodulin).

Bovine synaptotagmin from the glycoprotein-rich fraction of CGM fractionation with TX-114 was used as a positive control. The samples were incubated by rotating for 30 min at room temperature and the reaction terminated by pelleting the calmodulin-agarose as previously. The supernatants were removed and the pellets were washed four times with 1 ml of 10 mM Hepes.NaOH pH 7.2. Elution of bound material was carried out by resuspending in 500 µl of the buffer with 10 mM EGTA.NaOH pH 7.2 and incubating for 10 min at room temperature. The eluates were collected after centrifugation, lyophilised, resuspended in sample buffer and analysed by SDS-PAGE and Western blotting.

2.23 Fluorimetry

2.23a Titrations with terbium ions

Protein solution, ranging in concentration from 10 µg/ml - 200 µg/ml in 20 mM Hepes.NaOH pH 7.5 was placed in a Perkin-Elmer 3000 with excitation wavelength set to 290 nm and emission wavelength at 585 nm. Additions of 2 µl of 1 mM or 10 mM $TbCl_2$ were made to the protein solution so that final Tb^{3+} concentrations ranged from 4 µM to 1 mM and fluorescence emissions were recorded after each addition by integration of the signal over 5 s periods. Where required, the buffer was supplemented with 2 mM $CaCl_2$ or 2 mM EGTA.NaOH pH 7.5 . The experiment was performed using the purified cytoplasmic domain of synaptotagmin. Lysozyme was used as a negative control and calmodulin as a positive control.

2.23b Titrations with calmodulin

Production of dansyl calmodulin

Dansyl calmodulin was produced according to the method of Vorherr *et al* (1990). Calmodulin (obtained from Sigma) was dissolved at a concentration of 1.2 mg/ml in 20 mM NH_4HCO_3 pH 7.5. The concentration, assessed by its absorbance at 276 nm, was 51 μM. $CaCl_2$ was added to a final concentration of 1 mM. A 3 mg/ml stock solution of dansylchloride was made in acetone and enough was added to the calmodulin to give 74 μM dansylchloride. The reaction mixture was incubated at room temperature for 2 h and vortexed every 20 min. At the end of the reaction time the mixture was centrifuged at 100,000 rpm for 15 min in a Beckman TL-100.2 rotor to remove solids. Residual dansylchloride was removed from the supernatant by passing it through a 4 ml column containing Biogel P6DG equilibrated in the reaction buffer. Fractions of 0.5 ml were collected and assessed for calmodulin content by measuring A_{280}. The A_{320} was used to calculate the dansyl content of the fractions from the molar extinction coefficient for the dansyl moiety which is 3400 M^{-1} cm^{-1}. A molar ratio of 1:1 for calmodulin:dansyl was obtained.

Fluorescence spectra and titrations

All dilutions were carried out in 50 mM Hepes.NaOH pH 7.2, 100 mM NaCl. Dansyl calmodulin was diluted to 150 nM and the emission spectrum of the solution was recorded from 400 - 550 nm with the excitation wavelength adjusted to 340 nm. The spectrum was also measured with the addition of 100 μM EGTA.NaOH pH 7.2 or 100 μM $CaCl_2$ and by including SytC in various molar ratios. Titrations of Ca^{2+}, Ba^{2+} and Mg^{2+} were carried out with solutions of Dansyl calmodulin alone

(concentration as above) and with a mixture of dansyl calmodulin and SytC in a 1:1 molar ratio. In this case, 1 mM NTA.NaOH pH 7.2 was included so that free Ca^{2+} concentrations of 1-200 μM were obtained.

2.24 N-terminal peptide sequencing

N-terminal sequencing of the recombinant cytoplasmic domain of synaptotagmin was carried out by separation of SDS-PAGE followed by electroblotting onto PVDF membrane as described by Matsudaira (1987) with the particular modifications suggested by Dunbar and Wilson (1993). After the electroblotted protein had been stained and destained, the band of interest was excised and taken to the Welmet protein facility at the University of Edinburgh for automated peptide sequencing.

2.25 Circular dichroism

Measurements of UV and far UV circular dichroism spectra were carried out in a JASCO J-600 spectropolarimeter using purified synaptotagmin at a concentration of 0.5 mg/ml in 10 mM Tris.H_2SO_4 pH 7.4, 1mM NTA.NaOH pH 7.4. Additions of $CaCl_2$ were made to this solution so that free Ca^{2+} concentrations ranged from 1 - 200 μM and successive spectra were measured and then compared to see whether Ca^{2+} had any effect of the peptide secondary structure. This was also performed with $TbCl_3$ to give Tb^{3+} concentrations of up to 90 μM. Similar Ca^{2+} titrations were also carried out in the presence of equimolar concentrations of calmodulin and in the presence of 100 μg/ml phospholipid vesicles.

2.26 Molecular dynamics

Molecular dynamics or light scattering properties of the purified cytoplasmic domain of the protein were carried out using a DynaPro-801

light scattering spectrometer following manufacturer's instructions. The protein was used at a concentration of 0.5 mg/ml or 1 mg/ml in 20 mM Tris.HCl pH 7.2, 100 mM NaCl, 1mM NTA.NaOH pH 7.2. Additions of $CaCl_2$ were made to the protein solution so that free Ca^{2+} concentrations of 1, 5, 10, 20, 30, 50, 100 and 200 μM were obtained. After each addition a 200 μl sample of the protein was injected into the machine through a 0.02 μm nylon filter and the molecular dynamics parameters were measured. The machine was flushed with distilled water after each measurement to prevent residue build-up which distorted the measurement. A similar titration with $CaCl_2$ was also performed using a solution containing equimolar concentrations of synaptotagmin and calmodulin.

2.27 Digestion with trypsin

Analytical digestion of purified synaptotagmin with trypsin was performed in 200 μl reaction volumes in 50 mM Hepes.NaOH pH 7.2, 100 mM NaCl containing 0.2 mg/ml of the protein and 100 μg/ml of phospholipid vesicles (40% (w/v) each of PS and PC, 20% (w/v) cholesterol) and either 100 μM $CaCl_2$ or 1 mM EGTA. NaOH pH 7.2. Trypsin was added in the concentrations 0, 6.25, 12.5, 25, 50 and 100 μg/ml and the reactions incubated at 37°C for 45 min. The reaction was terminated by adding hot SDS-PAGE sample buffer and heating the samples further at 95°C for 10 min. The digestion was analysed by electrophoretic separation and Western blotting.

2.28 Digestion with thrombin

2.28a Digestion in solution

The soluble fraction prepared from a bacterial culture expressing protein

A-SytC fusion protein was digested using purified thrombin obtained commercially. Thrombin was added to the protein, prepared in 50 mM Tris.HCl pH 7.8, 150 mM NaCl, 2.5 mM $CaCl_2$, in an enzyme:substrate protein ratio of 1:500 (w/w) and then incubated at 37°C for 1 h. The reaction was stopped by adding SDS-PAGE sample buffer and the digest analysed by gel electrophoresis.

2.28b Digestion of immobilised protein

Thrombin was also used to digest the fusion protein after it had been bound to IgG-Sepharose and the Sepharose washed with TST and ammonium acetate pH 5.0. The Sepharose (2 ml) was then washed 3 times in 20 ml of 50 mM Tris.HCl pH 7.8, 150 mM NaCl, 2.5 mM $CaCl_2$ and finally resuspended in 2 ml of the same buffer. Two units of thrombin (corresponding to a thrombin:recombinant protein weight ratio of 1:40000) were then added and the Sepharose incubated at 37°C for 9-13 h. The buffer was removed from the top of the Sepharose and retained. Two further washes of 2 ml wash buffer (50 mM Tris.HCl pH 7.8, 400 mM NaCl, 4 mM EGTA, 10% (w/v) glycerol) were collected and retained and the IgG-Sepharose was then treated with acetic acid pH 3.4 and reequilibrated as previously described. Samples of 30 µl of the thrombin digest buffer and subsequent wash buffers were taken, 10 µl SDS-PAGE sample buffer added and the protein content analysed by gel electrophoresis. All the washes and the Sepharose were treated with 0.1 mM PMSF after the digestion to ensure the thrombin activity was inhibited.

2.29 Blue native gels

Blue native gel electrophoresis was performed using the method of

Schagger & von Jagow (1994). Solutions used for blue native electrophoresis are outlined below.

First dimension

Cathode buffer	50 mM tricine 15 mM bis Tris 0.02% (w/v) Serva Blue G
Anode buffer	50 mM bis Tris.HCl pH 7.0
3x gel buffer	150 mM bis tris.HClpH7.0 1.5 M aminocaproic acid
Acrylamide	48% (w/v) acrylamide 1.5% (w/v) bisacrylamide
2x Sample buffer	1.5 M aminocaproic acid 0.1 M bis Tris.HCl pH 7.0
Blue dye	5% (w/v) Serva Blue G 0.5 M aminocaproic acid
Detergent	10% (w/v) dodecylmaltoside.

Second dimension

10x cathode buffer	1 M tris 1 M tricine 1% (w/v) SDS

10x anode buffer	1 M Tris.HCl pH 8.9
3x gel buffer	3 M Tris.HCl pH 8.45 0.3% (w/v) SDS
Stain solution	0.025% (w/v) Serva Blue G 10% (v/v) acetic acid
Destain	10% (v/v) acetic acid

Gel mixtures were made up as outlined in tables 1 and 2.
Standard Hoefer Tall-Mighty-Small units were used for first dimension gels. The first dimension gel was prepared with 1.5 mm spacers using a peristaltic pump to create an exponential acrylamide gradient from 12% at the bottom of the gel to 4.8% at the top of the separating gel with a 4% stacking gel on the top.

Samples of chromaffin granule membranes were prepared by centrifuging membranes containing 600 µg total protein at 100,000 rpm in a Beckman TL100.2 rotor for 10 min. The pellet was resuspended in 80 µl of distilled water and 80 µl of 2x sample buffer added.

30 µl 10% (w/v) dodecylmaltoside was then added and the sample centrifuged again as before. The supernatant was removed and 15 µl 5% (w/v) Serva Blue G added. 80µl of this prepared sample was loaded per lane of the gel.

Bovine heart mitochondria were prepared as standard markers for the first

dimension gel. Mitochondria containing 800 µg protein were diluted with 60 µl water, 80 µl 2x sample buffer and 40 µl of the same detergent was added. Finally, 20 µl of blue dye was added and 60 µl of this sample was loaded.

Table 2.1 **Blue native gel first dimension solutions**

	volume of solution (ml)		
	Stack 4%	Top 4.8%	Bottom 12%
Acrylamide	0.5	0.6	1.5
3X gel buffer	2.0	2.0	2.0
Glycerol	-	-	1.2 g
Water	3.45	3.35	1.48
TEMED	0.005	0.003	0.002
10% (w/v) ammonium persulphate	0.05	0.03	0.02

Table 2.2 Blue native gel second dimension solutions

	volume of solution (ml)				
	stack	overlay	separating		
			10%	12%	16%
Acrylamide	3.0	3.0	6.0	7.5	10.0
3x gel buffer 1D	-	5.0			
2D	5.0	-	10.0	10.0	10.0
Glycerol	1.5g	1.5g	3.0g	3.0g	3.0g
Water	5.75	5.75	11.5	10.0	7.5
TEMED	0.009	0.015	0.015	0.015	0.015
10%(w/v) ammonium persulphate	0.09	0.15	0.15	0.15	0.15

The gel was subjected to electrophoresis at 100 V constant voltage for 1 h, 200 V for a further 2 h and then 300 V until the dye had reached the bottom. If the first dimension was to be electroblotted to nitrocellulose, the cathode buffer was replaced after 1 h with cathode buffer containing 0.002% (w/v) Serva Blue G. First dimension Western blotting was carried out as the standard protocol with the addition of a destaining step for the nitrocellulose with several changes of 50% (v/v) methanol immediately after transfer and prior to blocking.

For the second dimension, individual gel strips corresponding to single lanes of 1D gel were soaked twice for half an hour in 200 µl of 1% (w/v) SDS, 0.1 M DTT. The strips were then placed near the top of a notched 15 cm x 15 cm glass plate; 3 mm spacers and a straight glass plate were then placed on the top. Holding the assembly together with bulldog clips, the plates were carefully sealed on all straight sides using 1.5% (w/v) agar. The separating gel was poured into the cassette to 1 cm below the gel strip; the stacking gel was poured to 2 mm below the gel strip and overlay gel was used to fill the remainder of the space including a few millimetres above the gel strip. The gel was then run at 50 mV constant voltage for 1 h and then switched to 30 mA constant current for a further 8 h until the blue dye was just starting to come off the bottom. The gel was fixed in 10% (v/v) acetic acid, 50% (v/v) methanol for several hours and stained in 5% (v/v) acetic acid containing 0.025% (w/v) Serva Blue G for 2 h. Destaining was carried out with 5% (v/v) acetic acid over night. Second dimension gels for electroblotting were treated as normal SDS-PAGE gels.

Chapter 3

Production and purification of a synaptotagmin-ProteinA fusion protein and a synaptotagmin-His10 fusion protein

3.1 Introduction

Many proteins thought to be involved in exocytosis have been identified and the study of these proteins may help to elucidate the mechanisms involved in this biological process. Such investigations are often hampered by the relatively low abundance of these proteins which makes it difficult to accumulate enough protein for biochemical study. Molecular cloning technology circumvents this problem by allowing the cloning and bacterial expression of eukaryotic genes encoding secretory proteins in large amounts. In addition, it is possible to add DNA sequences to the gene of interest to create convenient 'tags' on the protein product for ease of identification, purification and experimental manipulation.

One such protein is synaptotagmin which, apart from being positioned in the secretory vesicle membrane of cells which exhibit regulated exocytosis, is further implicated as having a role in regulated secretion by the existence of two putative Ca^{2+} binding sites in its sequence. Most of the sequence of synaptotagmin is cytoplasmic. It is therefore assumed that any interaction with other vesicle, cytoplasmic and plasma membrane proteins must occur in this portion of the molecule (referred to as SytC).

For this project, a molecular cloning approach was adopted to study bovine synaptotagmin I. The DNA encoding the cytoplasmic domain of the protein (*sytc*) was cloned into two different vectors creating gene fusions with either DNA encoding a ten-histidine peptide or DNA encoding part of Protein A (*pra*). Both strategies gave a fusion protein which was easy to purify by affinity chromatography either with Ni-NTA agarose (affinity to histidine) or IgG-Sepharose (affinity to Protein A). Creating two fusions would then enable a comparative evaluation of gene expression efficiency,

ease of purification and final protein yield.

3.2 Construction of a gene encoding pra-tagged synaptotagmin

Nucleotide primers delineating the sequence encoding the cytoplasmic domain of synaptotagmin (approximately 1 kb) were designed and used in PCR to amplify the portion of the gene from a bovine adrenal library using *Taq* polymerase (see Appendix 2, table A2b). This polymerase adds adenosine extensions to the 3' ends of the amplified product. This was utilised in the initial cloning into a pGEM-T vector. The vector pGEM-5Zf(+) has been linearised with *Eco*RV and modified with T extensions at the 3' ends which will efficiently anneal to the 3' A extensions of the PCR product.

The pAX11 plasmid contains a sequence encoding a Pra-lacZ fusion protein of 26 kDa containing the N-terminal portion of Protein A (two and a half IgG-binding domains of approximately 16.9 kDa). The multiple cloning region of the plasmid is situated in between the *pra* and *lac*Z DNA so that insertion of *sytc* into it will form an in-frame fusion of *pra* and *sytc* and disrupt transcription of the *lac*Z giving blue/white selection of recombinant plasmids in an *E.coli* strain containing ZΔM15.

Once the *sytc* sequence had been cloned into the pGEM-T plasmid, it was excised using *Eco*RI and *Sal*I DNA restriction enzymes (the recognition sequences for these enzymes had been included in the primer sequences flanking the coding DNA) and ligated to pAX11 plasmid DNA which had been similarly digested. The resultant recombinant plasmid was labelled pLC100. The sequence of the gene junction and the *sytc* portion of the construct was verified experimentally and found to be as expected. The

gene junction is shown in figure 3.i below.

Figure 3.i DNA and protein sequence of the junction between *pra* and *sytc* in the fusion construct

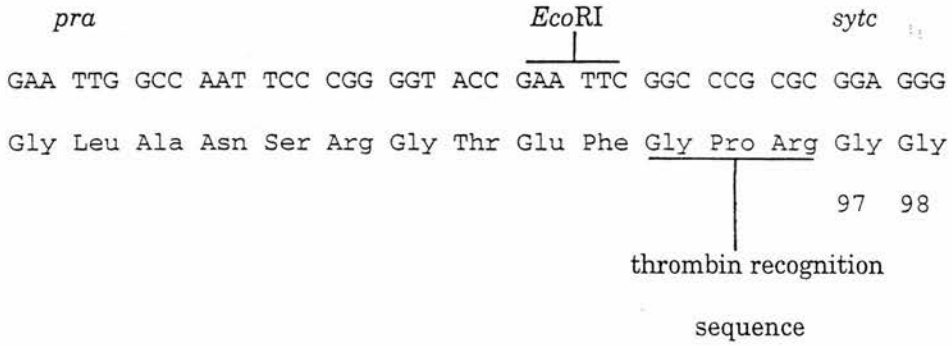

The full sequence of the Synaptotagmin I gene is shown in Appendix 3 giving the DNA sequence relevant to the cloning and the aminoacid residue numbers as shown on the previous diagram. It was then possible to express this construct in bacterial cells under *lac* promoter control producing a fusion protein, Protein A-SytC with Protein A (PrA) at the N-terminus. The primer encoding the N terminus of SytC was also designed to contain the DNA encoding the three-amino acid recognition site for the protease thrombin. Thrombin could therefore be used to cleave Protein A from SytC enabling purification of the cytoplasmic domain alone.

3.3 Induction of fusion gene expression

The cloned portion of the synaptotagmin gene had been placed under *lac* promoter control in the pAX11 plasmid. Expression of the chimaeric gene should therefore be induced by the addition of IPTG to a growing culture of transformed bacterial cells giving rise to the production of fusion protein. Conversely, addition of glucose to a culture should ensure that no protein

appears in the cells and is a useful way of controlling the onset of protein production. Figure 3.1 shows that IPTG induced the production of a protein which was recognised by the synaptotagmin-specific monoclonal antibody cgm67 and was of the size expected (approximately 50 kDa) for the expected fusion protein.

Levels of the fusion protein were found to increase over time reaching high levels after 3 h of growth after induction with IPTG (figure 3.2). This information was useful to set the initial growth conditions for a good yield of the recombinant protein.

3.4 Fractionation studies showing intracellular distribution of the fusion protein

Recombinant proteins produced in *E.coli* can often be made in such large quantities that they aggregate and form insoluble inclusion bodies. These can be isolated by differential centrifugation but the protein is not suitable for functional studies due to its assuming a misfolded or unfolded conformation which presumably causes the aggregation. Before purification of the protein can be attempted therefore, it is important to ascertain its location within the cell; if it is soluble, this will be an indication that the protein is in a correctly folded conformation and will be amenable to affinity chromatography. Figure 3.3 shows the P20, S20 and P3 fractions from a bacterial culture containing the recombinant plasmid after 3 h induction at 37°C. Since the P20 and P3 fractions have a much smaller volume than S20, the material from them was resuspended in the same total volume as S20 and equal volumes of each were analysed by SDS-PAGE. Analysing equivalent volumes in this way gives a true representation of the total amount of fusion protein present in each

fraction. The P20 fraction (inclusion bodies) and the P3 fraction (whole cells and nuclear debris) contain substantial amounts of the fusion protein but the soluble S20 fraction contains more. The culture conditions are therefore suitable for producing large amounts of soluble fusion protein for purification.

3.5 Digestion with thrombin

The fusion protein was designed with a cleavage site for the protease thrombin. Initially, the accessibility of this site was tested with the unpurified protein in the soluble S20 fraction. A time course of digestion (figure 3.4) showed the main protein band in the extract was one of the correct size for the Protein A-SytC fusion (57 kDa) and this disappeared over a period of digestion with thrombin and was accompanied by the appearance of a band of the correct position to be the SytC portion of the protein (36 kDA). The synaptotagmin-specific antibody recognises both the disappearing upper band and the appearing lower band (figure 3.5) confirming that the lower band is the SytC product.

A titration with successively smaller amounts of thrombin (figure 3.6) showed that a ratio of thrombin to total protein of 1:10000 was sufficient to give substantial digestion of the fusion protein over short periods. This was encouraging as it suggested that thrombin could be used in the purification without it becoming a major protein contaminant. Figure 3.7 illustrates the appearance of Protein A during thrombin digestion. Any non-specific IgG can be used to detect the fusion protein or Protein A alone due to the affinity between Protein A and IgG but SytC will not be detected. The large Protein A - containing band is shown to disappear and a much smaller band the size of the Protein A domain alone appears upon

digestion with thrombin giving further evidence that the fusion protein is indeed being cleaved into SytC and PrA. The purification strategy planned would require the thrombin digestion to act on fusion protein immobilised on IgG-Sepharose. A small-scale pilot study was therefore conducted to establish whether this was feasible. Figure 3.8 shows that the fusion protein binds to IgG-Sepharose although the amount applied probably exceeds the capacity of the Sepharose used because there was still soluble protein left in the S20 after binding. Buffer removed from the protein-bound Sepharose after 4 h digestion with thrombin was found to contain the 36 kDa protein recognised by the monoclonal antibody cgm67 suggesting that the thrombin site is accessible to the enzyme even in the immobilised protein and that digestion in this way would be a convenient method to purify SytC in one step, without the need for separation of PrA and SytC after digestion as would be necessary if the cleavage was carried out on soluble fusion protein. More of the SytC was recovered in the wash steps and the final elution contains mainly the PrA portion of the construct (data not shown) Some of the Pra portion of the fusion protein appeared to leach off the Sepharose with SytC straight after the thrombin digestion. This was not a large amount but was amplified by the sensitivity of the detection method. Furthermore, the leaching was not seen in subsequent purifications (eg figure 3.9) and so was probably an effect of a pH inaccuracy in this experiment alone.

3.6 Affinity purification of the PrA-SytC fusion using IgG Sepharose

A scaled-up version of the thrombin digestion of the fusion protein immobilised on IgG-Sepharose was attempted in order to purify a larger amount of SytC. The basic procedure for binding Protein A fusion proteins

to IgG-Sepharose was followed and after extensive washing of the Sepharose to remove residual contaminating proteins, thrombin was added in the lowest dilution previously found to be effective and incubated overnight at 37°C. Figure 3.9 shows that not all of the fusion protein is removed from the bacterial lysate, presumably because the quantity present exceeds the capacity of the Sepharose used, but the digestion with thrombin released essentially pure SytC with a yield of 15-20 mg per litre of bacterial culture. The main problem to be solved with this step was that an equal amount of SytC remains bound to the IgG-Sepharose and is only recovered in the low pH eluate when the resin is recycled. The Pra portion of the chimaeric protein was not seen in the glycine eluate. It is possible that the pH of the Sepharose was not lowered sufficiently for successful elution of Pra. Alternatively, it is possible that the Pra has not stained well on figure 3.9 since the Pra eluted well in subsequent purifications but showed variability of staining on gels.

The nature of the interaction which was keeping SytC bound to the Sepharose was not known so various wash conditions were tried after thrombin digestion. Figures 3.10a and 3.10b show that no SytC is left bound to the Sepharose in the presence of RIPA detergents and very little is left bound with EGTA. It was therefore decided to include EGTA washes in the purification when recovering the SytC protein rather than introducing detergents into the preparation which may be difficult to remove completely and may adversely affect the conformation of the protein.

3.7 Further purification by exclusion chromatography

Figure 3.11 shows the protein purity (estimated by densitometry as 80%)

after initial affinity purification and concentration by precipitation with ammonium sulphate. The main contaminants are high-molecular weight proteins, which are probably derived from the IgG heavy chain or *E.coli* chaperone proteins such as hsp70 which may be complexed with the fusion protein. A wash step with buffer containing 10 mM MgATP was attempted before the thrombin digest because ATP is required for the binding/release cycle of chaperones. Some high molecular weight contaminants were released from the Sepharose but approximately half of the bound fusion protein was also removed from the resin (data not shown) giving a much lower final yield of SytC. Gel exclusion chromatography was therefore selected as the method for further purification. The elution profile and calibration curve for the column using marker proteins are shown in figures 3.12a and 3.12b respectively and the elution profile for the SytC preparation is shown in figure 3.13a. The composition of the main peak fractions was analysed by gel electrophoresis and is shown in figure 3.13b. Fractions 24-29 all contain protein which was 90% pure (estimated by densitometry). The purest fractions are 95-98% SytC and had a protein concentration of 1.5-2.0 mg/ml.

3.8 N terminal peptide sequencing

The purified SytC protein was sequenced at the N terminus by automated peptide sequencing of the protein bound to PVDF membrane. The N terminus was found to be N A I N M. The original construct was designed to have the sequence G G K N A I N M at the N terminus of the protein. The missing three amino acids are likely to be the result of other protease activity in the thrombin used or residual protease activity from the *E.coli* lysate although this is treated with a mixture of protease inhibitors during the preparation of the lysate and also during binding to IgG-Sepharose. It

is also possible that the G G K sequence is acting as a 'pseudo-recognition' sequence for thrombin mimicking G P R (the accepted thrombin recognition sequence)

3.9 Construction of a gene encoding His10 N-terminally tagged synaptotagmin

The *sytc* gene was amplified by PCR and initially cloned into pGEM-T as previously described. The primers contain DNA recognition sequences for the restriction enzymes *Nde*I and *Bam*HI so that *sytc* can be excised from pGEM-T and ligated to the vector pET16b similarly digested with these enzymes. pET16b is designed to create an in-frame fusion to the gene inserted at this cloning site consisting of a sequence encoding a 10-histidine peptide separated from the cloned gene by a sequence encoding the Factor Xa protease site. The resulting fusion protein has therefore a cleavable N-terminal oligohistidine tag referred to as His10. The DNA and protein sequence of the junction between the His10 and SytC portions of the construct are shown in figure 3.ii below.

Figure 3.ii DNA and protein sequence of the junction between *his10* and *sytc* in the fusion construct

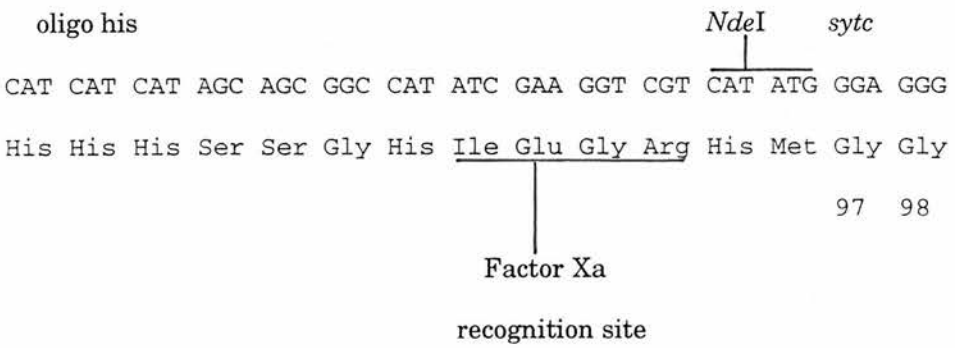

The junction sequence and the *sytc* portion were verified experimentally by

DNA sequencing.

3.10 Synthesis of the His10-SytC protein

The gene cloned in pET16b is under T7 promoter control so it must be expressed in a strain which has an inducible T7 polymerase to transcribe the gene. The *E.coli* strain BL21(DE3) was used which carries a T7 polymerase gene under *lac* promoter control. This enables the induction of gene expression, again by the addition of IPTG and its repression with glucose. Figure 3.14 shows induction of a protein, upon addition of IPTG, recognised by cgm67 in cultures of cells transformed with different recombinant plasmids. There is good repression of expression in the presence of glucose and moderate induction with IPTG and there appear to be three forms of the protein recognised by the monoclonal antibody. Analysis of the construct sequence reveals the presence of three potential methionine 'start' codons so alternative initiation events could be responsible for the appearance of smaller cgm67 - reactive proteins (Appendix 4). In this case, it may be predicted that only the largest product will have a his-tag and therefore will be the only form purified on Ni-NTA agarose.

The levels of expression of the His10-fusion protein were not very high even after 4 h growth following induction (cell death occurs if cells are grown for longer than this). In an attempt to increase levels of the protein, alternative *E.coli* DE3 strains were used which contain a plasmid encoding T7 lysozyme (pLysS). This is a natural inhibitor of T7 RNA polymerase and should prevent 'leaky' expression by low background levels of T7 polymerase. When IPTG is added this inhibition should be overcome by the transcription of large amounts of the polymerase from the stronger *lac*

promoter. The strain containing pLysE gives even tighter control of expression of the cloned gene. Figure 3.15 shows the distribution of fusion protein in the S20, P20 and P3 fractions in three DE3 strains. Although the LysE strain gives less of the smaller products, neither of the two alternative strains gave an increase in protein levels. A His10 chimaeric protein (of the 39 kDa subunit of the V ATPase) had previously been purified in large quantities which suggests that this strategy is variable with different proteins.

3.11 Affinity-purification of His10-SytC with Ni-NTA agarose

The fusion protein produced can be purified by affinity chromatography on Ni- agarose. Figures 3.16a and 3.16b show the purification of the fusion protein with a step-wise gradient of imidazole which first elutes non-specifically bound proteins at 50-100mM imidazole and then elutes the specifically bound His10-tagged protein at 150-200mM imidazole. As predicted by the sequence analysis, only the largest product produced by the cells is purified on Ni-NTA agarose suggesting it is indeed the only product carrying the oligohistidine tag. This is shown in figure 3.17. It was decided to leave the his-tag on the protein since it is only small and unlikely to interfere structurally with the protein.

3.12 Conclusion

The construction of two gene fusions encoding affinity-tagged versions of SytC has been described along with the identification and purification of the protein products.

Both constructs encode soluble fusion proteins which are accessible to affinity chromatography although the Protein A chimaera is produced in

much larger quantities than the His10 chimaera. Conversely, the Ni-NTA agarose purification procedure is more straightforward and gives a purer product in one step. In addition, no other proteins are introduced during Ni-NTA agarose purification whereas the IgG-Sepharose procedure involves both IgG, probably responsible for the high molecular weight contamination, and also thrombin. It was therefore difficult to decide at this stage whether to work with one particular construct or to carry out experiments using both. Anomalous behaviour of the his-tagged protein, discovered later, along with structural studies eventually led to the use of the Protein A fusion as the source of SytC for this study.

Figure 3.1 Induction of *pra-sytc* expression

Two flasks containing 50 ml medium (L-broth) with 50 μg/ml kanamycin were inoculated with one fiftieth the volume of an overnight culture of *E.coli* NM522(pLC100) grown in medium containing 0.4% (w/v) glucose. One 50 ml culture still contained the same amount of glucose. The two cultures were incubated at 37 °C for 0.5 h (to an $O.D_{600}$ of 0.2) before the addition of 0.1 mM IPTG to the culture not containing glucose. After 2 h further incubation, 1 ml of each culture was centrifuged for 1 min at 13000 rpm in a MSE MicroCentaur and the pellet resuspended in 100 μl SDS-PAGE sample buffer. These were analysed by gel electrophoresis (10 μl loaded) and Western blotting using a synaptotagmin-specific monoclonal antibody (cgm67) at a dilution of 1:5.

Lane 1	Culture induced with IPTG
Lane 2	Culture grown with 0.4% (w/v) glucose

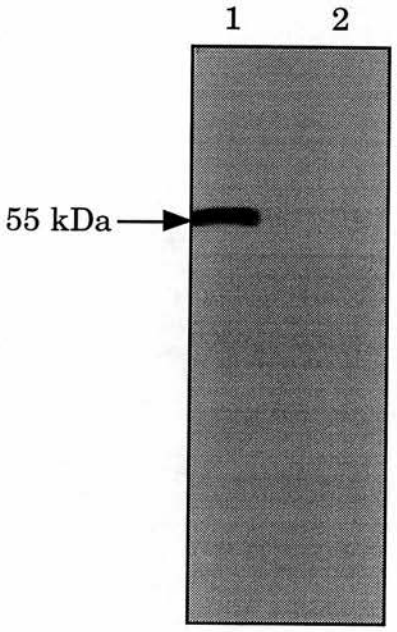
1
2
55 kDa

Figure 3.2 Time course of PrA-SytC fusion protein production

Medium containing 50 μg/ml kanamycin (100 ml) was inoculated with one fiftieth the volume of an overnight culture of *E.coli* NM522(pLC100). After growing to an OD_{600} of 0.4 (45 min at 37°C), 0.1 mM IPTG was added and 1 ml samples withdrawn from the culture after 0.5, 1, 2, 3 h growth. The 1 ml samples were centrifuged for 1 min at 13000 rpm in a MSE MicroCentaur and the pellet resuspended in 100 μl of SDS-PAGE sample buffer. 15 μl of the first sample was loaded and the volumes loaded of the other samples were adjusted according to the cell mass present in each sample (estimated from the culture A_{600} when the sample was taken). Gel electrophoresis and Western blotting were carried out using cgm67 at a dilution of 1:5 for detection of the protein.

Lane 1	0.5 h growth after induction
Lane 2	1.0 h growth after induction
Lane 3	2.0 h growth after induction
Lane 4	3.0 h growth after induction

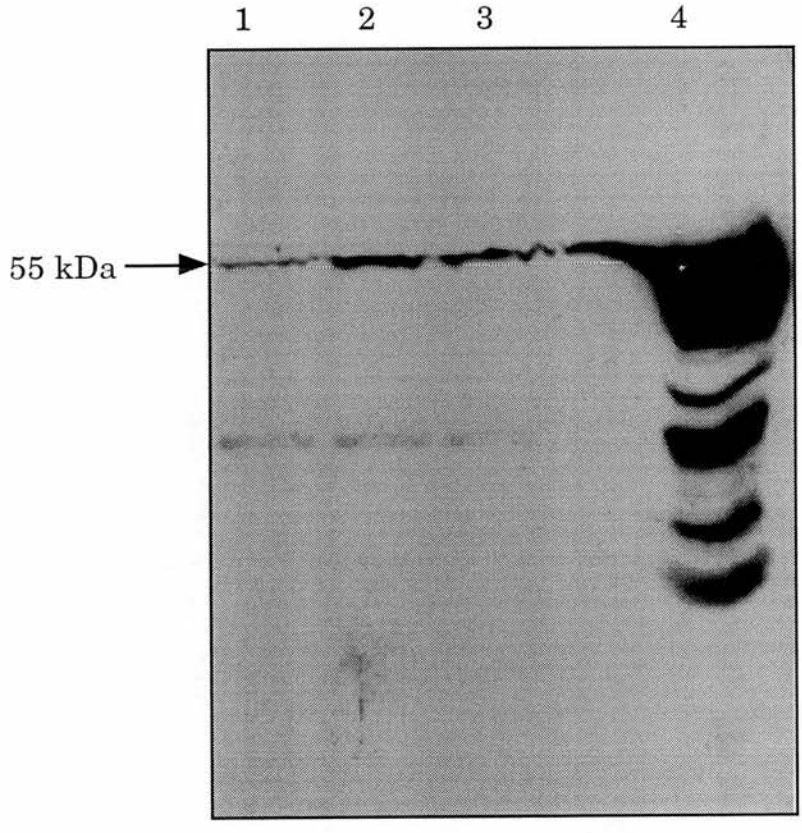
1
2
3
4
55 kDa

Figure 3.3 Fractionation of a bacterial culture expressing the *pra-syt* gene

Fractionation was carried out with a 1 l culture of *E.coli* NM522(pLC100) as already outlined in Materials and Methods. All the fractions were made up to a volume of 10 ml and samples of 10 µl were analysed by SDS-PAGE followed by Western blotting using cgm 67 at a 1:5 dilution for detection.

Lane 1	P20 pellet (inclusion bodies)
Lane 2	S20 soluble fraction (cytosol)
Lane 3	P3 pellet (whole cells and cell debris)

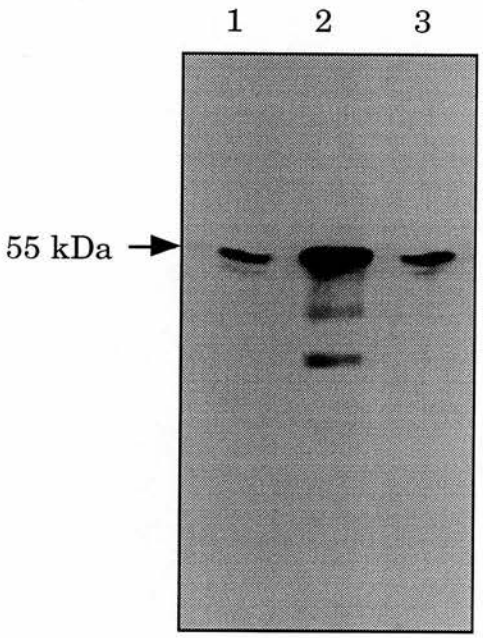
1
2
3
55 kDa

Figure 3.4 SDS-PAGE gel showing the time course of thrombin digestion of the PrA-SytC protein

The S20 fraction was prepared from a 100 ml culture of *E.coli* NM522(pLC100) . A 100 µl digest was carried out as described in Materials and Methods using a thrombin:total protein weight ratio of 1:2000. Samples of 10 µl were removed from the digest at intervals of 0, 15, 30, 45, 60, 90, 120 and 150 min after the start of incubation and 3 µl SDS-PAGE sample buffer added. 5 µl of each sample was analysed by gel electrophoresis and Coomassie staining

Lane 1	Molecular weight standards
Lane 2	S20 incubated for 150 min at 37 °C without thrombin
Lane 3	0 min sample
Lane 4	15 min sample
Lane 5	30 min sample
Lane 6	45 min sample
Lane 7	60 min sample
Lane 8	90 min sample
Lane 9	120 min sample
Lane 10	150 min sample

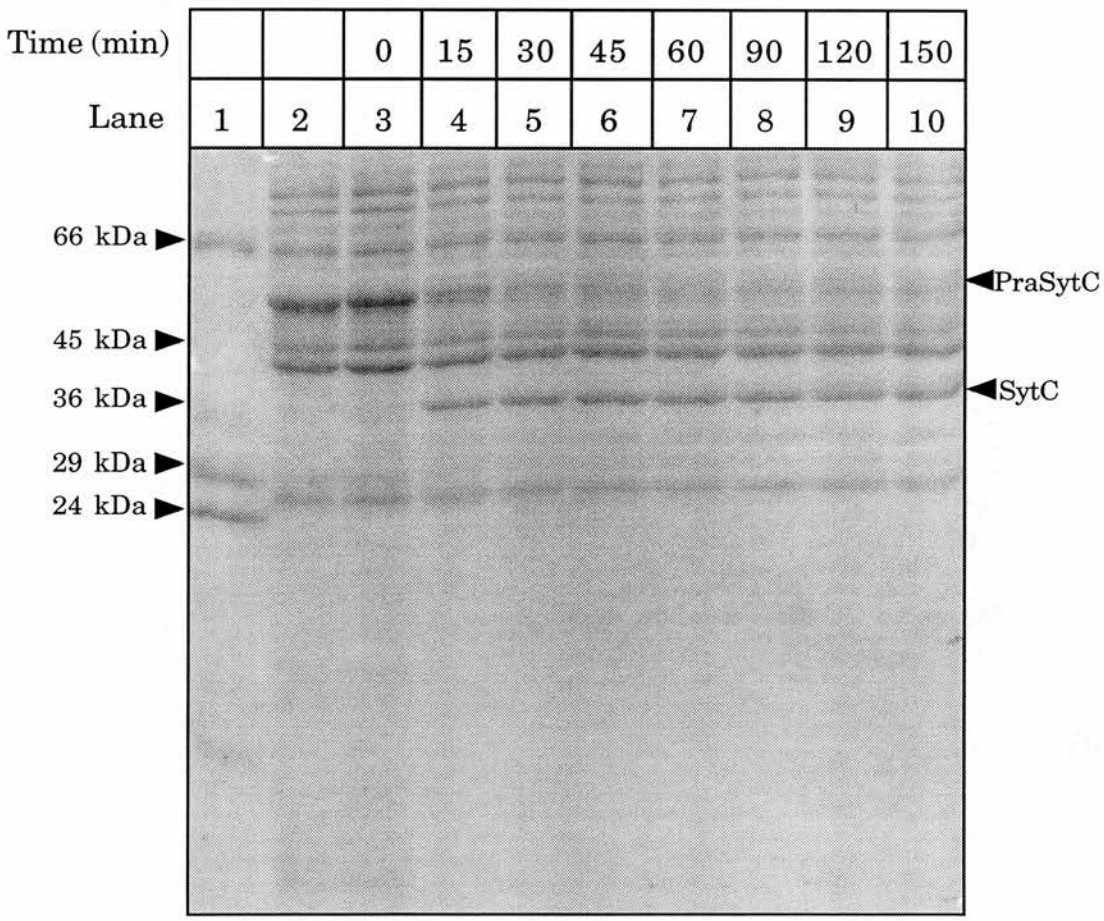
Time (min)
0
15
30
45
60
90
120
150
Lane
1
2
3
4
5
6
7
8
9
10
66 kDa
45 kDa
36 kDa
29 kDa
24 kDa
PraSytC
SytC

Figure 3.5 Western blot showing time course of digestion with thrombin of Pra-SytC protein

A 200 µl thrombin digest was performed with the S20 fraction from a 100 ml culture of NM522(pLC100) using a thrombin:total protein weight ratio of 1:2000 and 10 µl samples withdrawn after 0, 5, 10, 15, 20, 25, 30, 45, 60, 90, 120 and 150 min after the start of incubation. SDS-PAGE sample buffer was added (3 µl) to each sample and 2 µl analysed by gel electrophoresis followed by Western blotting using the monoclonal antibody cgm67 at a dilution of 1:5.

Lane 1	0 min sample
Lane 2	5 min sample
Lane 3	10 min sample
Lane 4	15 min sample
Lane 5	20 min sample
Lane 6	25 min sample
Lane 7	30 min sample
Lane 8	45 min sample
Lane 9	60 min sample
Lane 10	90 min sample
Lane 11	120 min sample
Lane 12	150 min sample

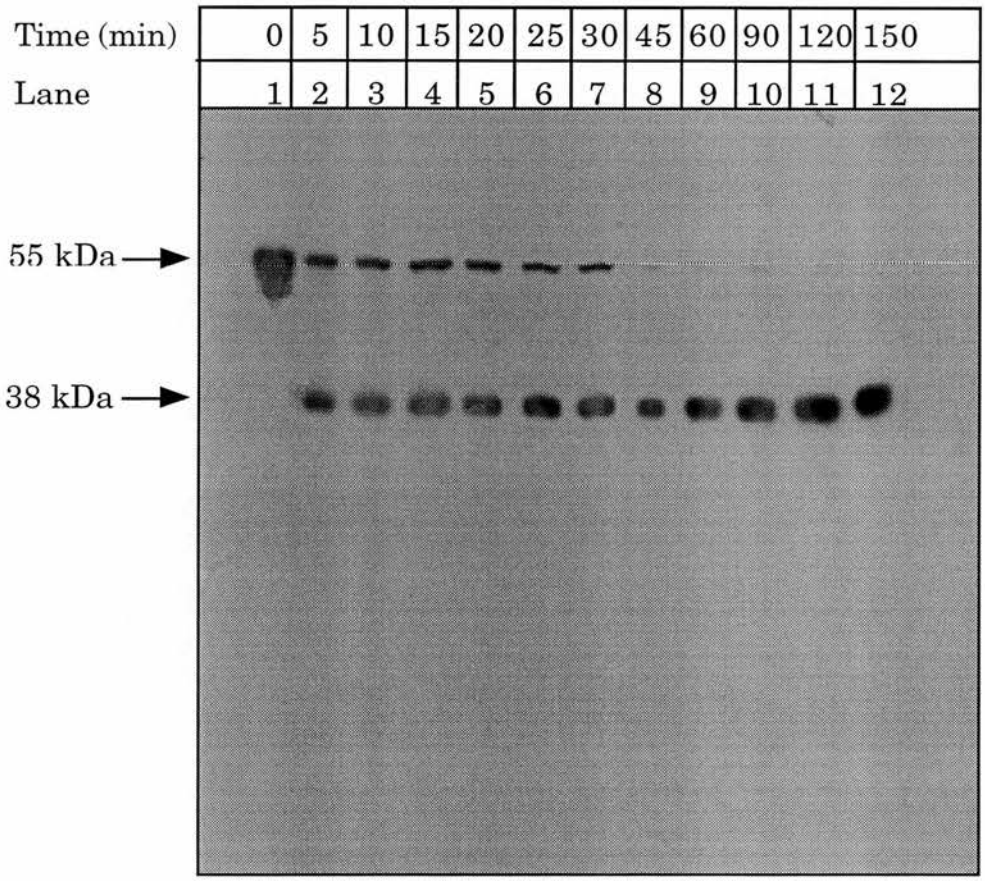
Time (min)
0 5 10 15 20 25 30 45 60 90 120 150
Lane
1 2 3 4 5 6 7 8 9 10 11 12
55 kDa
38 kDa

Figure 3.6 Gel showing titration of Pra-SytC protein with thrombin

Protein from the S20 fraction of a 100 ml culture of *E.coli* NM522(pLC100) was used to set up 20 µl thrombin digests incubated at 37 °C for 4 h following the basic procedure already outlined but with different weight ratios of thrombin:total protein. The reaction was terminated by adding 7 µl SDS-PAGE sample buffer and 5 µl analysed by gel electrophoresis and Coomassie blue staining.

Lane 1	Thrombin:total protein weight ratio of 1:1000000
Lane 2	Thrombin:total protein weight ratio of 1:100000
Lane 3	Thrombin:total protein weight ratio of 1:10000
Lane 4	Thrombin:total protein weight ratio of 1:5000
Lane 5	Thrombin:total protein weight ratio of 1:2000
Lane 6	Thrombin:total protein weight ratio of 1:1000
Lane 7	S20 incubated at 37 °C for 1.5 h without thrombin
Lane 8	S20 at 0 time

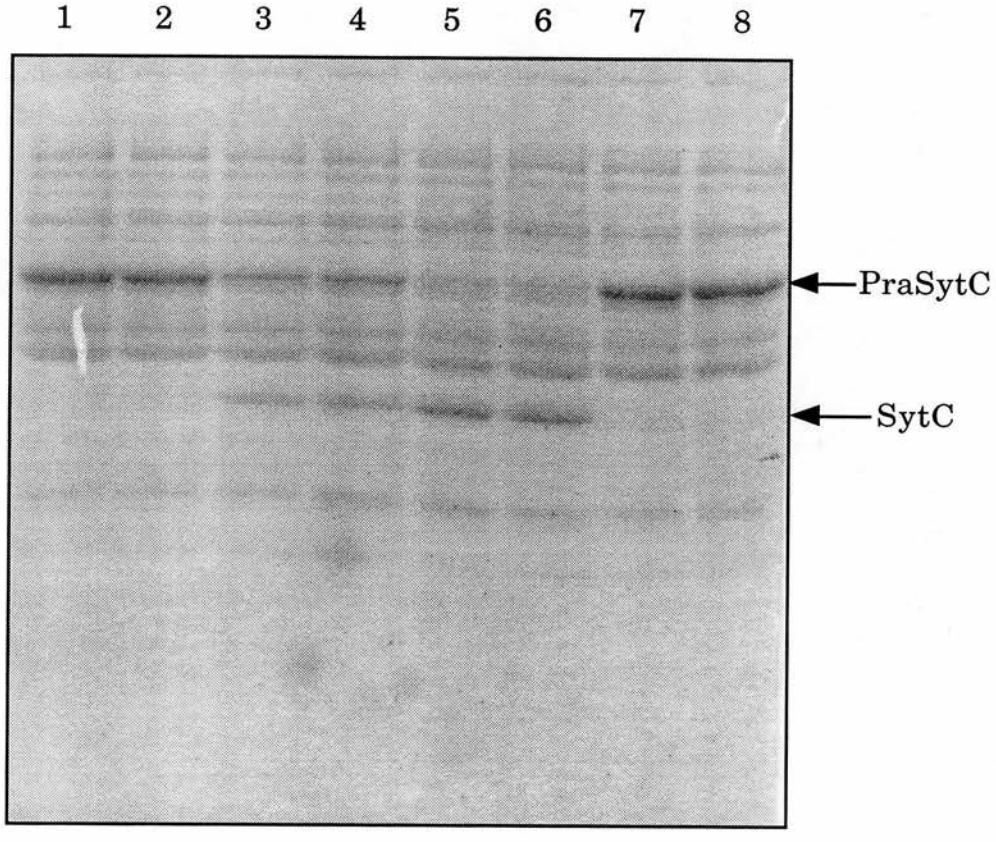
1
2
3
4
5
6
7
8
PraSytC
SytC

Figure 3.7 Western blot showing titration of Pra-SytC protein with thrombin

Thrombin digests of of 20 µl using S20 protein were incubated at 37 °C for 1.5 h with larger amounts amounts of thrombin than previously used to ensure complete digestion in a short time. Reactions were terminated by the addition of 7 µl SDS-PAGE sample buffer and 2 µl of the samples analysed by gel electrophoresis and Western blotting using anti-bovine IgG-HRP conjugate for detection at a dilution of 1:10000.

Lane 1	Thrombin:total protein weight ratio of 1:1000
Lane 2	Thrombin:total protein weight ratio of 1:500
Lane 3	Thrombin:total protein weight ratio of 1:350
Lane 4	Thrombin:total protein weight ratio of 1:250

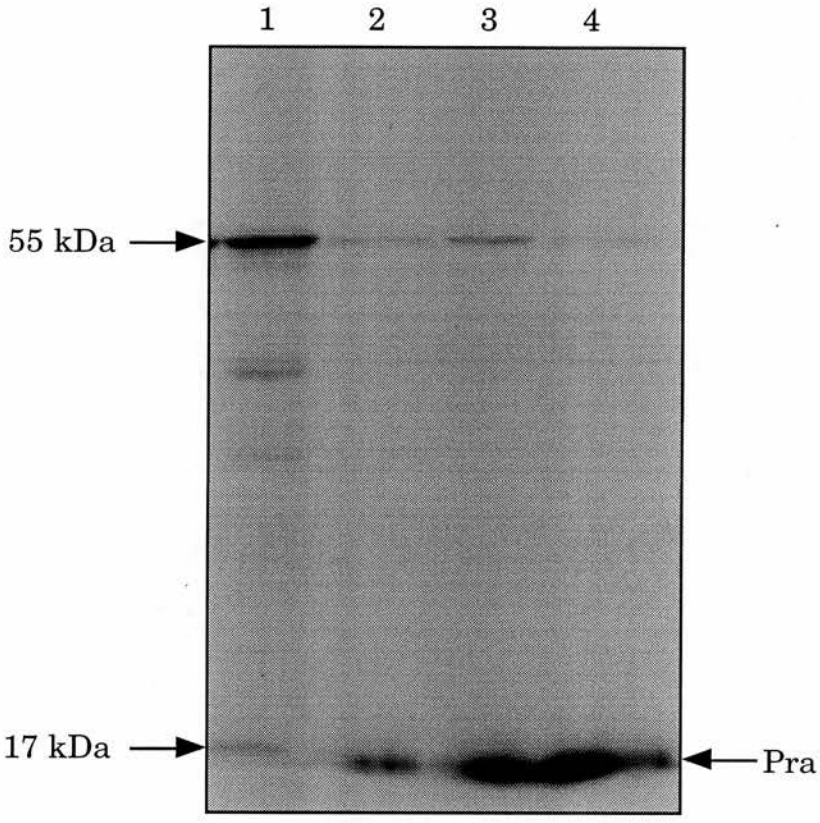
1
2
3
4
55 kDa
17 kDa
Pra

Figure 3.8 Thrombin digestion of Pra-SytC immobilised on IgG Sepharose

3 ml of S20 (containing approximately 10 mg recombinant protein), prepared from a culture of E.coli NM522(pLC100), was mixed with 400 µl IgG-Sepharose, incubated overnight and washed as described in Materials and Methods. The Sepharose was then equilibrated in thrombin digest buffer (50 mM Tris.HCl pH 7.8, 2.5 mM $CaCl_2$, 100 mM NaCl) and 100 µl of the buffer added along with 10 units of thrombin, corresponding to a PraSytC:thrombin weight ratio of 4000:1. After incubation at 37°C for 4 h, the buffer was removed and the IgG-Sepharose washed twice with 100 µl of digest buffer. Finally, 100 µl of 0.2 M glycine pH 2.8 was used to elute any protein left bound to the column. 20 µl samples were taken from the initial digest buffer and the washes. SDS-PAGE sample buffer was added and 5 µl of each sample was loaded on a gel and subjected to electrophoresis followed by Western blotting using the monoclonal antibody cgm67 for detection at a dilution of 1:5 together with anti-bovine IgG-HRP at a dilution of 1:10000 for detection of Pra.

Lane 1	S20 before binding to IgG-Sepharose
Lane 2	Blank
Lane 3	S20 after binding IgG-Sepharose
Lane 4	Digest buffer after incubation at 37 °C with thrombin
Lane 5	First wash after digestion
Lane 6	Second wash after digestion
Lane 7	Elution with glycine

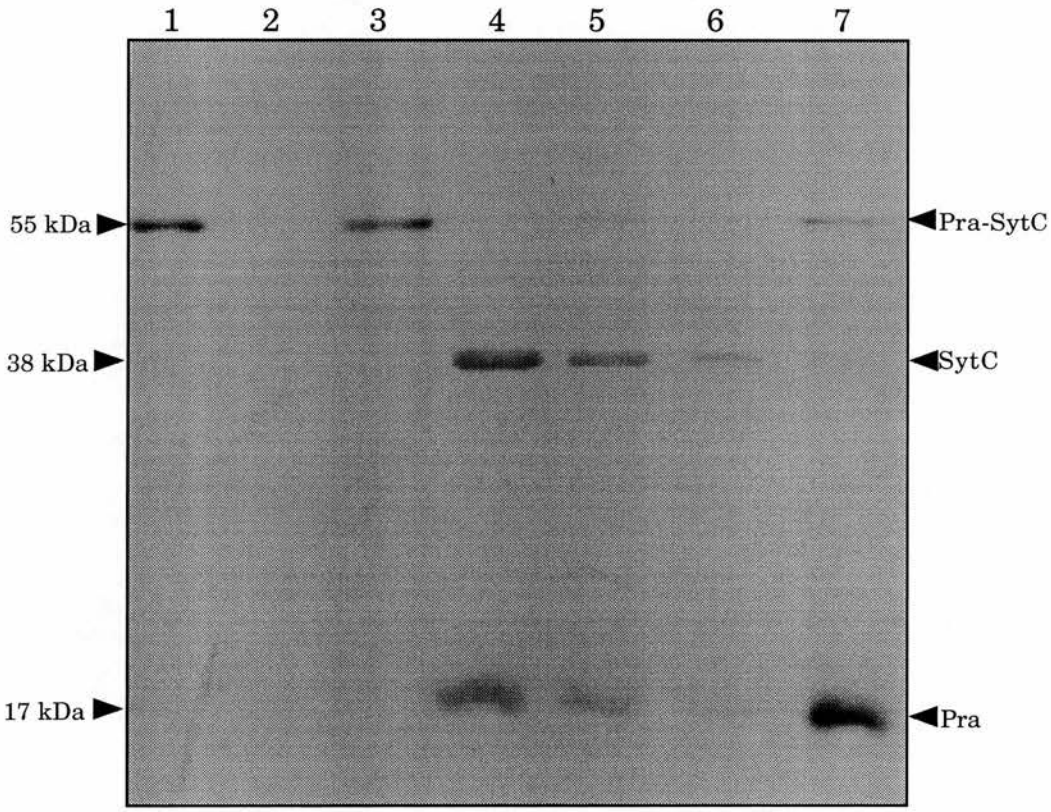
1
2
3
4
5
6
7
55 kDa
38 kDa
17 kDa
Pra-SytC
SytC
Pra

Figure 3.9 Large-scale preparation of SytC

Large scale purification was carried out with the S20 fraction from a 1 l culture of NM522(pLC100) by first binding the fusion protein to the resin and then carrying out a thrombin digest on the immobilised protein as described in Materials and Methods except the Sepharose was washed after thrombin digestion with two further washes of thrombin digest buffer without EGTA. Samples of the S20 fraction, the digest fraction and the washes were taken and 2 µl analysed by gel electrophoresis and silver staining.

Lane 1	Molecular weight standards
Lane 2	S20 before binding to IgG-Sepharose
Lane 3	S20 after binding to IgG-Sepharose
Lane 4	Thrombin digest buffer
Lane 5	First wash
Lane 6	Second wash
Lane 7	elution with glycine

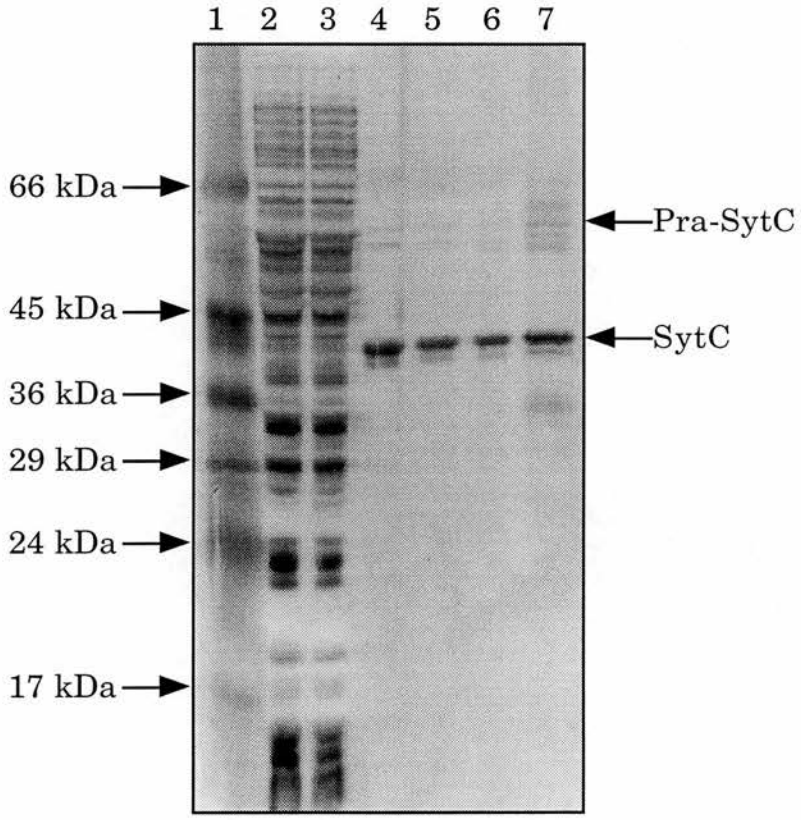
1 2 3 4 5 6 7
66 kDa
45 kDa
36 kDa
29 kDa
24 kDa
17 kDa
Pra-SytC
SytC

Figure 3.10 Recovering IgG-Sepharose - bound SytC protein using different wash conditions

Six identical tubes were set up with 1 ml of the S20 fraction from a 1 l bacterial culture and 200 µl of IgG-Sepharose and incubated overnight to bind the fusion protein to the resin. Thrombin digestion was then carried out on the immobilised fusion protein using 0.5 ml thrombin digestion buffer and 0.5 units of thrombin with overnight incubation at 37°C. After removal of the initial digestion buffer, the six tubes were washed twice with different washing buffers in each tube and then a final elution with 0.2 M glycine pH 2.8 was carried out. The washing conditions used were: condition 1- thrombin digestion buffer; condition 2- digestion buffer with 50% (v/v) ethylene glycol; condition 3 - digestion buffer with NaCl reduced to 25 mM; condition 4 - digestion buffer with NaCl increased to 400 mM; condition 5 - digestion buffer with RIPA detergents (1% (w/v) Np-40, 0.5% (w/v) deoxycholate, 0.1% (w/v) SDS); condition 6 - digestion buffer with 2 mM EGTA instead of $CaCl_2$.

Lane	Figure 3.10a	Figure 3.10b
1	Molecular weight standards	Molecular weight standards
2	S20 before binding to IgG-Sepharose	Blank
3	S20 after binding to IgG-Sepharose	Second wash with buffer condition 1
4	Initial digest buffer	Second wash with buffer condition 2
5	Initial digest buffer	Second wash with buffer condition 3
6	Initial digest buffer	Second wash with buffer condition 4
7	Initial digest buffer	Second wash with buffer condition 5
8	Initial digest buffer	Second wash with buffer condition 6
9	Initial digest buffer	Blank
10	First wash with buffer condition 1	Elution with glycine for condition 1
11	First wash with buffer condition 2	Elution with glycine for condition 2
12	First wash with buffer condition 3	Elution with glycine for condition 3
13	First wash with buffer condition 4	Elution with glycine for condition 4
14	First wash with buffer condition 5	Elution with glycine for condition 5
15	First wash with buffer condition 6	Elution with glycine for condition 6

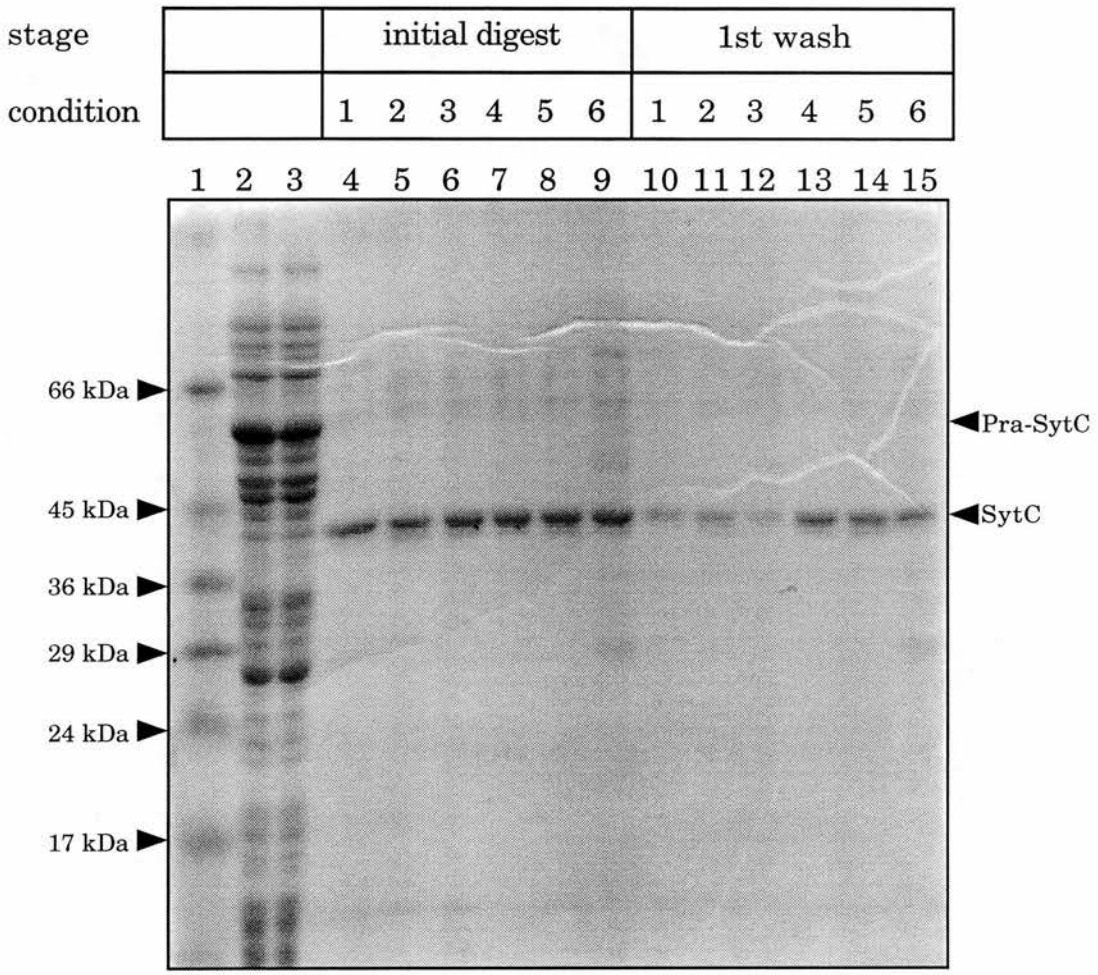
stage
initial digest
1st wash
condition
1 2 3 4 5 6 1 2 3 4 5 6
1 2 3 4 5 6 7 8 9 10 11 12 13 14 15
66 kDa
45 kDa
36 kDa
29 kDa
24 kDa
17 kDa
Pra-SytC
SytC

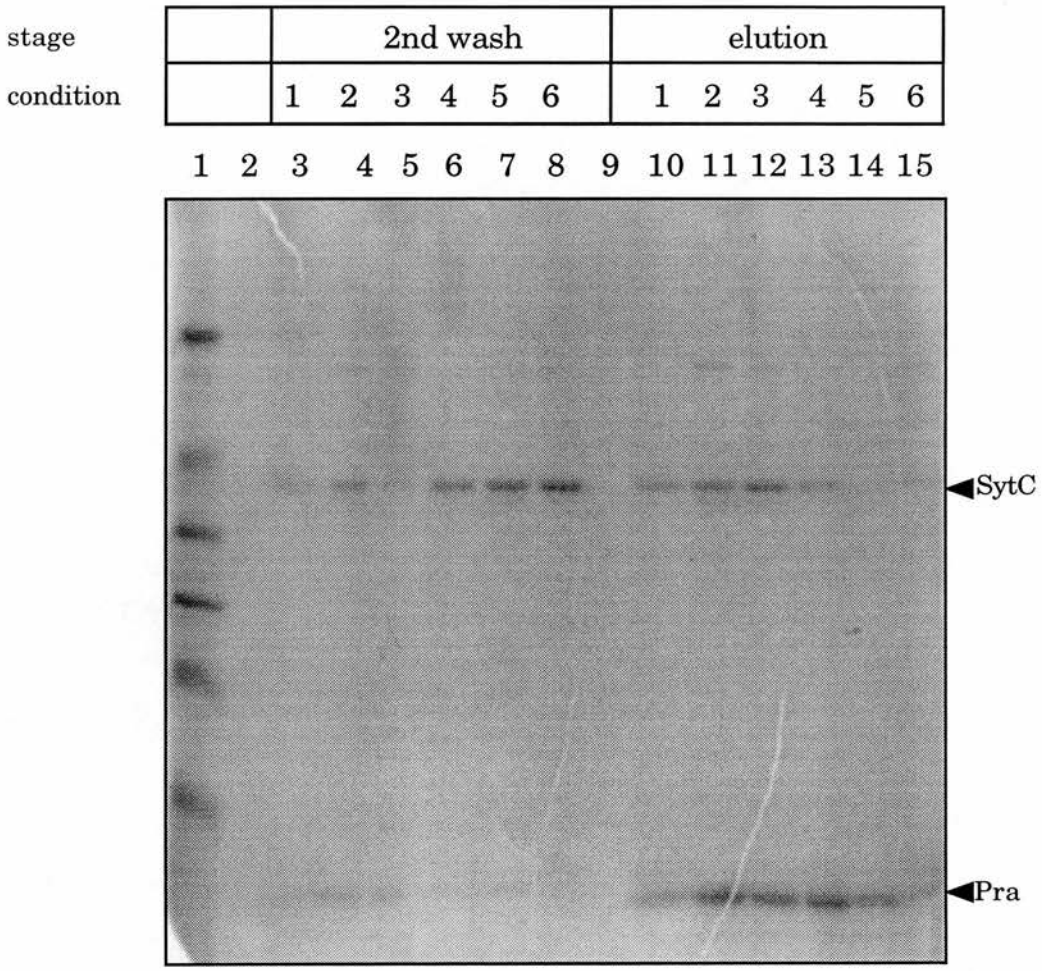
stage
2nd wash
elution
condition
1 2 3 4 5 6
1 2 3 4 5 6
1 2 3 4 5 6 7 8 9 10 11 12 13 14 15
SytC
Pra

Figure 3.11 Ammonium sulphate-precipitated SytC protein after affinity purification on IgG-Sepharose

The pooled washes from the thrombin digestion of immobilised PrA-SytC were precipitated using $(NH_4)_2SO_4$ to 80% saturation. 2 µl of the protein was analysed by gel electrophoresis and Coomassie staining.

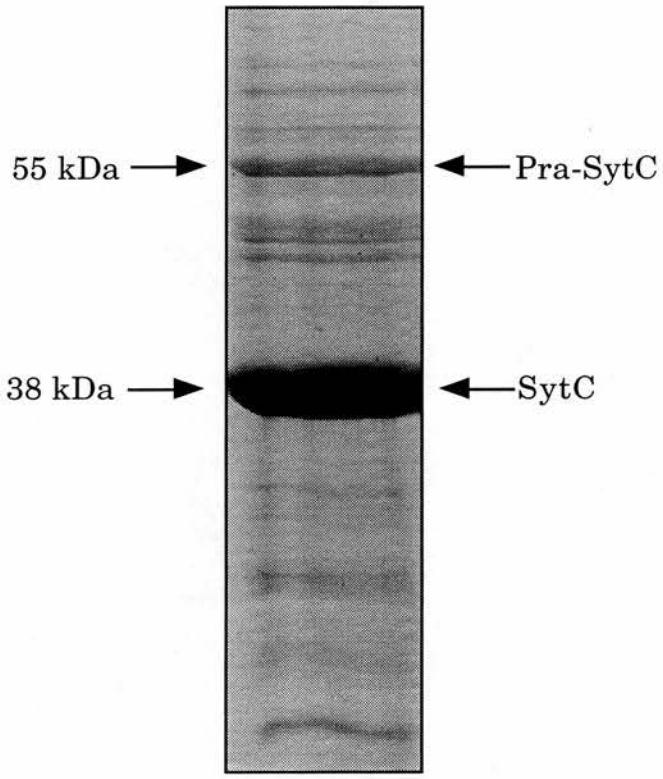
55 kDa
Pra-SytC
38 kDa
SytC

Figure 3.12a **Elution profile of molecular weight standard proteins in gel exclusion chromatography**

The A_{280} of the first eighty fractions was measured and the value obtained was plotted against the elution volume.

Peak 1	670 kDa thyroglobulin
	158 kDa γ globulin
Peak 2	44 kDa ovalbumin
Peak 3	17 kDa myoglobin
Peak 4	1.35 kDa vitamin B12

void volume = 10 ml

total volume = 42 ml

Figure 3.12b **Calibration curve for the gel exclusion column**

V_E was calculated from the peak fraction number for each protein given that the volume of each fraction is 0.5 ml. The curve was drawn assuming the exclusion limit of the resin was 100,000 Da.

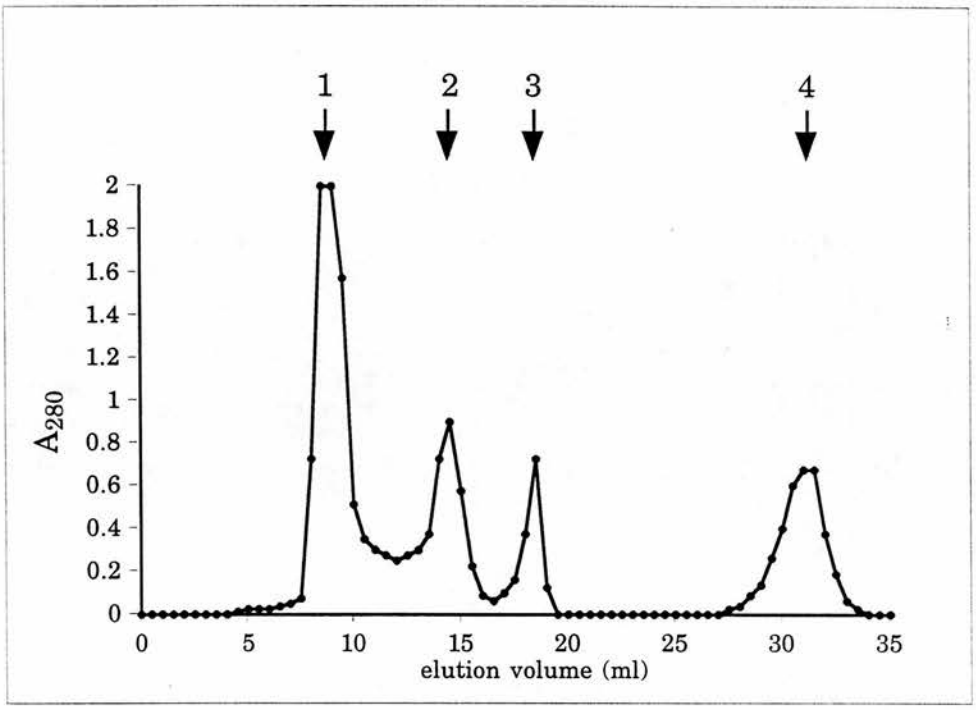
1
2
3
4
2
1.8
1.6
1.4
1.2
1
0.8
0.6
0.4
0.2
0
A280
0
5
10
15
20
25
30
35
elution volume (ml)

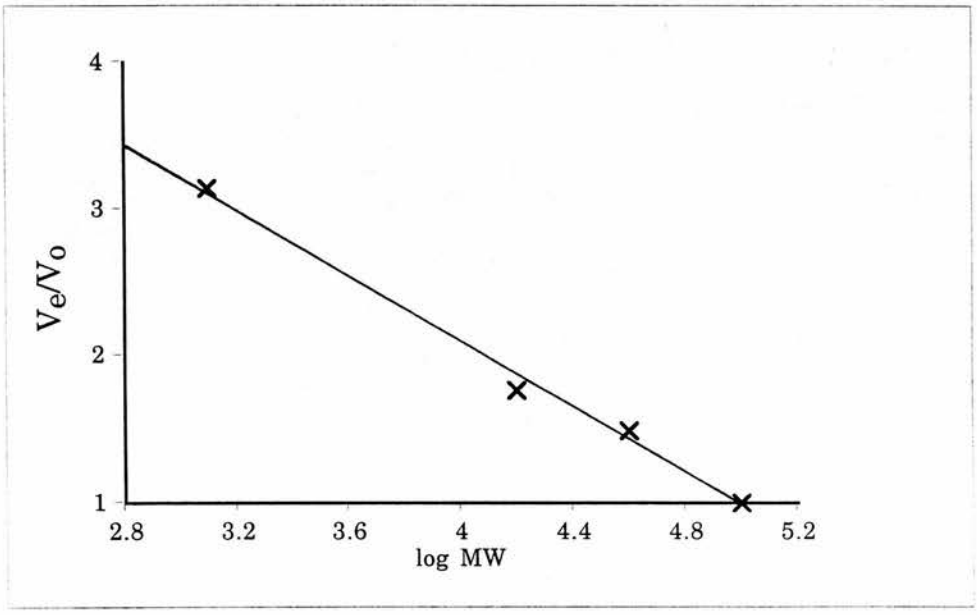
4
3
2
1
Ve/Vo
2.8
3.2
3.6
4
4.4
4.8
5.2
log MW

Figure 3.13a **Elution profile for the SytC protein in the gel exclusion column.**

The A_{280} of each fraction was measured and the value obtained for the first eighty fractions was plotted against the fraction number.

Figure 3.13b **Protein composition of the elution peak fractions in gel exclusion chromatography**

A 5 µl sample of each fraction from the main peak of absorbance was analysed by gel electrophoresis and Coomassie staining

3.13a

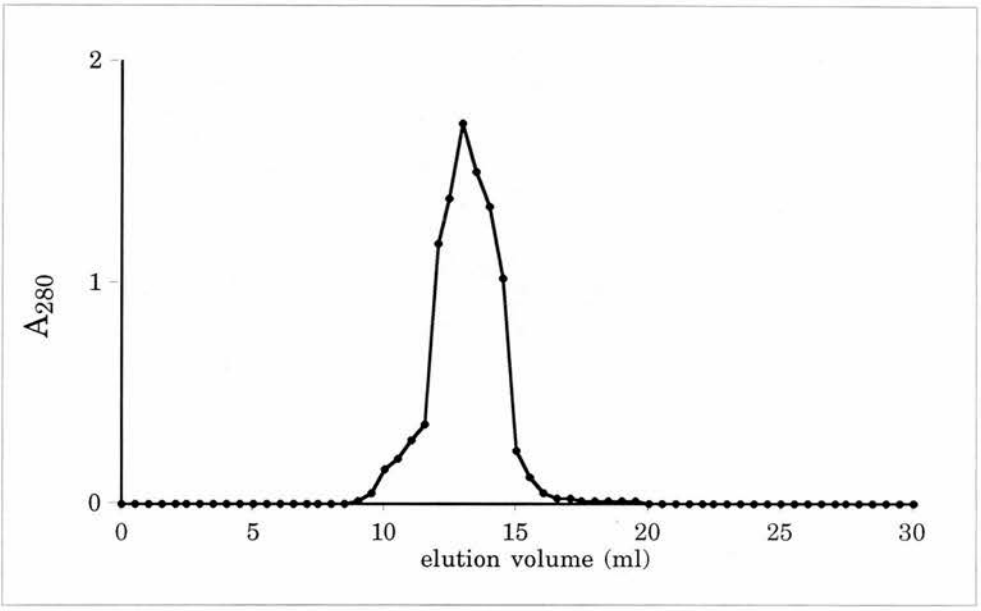
2
1
0
A_{280}
0
5
10
15
20
25
30
elution volume (ml)

3.13b

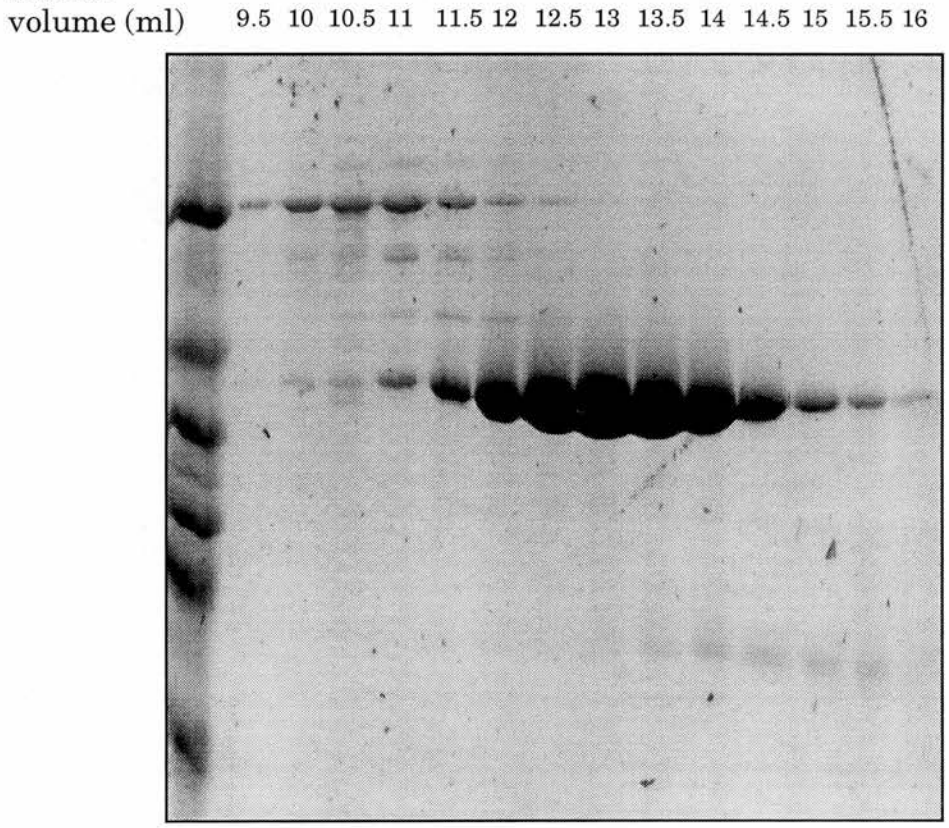
elution
volume (ml)
9.5 10 10.5 11 11.5 12 12.5 13 13.5 14 14.5 15 15.5 16

Figure 3.14 Production of His10-SytC

Seven 10 ml cultures containing 0.4% (w/v) glucose and 100 μg/ml ampicillin were inoculated from E.coli BL21 DE3 colonies transformed with different *his*$_{10}$*-sytc* recombinant plasmids. These were grown overnight and 1 ml of each was used to inoculate 50 ml cultures all containing ampicillin. One culture of each transformant contained 0.4% (w/v) glucose. The cultures were grown at 37°C for 1 h and then 0.1 mM IPTG was added to each culture not containing glucose. All the cultures were grown for a further 2 h and the S20 fraction prepared from each culture. A 20 μl sample was taken of all the S20 fractions, 7 μl SDS-PAGE sample buffer added and 10 μl analysed by gel electrophoresis and Western blotting using cgm 67 for detection at a 1:5 dilution.

Lane 1	Transformant 1 grown in glucose
Lane 2	Transformant 1 grown with IPTG
Lane 3	Transformant 2 grown in glucose
Lane 4	Transformant 2 grown with IPTG
Lane 5	Transformant 3 grown in glucose
Lane 6	Transformant 3 grown with IPTG
Lane 7	Transformant 4 grown in glucose
Lane 8	Transformant 4 grown with IPTG
Lane 9	Transformant 5 grown in glucose
Lane 10	Transformant 5 grown with IPTG
Lane 11	Transformant 6 grown in glucose
Lane 12	Transformant 6 grown with IPTG

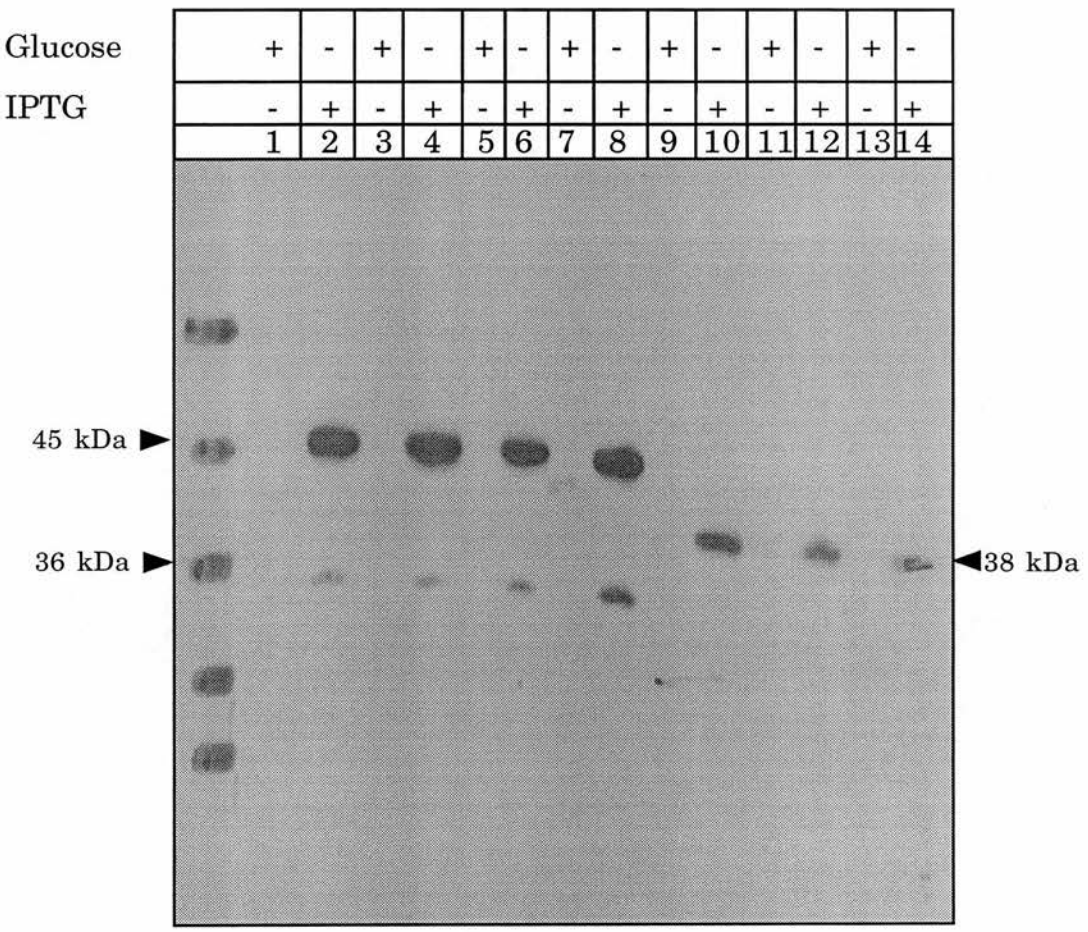
Glucose
IPTG
+ - + - + - + - + - + - + -
- + - + - + - + - + - + - +
1 2 3 4 5 6 7 8 9 10 11 12 13 14
45 kDa
36 kDa
38 kDa

Figure 3.15 Fractionation of three bacterial strains producing His10-SytC protein

100 ml cultures of three *E.coli* strains were set up; BL21 DE3(pLC600), BL21 DE3 pLysS(pLC600) and BL21 DE3 pLysE(pLC600). All the cultures contained 100 μg/ml ampicillin and were grown at 37°C for 2 h for a further 4 h after induction with IPTG (0.1 mM); the cultures all reached the same A_{600} in this time. P3, P20 and S20 fractions were prepared from each culture and 20 μl samples taken. SDS-PAGE sample buffer was added (7 μl) and 5 μl of each sample was analysed by gel electrophoresis and Western blotting using cgm67 at a dilution of 1:5.

Lane 1	BL21 S20 fraction
Lane 2	BL21 P20 fraction
Lane 3	BL21 P3 fraction
Lane 4	pLysS S20 fraction
Lane 5	pLysS P20 fraction
Lane 6	pLysS P3 fraction
Lane 7	pLysE S20 fraction
Lane 8	pLysE P20 fraction
Lane 9	pLysE P3 fraction

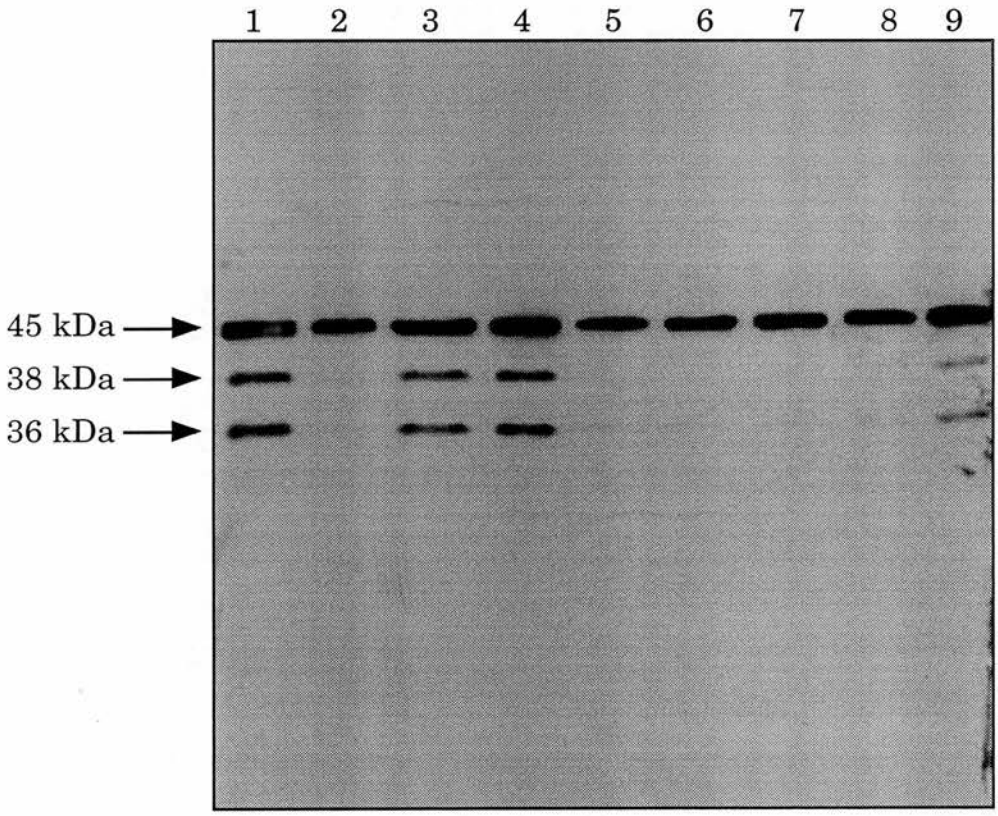
1
2
3
4
5
6
7
8
9
45 kDa
38 kDa
36 kDa

Figure 3.16 Purification of His10-SytC on Ni-Agarose

The S20 fraction was prepared from a 2 l culture of *E.coli* BL21 DE3(pLC600) and bound to Ni-NTA agarose overnight as already detailed in Materials and Methods and the agarose subsequently washed many times. Initially, to ascertain the imidazole concentration necessary for the elution of the fusion protein, a step-wise gradient of imidazole was applied by washing the agarose twice with 2 ml of each imidazole concentration from 50 mM to 500 mM in the pH 6 wash buffer. A sample of 20 µl was taken from all the washes, SDS-PAGE buffer added and 10 µl analysed by gel electrophoresis and Coomassie staining.

Lane	Figure 3.16a	Figure 3.16b
1	Molecular weight standards	Molecular weight standards
2	S20 before binding to Ni-agarose	First 250 mM imidazole wash
3	S20 after binding to Ni-agarose	Second 250 mM imidazole wash
4	First wash with pH 8.0 buffer	First 300 mM imidazole wash
5	Last wash with pH 8.0 buffer	Second 300 mM imidazole wash
6	Last wash with pH 6.0 buffer	First 350 mM imidazole wash
7	First 50 mM imidazole wash	Second 350 mM imidazole wash
8	Second 50 mM imidazole wash	First 400 mM imidazole wash
9	First 100 mM imidazole wash	Second 400 mM imidazole wash
10	Second 100 mM imidazole wash	First 450 mM imidazole wash
11	First 150 mM imidazole wash	Second 450 mM imidazole wash
12	Second 150 mM imidazole wash	First 500 mM imidazole wash
13	First 200 mM imidazole wash	Second 500 mM imidazole wash
14	Second 200 mM imidazole wash	

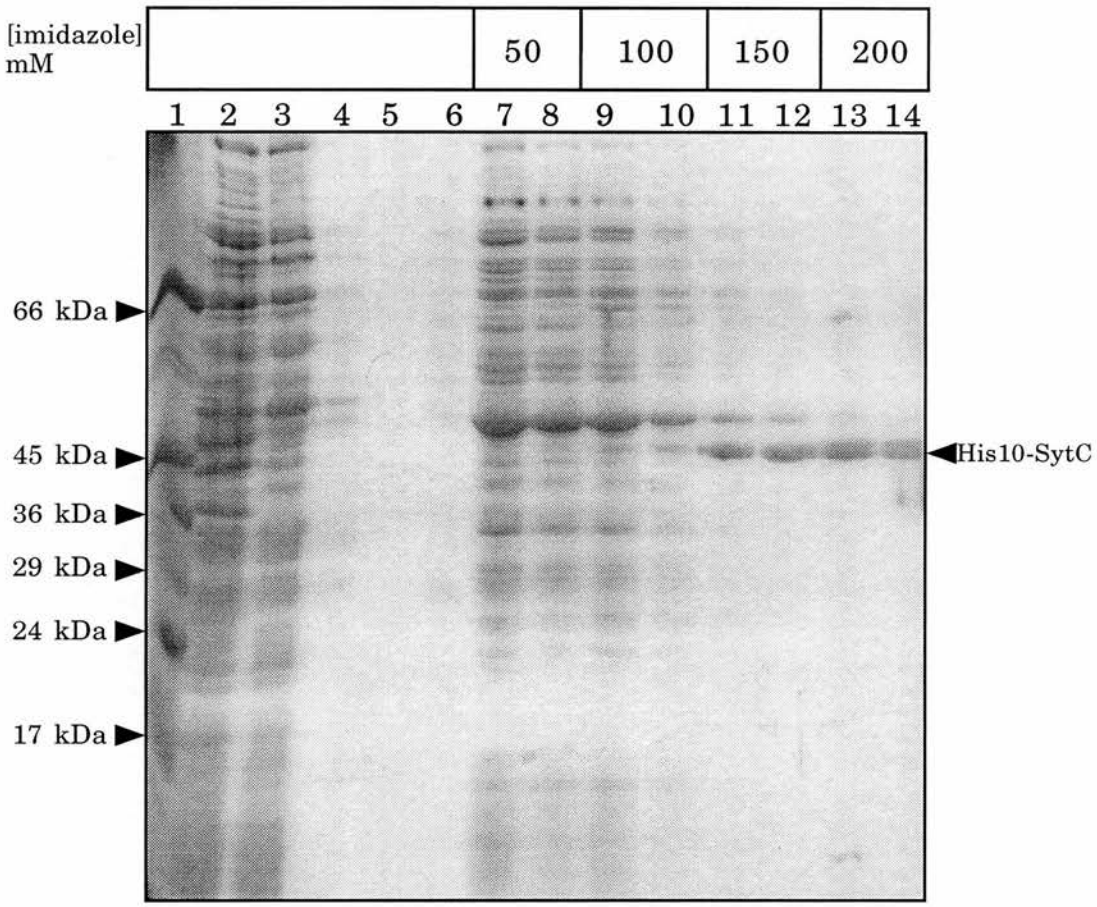
[imidazole]
mM
50
100
150
200
1 2 3 4 5 6 7 8 9 10 11 12 13 14
66 kDa
45 kDa
36 kDa
29 kDa
24 kDa
17 kDa
His10-SytC

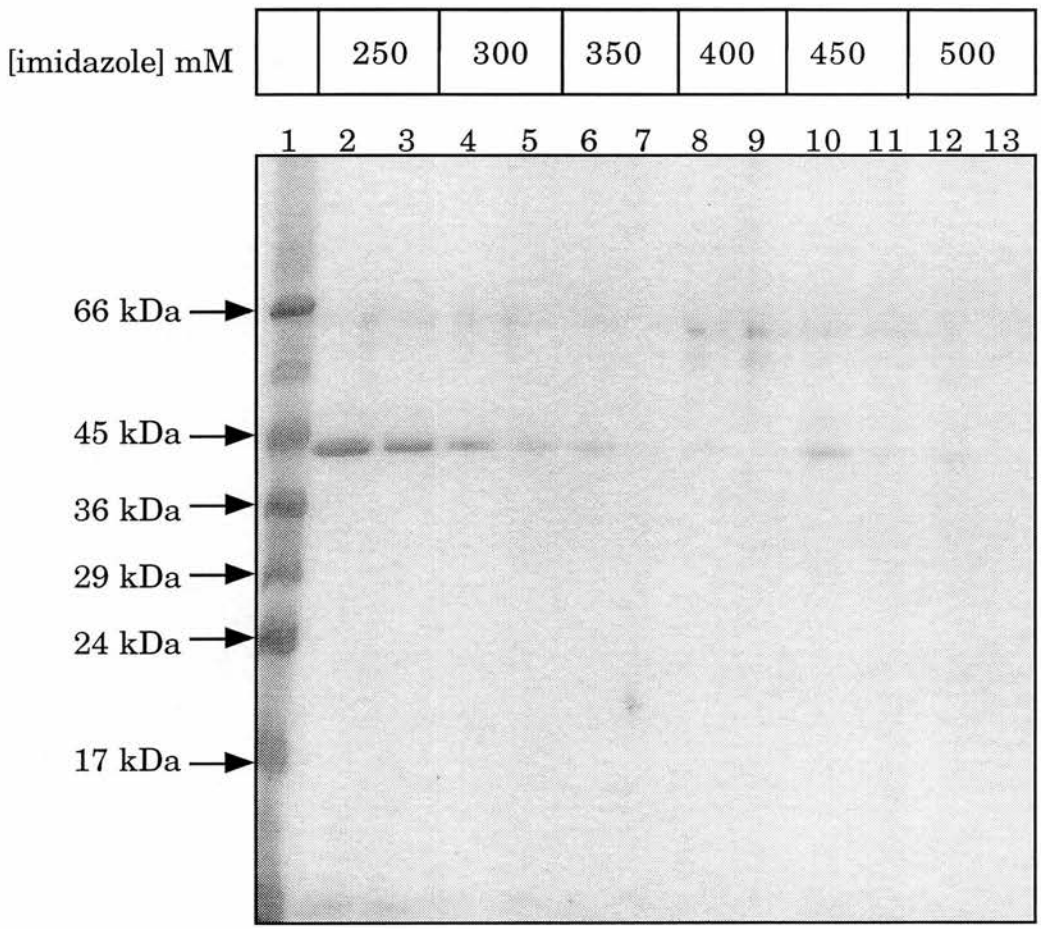
[imidazole] mM
250
300
350
400
450
500
1 2 3 4 5 6 7 8 9 10 11 12 13
66 kDa
45 kDa
36 kDa
29 kDa
24 kDa
17 kDa

Figure 3.17 Western blot showing final purification of His10-SytC protein

After the initial determination of elution conditions for the protein (Fig 3.17), purification was carried out as already outlined in Materials and Methods. Samples were taken of the starting protein and all the washes (20 µl), SDS-PAGE sample buffer added and 10 µl analysed by gel electrophoresis and Western blotting using cgm67 at a dilution of 1:5 for detection of the protein.

Lane 1	P20 fraction
Lane 2	S20 fraction before binding to Ni-NTA agarose
Lane 3	S20 fraction after binding to Ni-NTA agarose
Lane 4	First wash with buffer pH 8.0
Lane 5	First wash with buffer pH 6.0
Lane 6	Last wash with buffer pH 6.0
Lane 7	First 50 mM imidazole wash
Lane 8	Last 50 mM imidazole wash
Lane 9	First 200 mM imidazole elution
Lane 10	Second 200 mM imidazole elution
Lane 11	Third 200 mM imidazole elution
Lane 12	Fourth 200 mM imidazole elution
Lane 13	Fifth 200 mM imidazole elution
Lane 14	Sixth 200 mM imidazole elution

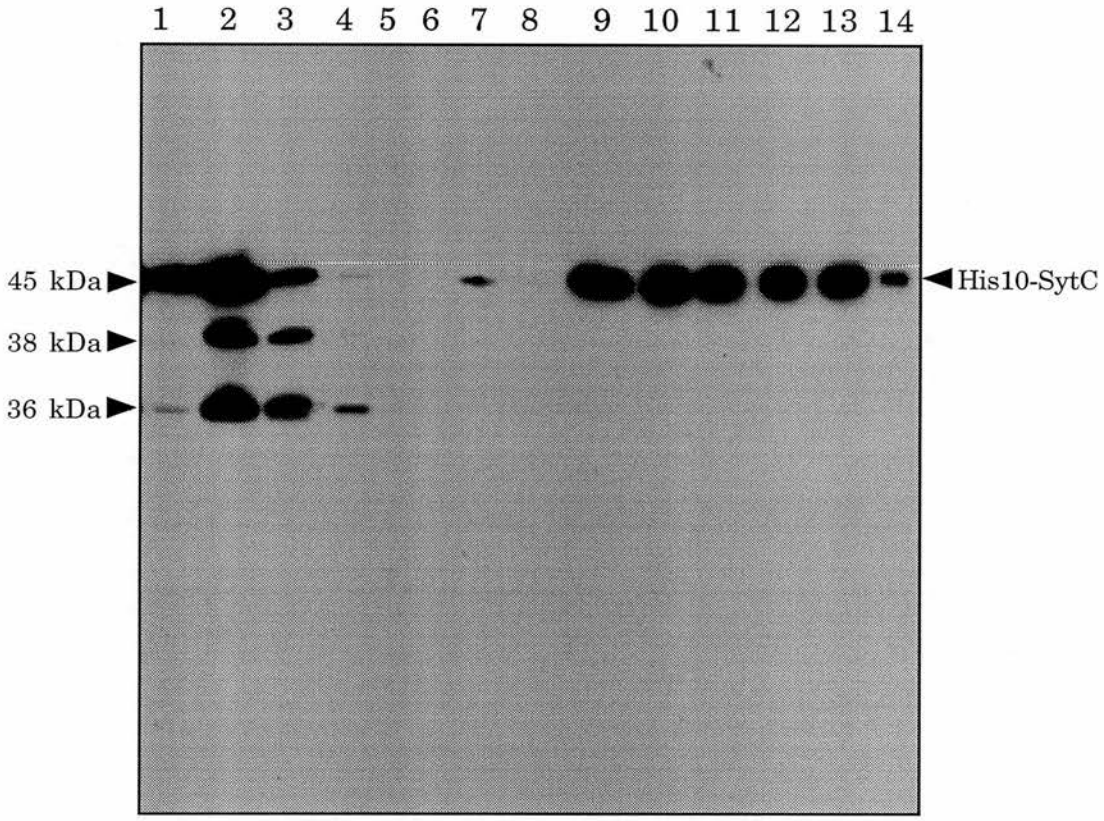
1 2 3 4 5 6 7 8 9 10 11 12 13 14
45 kDa
38 kDa
36 kDa
His10-SytC

Appendix to Chapter 3

Production of affinity purified polyclonal antibodies

Appendix to chapter 3

3.A.1 Production of affinity purified polyclonal antibody to SytC

During this study, a polyclonal antibody was raised against PrA-SytC. A fusion between the gene encoding Protein A from *S.aureus* and the *sytc* gene was made in the plasmid pLC100 and expressed in bacteria. The fusion protein produced was purified by affinity chromatography on IgG-Sepharose and used to immunise rabbits. Protein A fusions have been reported to give good immune responses (Lowenadler *et al* 1986) possibly due to the repetitive globular units of the Protein A moiety.

Affinity purification of the specific SytC antibodies was carried out as described in Materials and Methods using an analogous fusion between oligohistidine and SytC. The affinity-purified antibody was shown to recognise protein of the correct molecular size of 67 kDa in chromaffin granule membranes and synaptosomes as well as the His10-SytC fusion protein. It does not however detect the purified SytC protein very well even though this was part of the protein used to immunise the rabbits. Figures 3A1a and 3A1b show a comparison of the specificities of the affinity purified polyclonal antibody for SytC and the monoclonal anti-synaptotagmin cgm67.

It is difficult to explain this phenomenon. It may be possible that some structural property of SytC is absent in Western blots but this would certainly not explain why the antibody recognises other synaptotagmins and even SytC in another fusion protein. The antibody does of course recognise the PrA-SytC fusion protein but any IgG would also do the same. The only explanation in line with the facts, albeit the result of an

unfortunate coincidence, is that the polyclonal antibody has one main epitope on SytC at the junction region where thrombin cleaves the protein. As has been discovered, the thrombin recognition sequence and three extra amino acids are removed by the thrombin digestion process. It is likely that the sequence G P A G G K would be exposed at the junction between two globular domains of the fusion since it is relatively charged and therefore might be a potential target for the immune system.

Figure 3 A 1 **Specificities of polyclonal and monoclonal antibodies against synaptotagmin**

Samples of CGM (15 μg total protein), rat brain synaptosomes (10 μg protein), SytC (10 μg) and His10-SytC (10 μg) was subjected to gel electrophoresis and Western blotting. Polyclonal antibody raised against Pra-SytC and affinity purified using His10-SytC was used for detection at a dilution of 1:100 for 3A1a and monoclonal antibody cgm67 at a dilution of 1:4 was used for 3A1b.

3A1 a and b alike

Lane 1	Chromaffin granule membranes
Lane 2	Rat brain synaptosomes
Lane 3	SytC purified from Pra-SytC fusion
Lane 4	His10-SytC

3A 1a

3A 1b

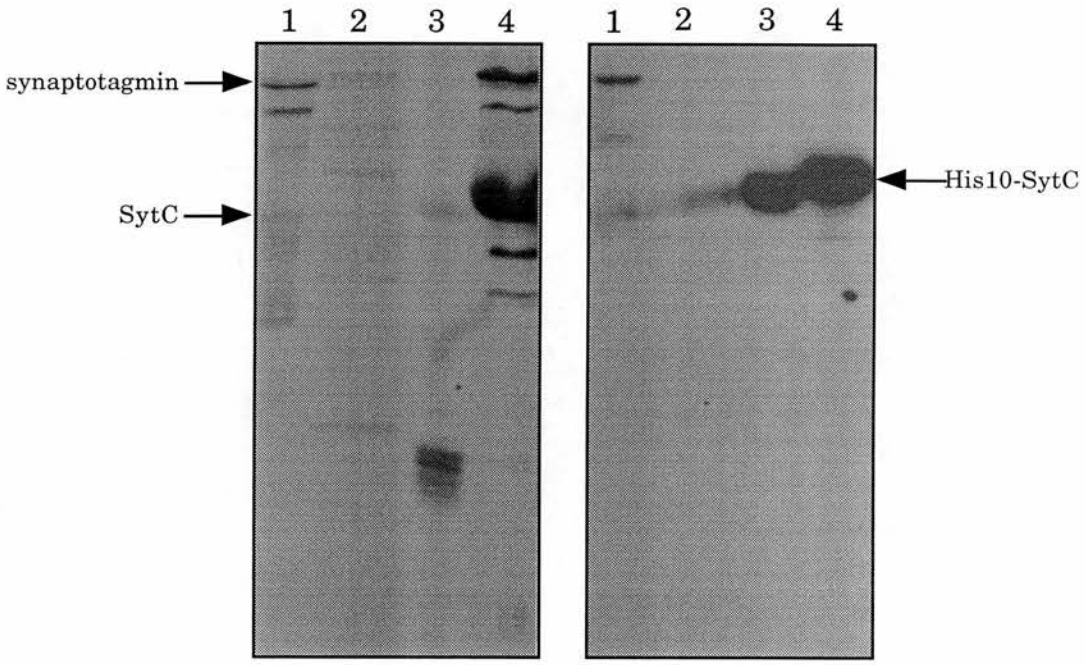

Chapter 4

Biochemical analysis of Ca^{2+}-dependent conformational change, interaction with calmodulin and phospholipids of recombinant SytC

4.1 Introduction

The recombinant cytoplasmic portion of synaptotagmin I (SytC) was purified using a combination of affinity chromatography and gel exclusion chromatography (see Chapter 3). It was then characterised using a variety of biochemical techniques.

4.2 Digestion of SytC with trypsin

SytC contains two regions with sequence homology to the regulatory domain of protein kinase C, which is responsible for Ca^{2+} and phospholipid binding in that protein and it has therefore been suggested that synaptotagmin also may have Ca^{2+} and phospholipid-binding properties. The binding of an ion such as Ca^{2+} to a protein may cause changes in its structure which can be detected by examining the structure of the protein. A simple and powerful technique for investigating conformational change in a protein is to examine its protease sensitivity in the presence and absence of the effector molecule.

Digestion of SytC with trypsin was performed at various trypsin concentrations for a fixed time period in the presence and absence of different divalent and trivalent metal cations. Figure 4.1 shows a comparison of the protease sensitivity of SytC in the presence of Ca^{2+}EGTA or with EGTA only. As can be seen in lane 4, the protein was completely digested with trypsin at 25 μg/ml in the absence of Ca^{2+} whereas it was resistant to even the highest trypsin concentration used (100 μg/ml) when Ca^{2+} was included (lane 12). One or both termini of the protein seem to be accessible to the protease as indicated by the appearance of a ladder of tryptic products, differing in size by only 2 kDa. This suggests that Ca^{2+} binds to SytC and causes the core of the protein to

fold up more tightly masking potentially trypsin-sensitive sites and leaving only the ends of the peptide chain available for proteolytic degradation. The same experiment was repeated substituting Ba^{2+}, Tb^{3+} or Mg^{2+} for Ca^{2+}. Ba^{2+} is reported to mimic Ca^{2+} in exocytosis whereas Mg^{2+} does not and Tb^{3+} has affinity for divalent cation binding sites (Hadad *et al* 1994, Zhang *et al* 1993). Figure 4.2a shows that Ba^{2+} also gave an increased resistance to trypsin digestion as did Tb^{3+} (figure 4.2b) whereas Mg^{2+} did not (figure 4.2c). These data suggest that Ba^{2+} and Tb^{3+} probably bind to the protein at the Ca^{2+} binding sites producing the same effect as Ca^{2+}. The efficiency of trypsin digestion with a control protein, lactate dehydrogenase, in the presence of each of these ions and EGTA alone was found to be unaffected (data not shown).

4.3 Probing Ca^{2+}-binding sites with Tb^{3+}

Tb^{3+} has been used to probe the divalent cation-binding sites of proteins (Hadad *et al* 1994, Zhang *et al* 1993) and has also been found to bind chromaffin granule membranes with affinity parameters suggesting protein involvement (Morris & Schober 1977). The ion has affinity for divalent cation binding sites in proteins and its fluorescence is greatly enhanced on binding to a protein. The fluorescence enhancement is then competitively inhibited by divalent cations with affinity for the protein. For this reason, Tb^{3+} was chosen as a convenient tool to probe the Ca^{2+}-binding sites of SytC.

Figure 4.3a shows the fluorescence enhancement of Tb^{3+} when added to a solution of SytC with the protein in excess. Under these conditions essentially all Tb^{3+} is bound at the start of the titration, allowing determination of the 'endpoint' when all the binding sites are filled. The

initial slope of the curve gave a specific change in fluorescence (ΔF) of 11 μM^{-1} and maximal binding of 24 μM Tb^{3+} overall as calculated from the fluorescence difference between the sample with protein and the background fluorescence due to Tb^{3+} alone at the maximum Tb^{3+} concentration used. Since the protein concentration used in this titration was 40 μM, the [Tb^{3+}] at the equivalence point would be expected to be at least 40 μM, or more if the protein has more than one binding site for the ion. It is however only just over half the expected value which suggests that not all the protein molecules are binding the cation. This is possibly due to overestimation of the concentration of SytC. However the the assumption that all the protein is functional may be incorrect or aggregation of the protein molecules may occur so that some of the cation-binding sites are inaccessible - certainly the protein is more prone to aggregation in a more concentrated solution. When titrations were performed with low concentrations of SytC, fluorescence enhancement showed typical hyperbolic characteristics (figure 4.3b). The curves appeared to approach saturation by 10-20 μM Tb^{3+} but there was a continued drift to higher fluorescence at the higher Tb^{3+} concentrations, even though the data was corrected for background Tb^{3+} fluorescence, suggesting that there was background light scattering due to protein aggregation which was distorting the result. In a third type of titration, successive quantities of SytC were added to solutions of fixed Tb^{3+} concentration; as expected, the fluorescence/protein concentration relationship was linear giving a series of almost parallel lines on a plot of fluorescence versus protein concentration (figure 4.4a). The slope of the lines for 10-50 μM Tb^{3+} is almost constant and gives a specific ΔF for Tb^{3+} binding of 0.19 nM^{-1} SytC when a plot of slope against [Tb^{3+}] was extrapolated to zero (figure 4.4b). To convert this to a specific fluorescence

as in figure 4.3a, it would be necessary to know how much protein in the titration is actually functional in the binding and also how many Tb^{3+} binding sites are on the protein. Although the number of binding sites could theoretically be estimated by Scatchard analysis, the amount of functional protein is impossible to measure without an assay for the protein's function. The fact that the gradient of the fluorescence enhancement changes dramatically at 100 μM Tb^{3+} is also an indication that the protein is being affected by the higher ion concentration. Indeed, aggregation became visible in the solution at 400 μM Tb^{3+} which called into question the specificity of the observed fluorescence increase.

Using the data obtained (figure 4.3b), a Hanes plot (figure 4.5a) was used to calculate K_d for Tb^{3+} from SytC. The value of K_d should be independent of the concentration of SytC and it was, in fact, fairly consistent in all the data sets at around 10 μM (table 4.1). The highest and lowest concentrations of SytC gave a value for K_d closer to 20 μM but this is still of the same order of magnitude as the other data sets. The Hill coefficient is close to 1 for all the measurements taken indicating that there is no cooperativity of binding.

The data were also analysed by a Scatchard plot using the specific fluorescence calculated in fig 4.3a (11 μM^{-1}) and this plot is shown in figure 4.6. Unfortunately, the specific fluorescence did not seem to be a reliable conversion factor since it gave values of bound Tb^{3+} greater than the total Tb^{3+} present for many data points which consequently had to be ignored when plotting the data if a straight line was to be obtained.[1] It is difficult to be confident of the accuracy of the specific fluorescence measurement

[1] The points that can be plotted will still represent an overestimate of Tb^{3+} bound since the specific fluorescence is erroneous.

since the sensitivity settings for the fluorescence spectrometer were different for separate experiments. The value of 11 μM^{-1} is however very close to the initial slope of the curve for the highest protein concentration in figure 4.3b and so could be considered a reasonable estimate. An alternative possibility is that the functional protein present in the determination of specific fluorescence is much lower than the apparent protein concentration giving rise to inaccurate parameters. The values of K_d obtained were fairly consistent in the region of 2-3 μM which although smaller are of the same order of magnitude than those obtained by the Hanes analysis. Scatchard analysis was attempted because it should give an indication of number of binding sites for Tb^{3+} on SytC which may be related to the number of Ca^{2+} binding sites if the two ions compete for the same sites. The values obtained ranged from 8 to 14 binding sites per SytC molecule. This is rather high given that the number of Ca^{2+} binding sites on the protein, assumed from structural analysis, is 4. The number of binding sites will be an overestimate because of the specific fluorescence used as a conversion factor but taken at face value this suggests that Tb^{3+} may not binding in the same way as Ca^{2+} to the protein. This conclusion was further supported when titrations were carried out using the two ions in a competitive binding assay discussed below.

Further titrations were carried out in the presence of various concentrations of Ca^{2+} in order to determine whether competition for binding to SytC was occurring between Ca^{2+} and Tb^{3+}. It was expected that Ca^{2+} would compete for binding sites on SytC and would therefore reduce the fluorescence enhancement seen when Tb^{3+} was added to a protein solution. This method would then be a convenient way of analysing Ca^{2+} binding fluorimetrically. As can be seen from figure 4.5b, Ca^{2+} did not

give parameters consistent with this hypothesis (except for the 15 μM Ca^{2+} condition). In addition to this, it was impossible to reduce fluorescence (displace Tb^{3+} from SytC) by the addition of Ca^{2+} after the Tb^{3+} had been added suggesting either that the Tb^{3+} was binding irreversibly to SytC or that it was binding to sites other than the Ca^{2+} binding site.

It is possible that Ca^{2+} is not binding optimally to SytC because the Ca^{2+}-binding properties of the protein are highly phospholipid dependent. Including phospholipid vesicles in this assay was not feasible because they interfered with the fluorescence measurements by scattering light and they also aggregated upon addition of Ca^{2+} further distorting the data. The methodology was tested using calmodulin as a model Ca^{2+} binding protein and was found to be satisfactory but of course, this is a protein with a very high affinity for Ca^{2+} and a much lower affinity for Tb^{3+} (table 4.1). The parameters calculated with the data obtained are summarised in table 4.1 but the fluorescence data for competition between Ca^{2+} and Tb^{3+} were considered too unreliable to interpret and it was decided to proceed no further with this analysis.

4.4 Binding of SytC to phospholipid vesicles

The phospholipid-binding properties of SytC were investigated by studying the binding of the protein to phospholipid vesicles of various compositions in the presence and absence of Ca^{2+}. SytC was mixed with phospholipid vesicles and incubated at room temperature for 15 minutes. The vesicles were then pelleted by centrifugation at 100,000g for 30 min. Figure 4.7a shows that the protein found bound to phospholipid vesicles after incubation at room temperature and separation of the vesicles from

solution by centrifugation. Figure 4.7b shows the corresponding protein left in the supernatant after the centrifugation to remove the vesicles. In the presence of EGTA (no Ca^{2+}) there was a low level of binding of SytC to the phospholipid vesicles, which did not appear to be dependent on the composition of the vesicles or even on the presence of vesicles at all, since the sample with no phospholipid also contains a small amount of protein in the pellet. This would suggest that there was a low level of aggregation of the protein even under these conditions. The amount of the protein in the pellets was very low and was probably over-represented because the immunological detection technique is very sensitive. The supernatants from this incubation still contained most of the protein. The background levels of protein in the lipid pellet completely disappeared in the presence of Ca^{2+} suggesting that the ion had had some effect on the solubility of the protein (lane 6). In these conditions, specific binding was seen with vesicles containing PS, PI and PC. The protein had bound in the largest quantities to PI-containing vesicles and this was supported by the fact that the PI supernatant was the only one to be depleted of SytC. An attempt was made to quantitate the binding of SytC using densitometric scanning but proved difficult because the Western blotting detection signal is very sensitive and easily saturated by even small amounts of protein. A calibration blot containing different amounts of protein did not give sufficiently linear measurements to use as a basis for quantitation.

A similar experiment was carried out using phospholipid vesicles of more complex lipid composition. In the presence of EGTA (figure 4.8a), most of the protein remained in solution although some specific binding was observed to PS/PI and PS/PE vesicles. Traces of protein could be seen bound to PS/PC and PI/PE vesicles but these amounts were negligible given the sensitivity of the detection method. None of the vesicles caused

enough protein to bind to reveal depletion of protein from the supernatant (figure 4.8b). In the presence of Ca^{2+}, substantial binding occurred particularly to PS/PE, PC/PI, PI/PE and PS/PC/PI vesicles since these conditions also showed protein depletion in the supernatant (figure 4.8c and d). Some protein also bound to PS/PI vesicles but although such binding was detectable in the pellets it was not accompanied by substantial depletion of the supernatant.

4.5 Interaction of SytC with immobilised calmodulin

Synaptotagmin from chromaffin granule membranes has been reported to bind calmodulin in a Ca^{2+} - dependent manner (Hikita et al 1984) and the cytoplasmic domain purified from a trypsin digestion of chromaffin granules was shown to contain the calmodulin binding site (H.B.Tugal, PhD thesis 1991). The Ca^{2+}-dependent calmodulin binding properties of SytC were therefore investigated by mixing purified recombinant protein with immobilised calmodulin in the presence or absence of Ca^{2+} using native synaptotagmin from the glycoprotein - rich fraction of CGM as a control for the experiment. Figure 4.9a shows that a large proportion of SytC bound to immobilised calmodulin in the presence of Ca^{2+} and was subsequently eluted by the addition of EGTA. All the native synaptotagmin also bound to the immobilised calmodulin in the presence of Ca^{2+}; although this suggests that binding of full-length synaptotagmin is more efficient, it was present at a much lower concentration (not determined) than the recombinant protein. The amount of recombinant protein used exceeded the binding capacity of the immobilised calmodulin used by a factor of 2. It has already been shown that Ba^{2+} mimics the effect of Ca^{2+} on SytC, as determined by proteolytic cleavage (section 4.2). Since Ca^{2+} binds both calmodulin and SytC whereas it is known that Ba^{2+}

does not bind calmodulin (Klee 1988), this experiment was repeated in the presence of Ca^{2+} or Ba^{2+} to determine which protein stimulated the binding. It can be seen from figure 4.9b that only Ca^{2+} caused significant depletion of protein from the supernatant with an equal quantity of protein in the eluate and still bound to the calmodulin agarose. No protein could be seen in the eluate when Ba^{2+} was used. This suggests that the binding between calmodulin and SytC is primarily stimulated by interaction between Ca^{2+} and calmodulin rather than between Ca^{2+} and SytC because Ba^{2+} would be expected to reproduce the protein interaction if it were dependent on SytC.

4.6 Fluorimetric analysis of interaction between calmodulin and SytC

The dansyl molecule gives a characteristic fluorescence and can be chemically attached to proteins.. The fluorescence may change if the protein interacts closely with another molecule. This was used as the basis of a fluorimetric assay for the Ca^{2+}-dependent interaction of calmodulin and SytC. Calmodulin was modified by the addition of a dansyl moiety in a 1:1 molar ratio.Figure 4.10 shows the typical spectrum obtained from a solution of dansyl-calmodulin. The fluorescence showed a large decrease of maximum fluorescence when 1 μM free Ca^{2+} was added (figure 4.11a) and smaller decreases up to 50 μM free Ca^{2+}. At higher Ca^{2+} concentrations, the fluorescence increased again and at any point in the titration, the starting fluorescence could be restored by the addition of enough EGTA to chelate virtually all of the Ca^{2+} added. It was also possible to increase the fluorescence by the addition of SytC in calmodulin:SytC molar ratios of 2:1. 1:1 and 1:2(data not shown). This could be due to an interaction between the two proteins or simply because

some of the Ca^{2+} is being removed from solution by binding to SytC (although this should be negligible in a Ca^{2+} buffered solution) but it is most likely to be due to a Ca^{2+}-independent protein interaction, which SytC caused even when added to dansyl calmodulin at zero Ca^{2+} (figure 4.11b). The intensity across the whole spectrum of dansyl fluorescence appeared to increase upon addition of SytC in the absence of Ca^{2+} and the peak of the spectrum shifted slightly to a lower wavelength as the SytC component was increased. This effect could not be accounted for by a change in fluorescence when SytC was added to a buffer solution with or without Ca^{2+} since the change was minimal. It was therefore decided to begin with a Ca^{2+}-buffered solution of dansyl calmodulin and SytC in a 1:1 molar ratio and add increments of Ca^{2+} to it since the starting spectrum would then already take into account the increase in fluorescence produced by mixing the two proteins and any further changes should be due to the Ca^{2+} additions alone. Figure 4.12a shows the change in fluorescence of dansyl calmodulin alone and of a protein mixture over a wide range of Ca^{2+} concentrations. The values are corrected for the difference in starting fluorescence due to the SytC component. Since no change occurred in the fluorescence of SytC alone in similar conditions, the difference indicates a Ca^{2+}-dependent interaction between the two proteins. Similar titrations with Ba^{2+} and Mg^{2+} caused no difference in the fluorescence response of the dansyl calmodulin alone compared to a protein mixture confirming that the interaction is due to the effect of Ca^{2+} on calmodulin rather than SytC. The main difference occurred within 5-20 μM Ca^{2+}. Figure 4.12b shows a titration in the 10 μM range with smaller increments of Ca^{2+} showing a steady fall in fluorescence in dansyl calmodulin whereas a mixture of the two proteins showed a fall in fluorescence followed by a reversal at 3 μM Ca^{2+} where the fluorescence began to increase.

4.7 Conclusions

Five biochemical approaches have been described which have allowed some assessment of the binding properties of SytC with other molecules. It has been shown that Ca^{2+}, and also other metal ions which have affinity for Ca^{2+} binding sites, bind to SytC causing it to alter conformation to the extent that it becomes resistant to trypsin digestion. An attempt to further study the Ca^{2+} binding properties of the protein using Tb^{3+} as a fluorescent probe and competitive substrate for Ca^{2+} binding sites was unsuccessful because the Tb^{3+} appeared to bind irreversibly to the protein, probably due to some adverse effect the ion had on the tertiary structure and solubility of the protein. SytC also demonstrates Ca^{2+}-stimulated phospholipid binding properties as would be predicted from the presence of regions homologous to the regulatory domain of protein kinase C. SytC shows particular affinity for phosphatidyl inositol and for combinations of lipids which are charged. The binding of SytC to calmodulin has been illustrated by the interaction with immobilised calmodulin and also by a change in fluorescence of a reporter molecule attached to the calmodulin when the two proteins were mixed. Both of these techniques show that the interaction is stimulated by the effect of Ca^{2+} on calmodulin rather than on SytC.

Figure 4.1 Trypsin digestion of SytC with Ca^{2+}

Digestions of SytC with varying trypsin concentrations were performed in the presence of 100 μg/ml phospholipid vesicles (40% (w/v) each of PS and PC, 20% (w/v) cholesterol) and in the presence or absence of 100 μM Ca^{2+} in 200 μl digest volumes as described in Materials and Methods. 5 μl of each reaction was analysed by SDS-PAGE and Western blotting using cgm67 at a dilution of 1:5 for detection.

Lanes 1-6	Digestions in the presence of EGTA
Lanes 8-13	Digestions in the presence of 100 μM free Ca^{2+}

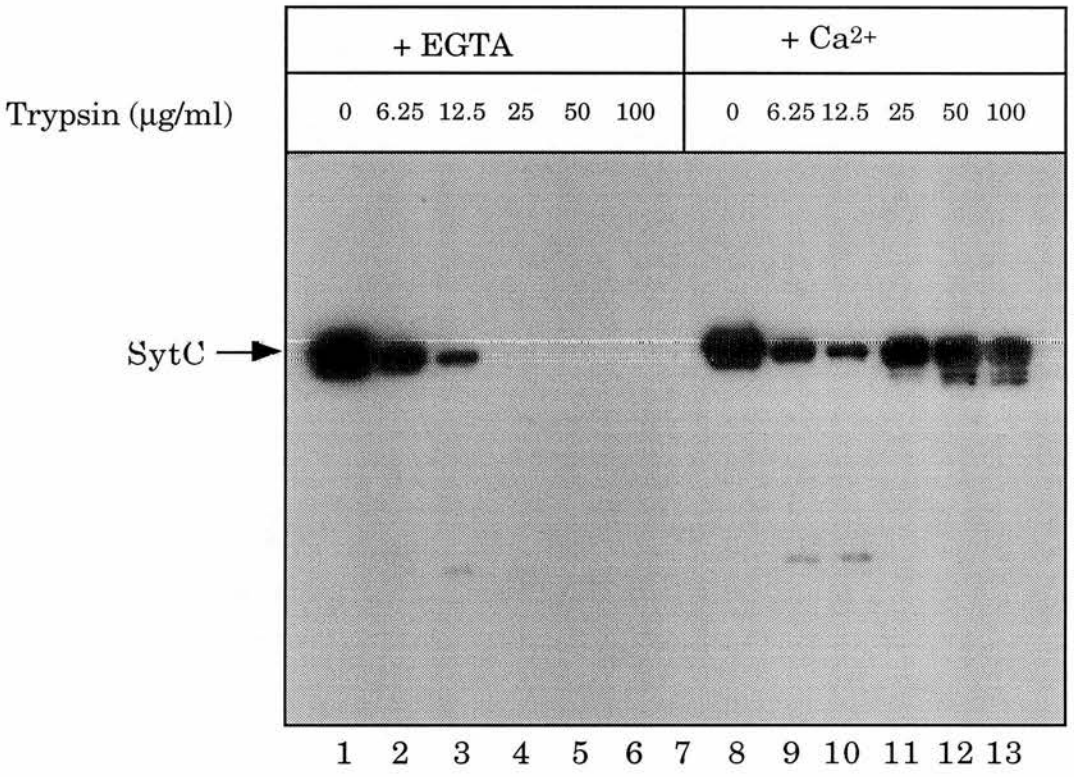
+ EGTA
+ Ca2+
Trypsin (μg/ml)
0 6.25 12.5 25 50 100
0 6.25 12.5 25 50 100
SytC
1 2 3 4 5 6 7 8 9 10 11 12 13

Figure 4.2 Trypsin digestion of SytC with Ba^{2+} Tb^{3+} and Mg^{2+}

Digestions were performed as described in Materials and Methods substituting 100 μM Ba^{2+}, Tb^{3+} or Mg^{2+} for Ca^{2+}. 5 μl of each reaction was analysed by SDS-PAGE and Western blotting using cgm67 at a dilution of 1:5 for immunodetection.

Figure 4.2a	Lanes 1-6	Digestions performed with Ba^{2+}
Figure 4.2b	Lanes 1-6	Digestions performed with Tb^{3+}
Figure 4.2c	Lanes 1-6	Digestions performed with Mg^{2+}

4.2a

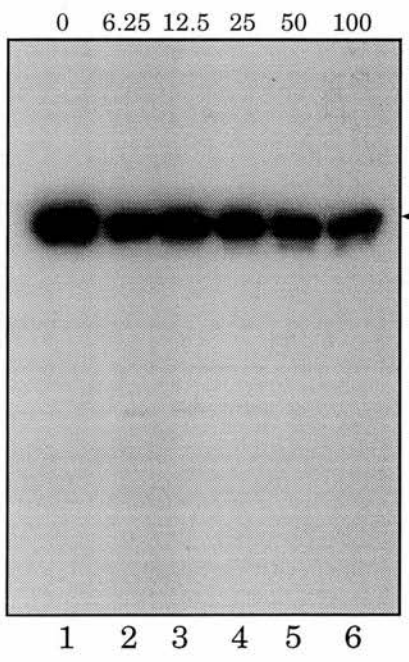

[Trypsin] µg/ml

SytC

4.2b

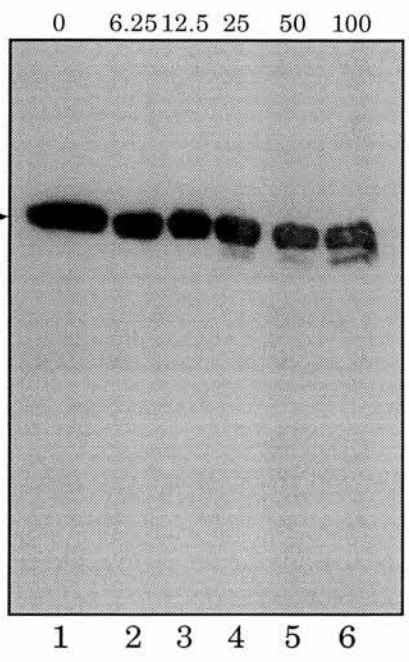

4.2c

[Trypsin] µg/ml

SytC

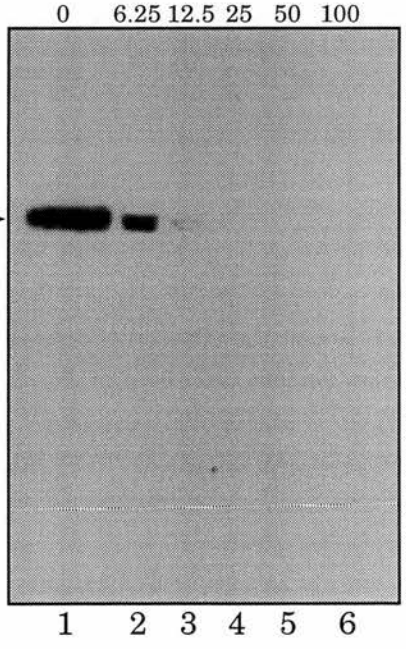

Figure 4.3 Titration of SytC with Tb^{3+}

Fluorimetric titrations were performed as outlined in Materials and Methods. A 10 mM $TbCl_3$ solution was used to make additions to a 40 μM solution of SytC in Hepes.NaOH pH 7.4 to give Tb^{3+} concentrations of up to 120 μM. The emission was recorded at 580nm. All figures were corrected for dilution effects which were no greater than 5%.

Figure 4.3a Fluorescence enhancement versus Tb^{3+} added in a 40 μM protein solution

Figure 4.3b Fluorescence enhancement versus Tb^{3+} added in solutions of 1 - 4 μM protein concentration. Figures are corrected for background fluorescence due to Tb^{3+} alone which is also shown as a separate line 'no SytC'. Note that the fluorimeter sensitivity is set higher in figure 4.3b than in 4.3a

4.3a

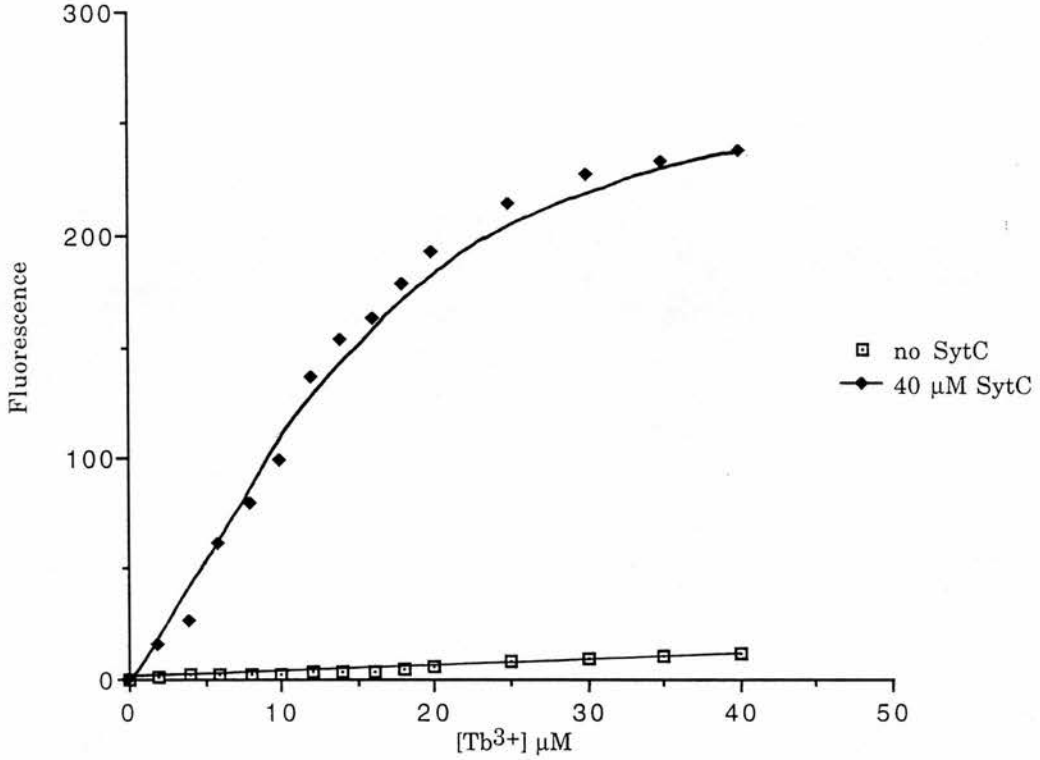
300
200
100
0
Fluorescence
0
10
20
30
40
50
[Tb3+] µM
no SytC
40 µM SytC

4.3b

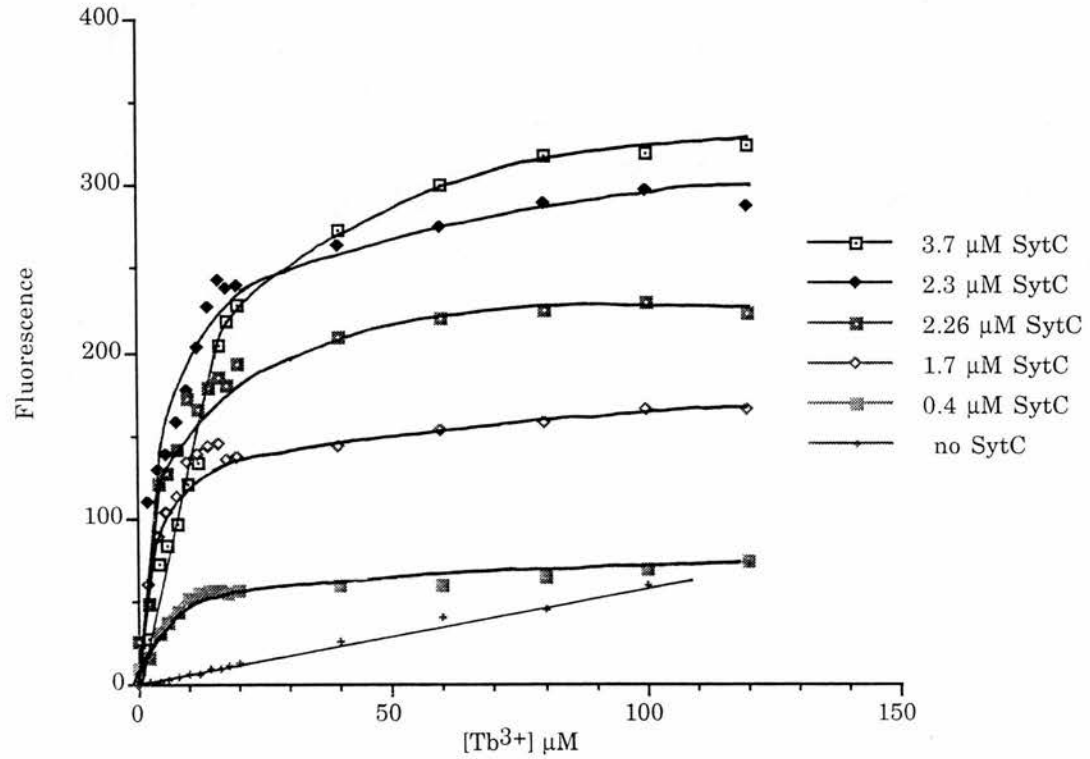
400
300
200
100
0
Fluorescence
0
50
100
150
[Tb3+] µM
3.7 µM SytC
2.3 µM SytC
2.26 µM SytC
1.7 µM SytC
0.4 µM SytC
no SytC

Figure 4.4 Titration of Tb^{3+} with SytC

Additions of SytC protein were made to $TbCl_3$ solutions in Hepes.NaOH pH 7.4 to give protein concentrations of up to 400 nM (4.4a). The slope of the line for the concentrations between 10-50 μM Tb^{3+} in figure 4.4a were plotted against the Tb^{3+} concentration and extrapolated to zero in figure 4.4b.

4.4a

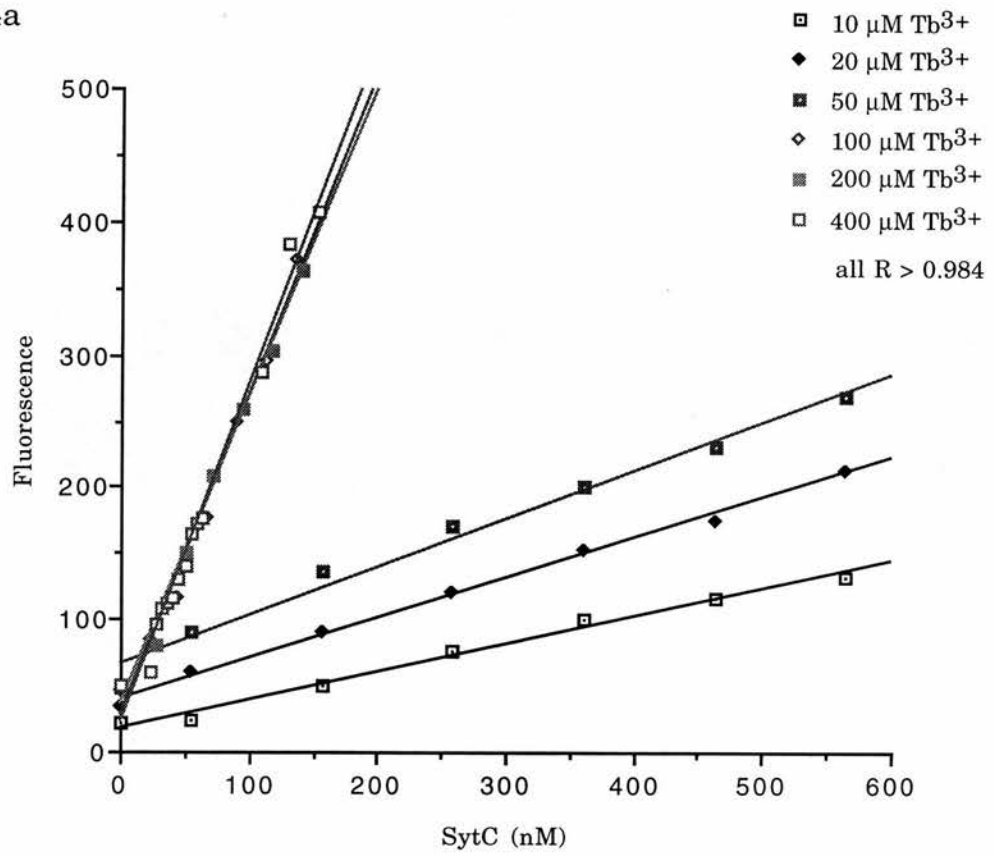
10 μM Tb3+
20 μM Tb3+
50 μM Tb3+
100 μM Tb3+
200 μM Tb3+
400 μM Tb3+
all R > 0.984
Fluorescence
SytC (nM)
0
100
200
300
400
500
600

4.4b

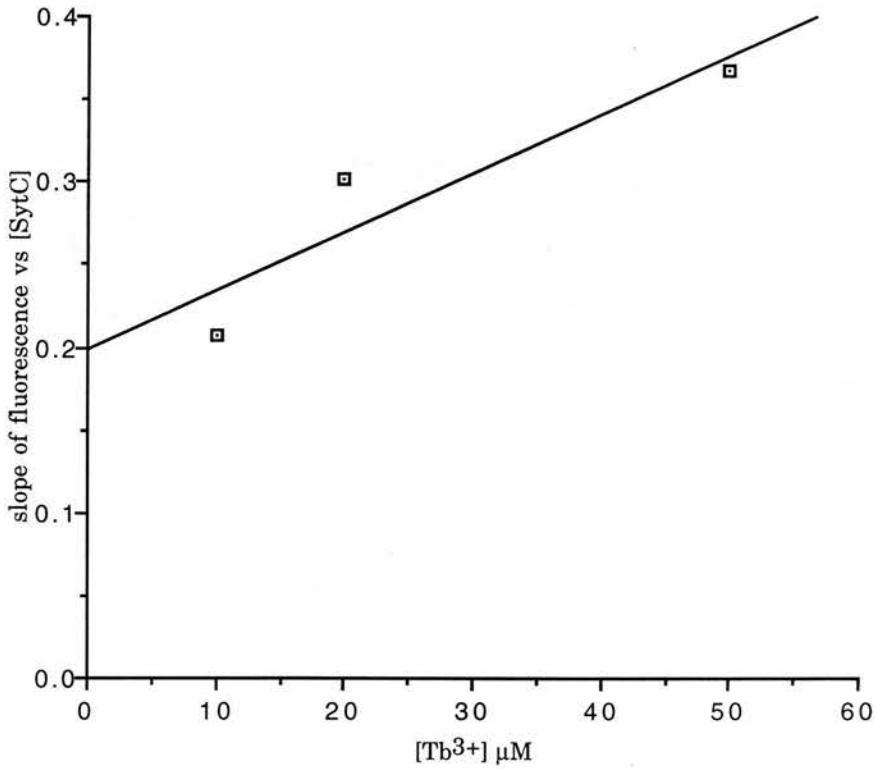
slope of fluorescence vs [SytC]
[Tb3+] μM
0.0
0.1
0.2
0.3
0.4
0
10
20
30
40
50
60

Figure 4.5a **Hanes plot of binding of Tb^{3+} to SytC**

Fluorescence emissions were recorded in protein solutions of 0.4 - 3.7 μM with additions of $TbCl_3$ up to 120 μM (see figure 4.3b). The data were plotted in a Hanes transformation and the K_d for Tb^{3+} found from the graph. Regression lines were fitted using a computer program.

Figure 4.5b **Inhibition of Tb^{3+} fluorescence enhancement by Ca^{2+}**

Titrations of up to 80 μM Tb3+ were made to a 0.5 μM SytC solution including Ca^{2+} in varying concentrations. Figures are corrected for background fluorescence due to Tb^{3+} alone.

4.5a

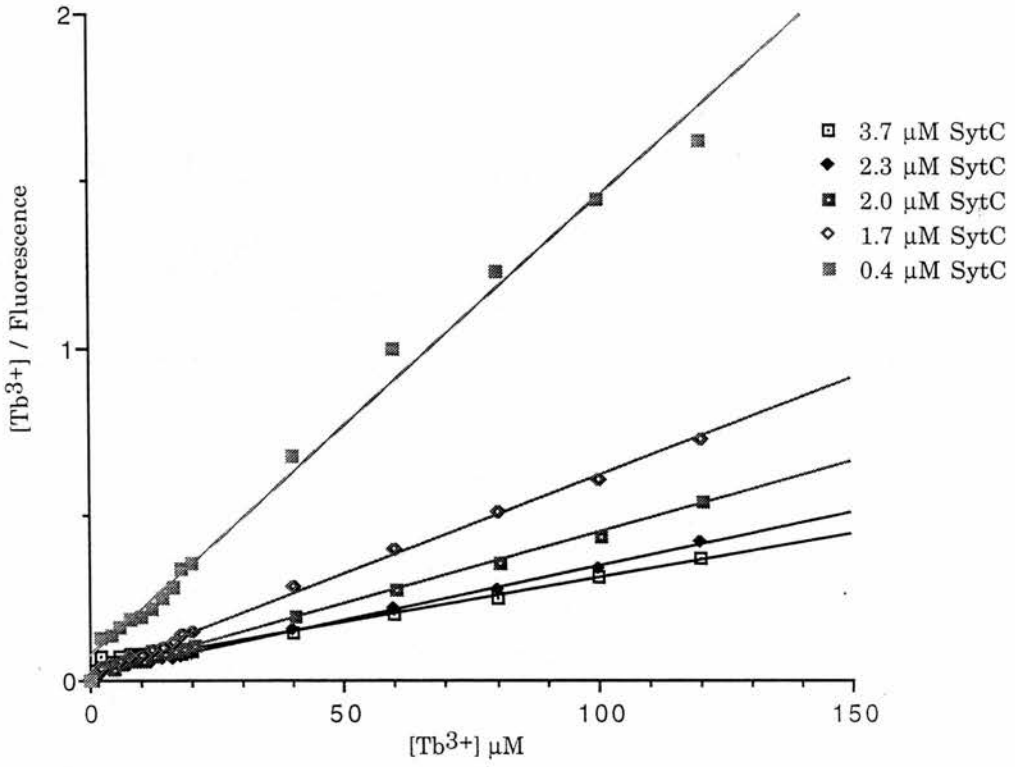
2
1
0
0
50
100
150
[Tb3+] / Fluorescence
[Tb3+] µM
3.7 µM SytC
2.3 µM SytC
2.0 µM SytC
1.7 µM SytC
0.4 µM SytC

4.5b

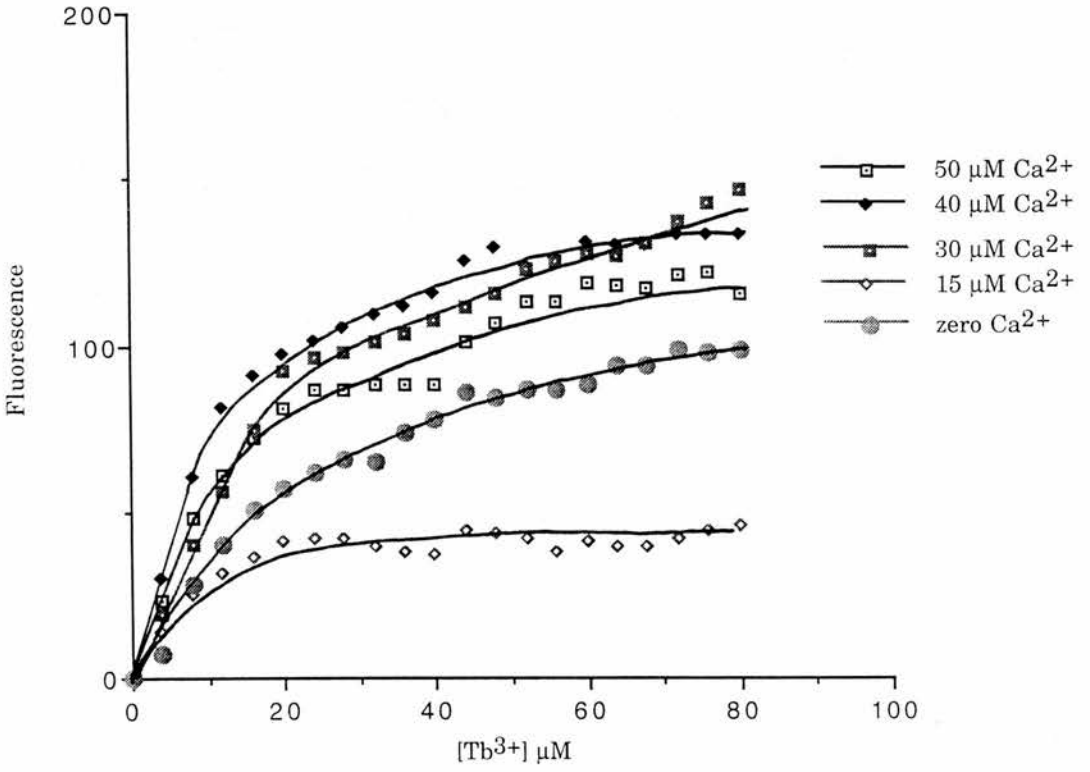
200
100
0
0
20
40
60
80
100
Fluorescence
[Tb3+] µM
50 µM Ca2+
40 µM Ca2+
30 µM Ca2+
15 µM Ca2+
zero Ca2+

Table 4.1 Parameters for interaction of SytC and Tb^{3+}

The table shows K_d for Tb^{3+} calculated from Hanes plots of the fluorescence data obtained and the Hill coefficient for the data. The Hill coefficient was calculated from the gradient of a plot of $\log_{10} [\Delta F / \Delta F_{max} - \Delta F]$ versus $\log_{10} Tb^{3+}$. ΔF_{max} was calculated from the gradient of the Hanes transformations of the data. Parameters are shown for SytC and calmodulin used as a control protein.

[SytC] μM	K_d (Tb^{3+}) μM	Hill coefficient
3.7	17.2	1.09
2.3	8.49	1.04
2.0	8.34	1.08
1.7	6.78	1.04
0.4	5.1	0.83
Calmodulin	55	0.84

Figure 4.6 Scatchard analysis of Tb^{3+} binding

Using the specific fluorescence value determined from figure 4.3a to calculate the concentration of bound and free Tb^{3+}, the data from figure 4.3b were transformed and plotted according to Scatchard and used to calculate number of binding sites for Tb^{3+} on SytC.

Scatchard plot for
0.4 μM SytC

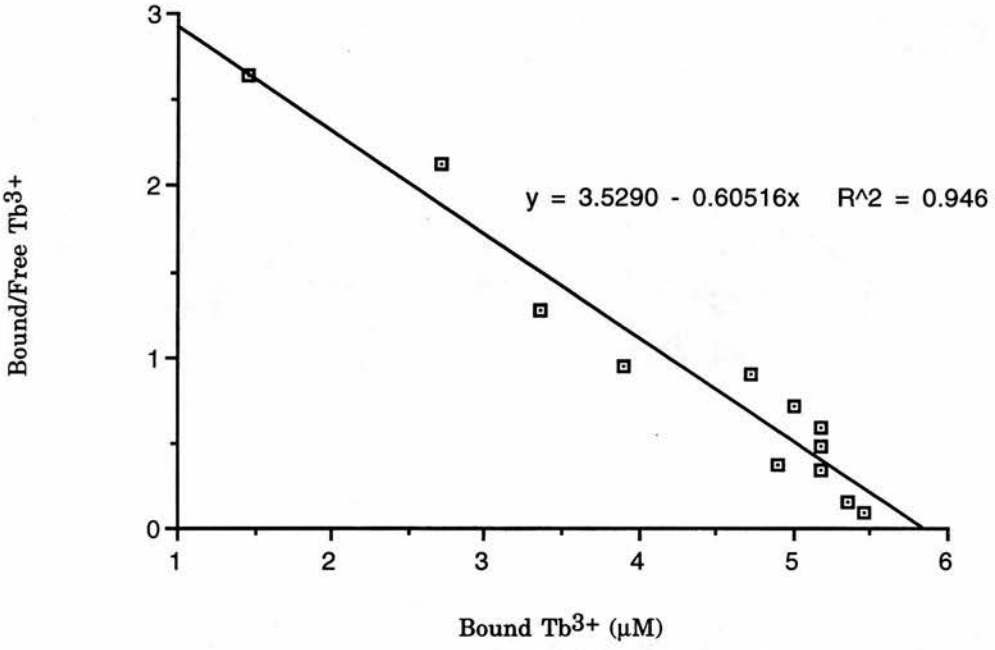

Scatchard plot for
2.3 μM SytC

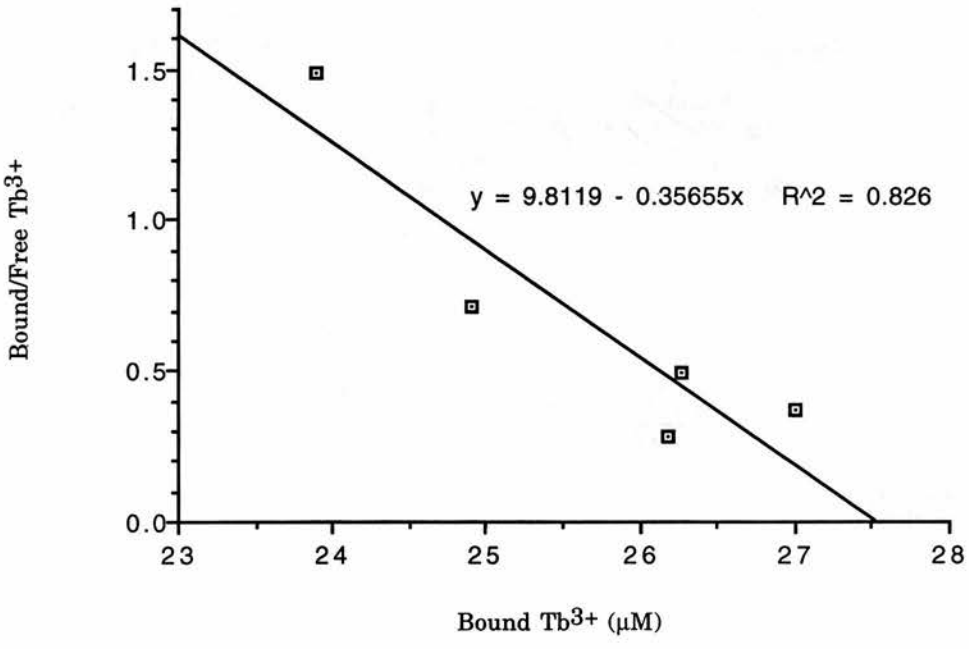

Scatchard plot for
3.7 μM SytC

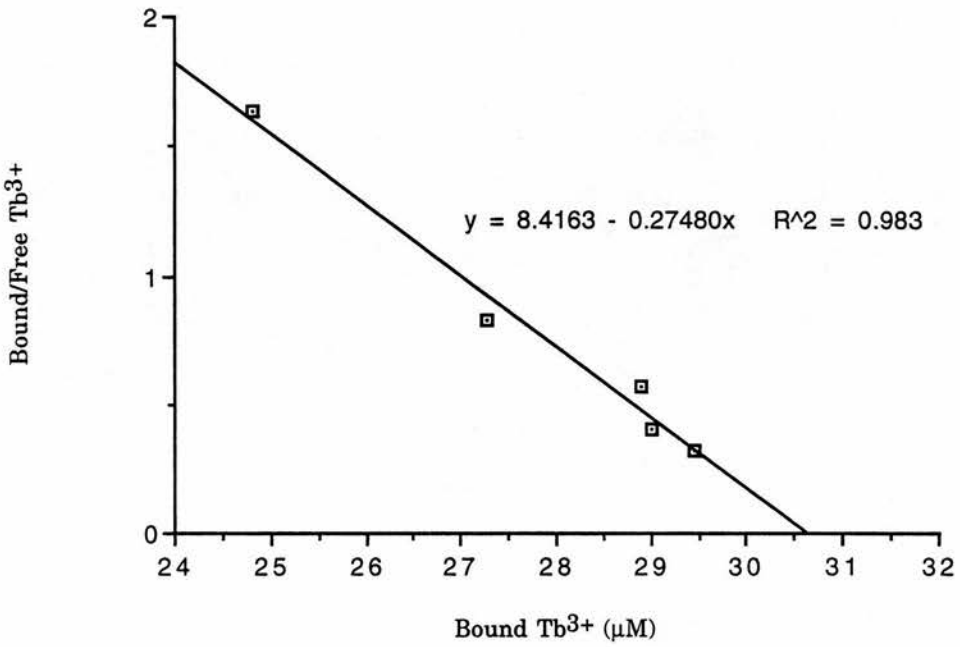

Parameters obtained by Scatchard analysis

SytC (μM)	K_d (μM)	Bmax (μM)	binding sites for Tb^{3+}
0.4	1.67	5.8	14
2.3	2.77	27.5	12
3.7	3.70	30.6	8

Figure 4.7 Binding of SytC to phospholipid vesicles of simple composition

Binding of SytC to phospholipid vesicles was carried out as described in Materials and Methods using vesicles composed of 20% (w/v) cholesterol and 80% (w/v) PS, PI, PC or PE. 5 µl samples of the lipid pellets and the TCA precipitated supernatants were analysed by SDS-PAGE and Western blotting using cgm67 at a dilution of 1:5 for detection.

Figure 4.7a

Lane 1 Molecular weight standards
Lane 2 Blank
Lane 3 Protein pellet with no lipid+EGTA
Lane 4 Protein pellet with PS+EGTA
Lane 5 Protein pellet with PI+EGTA
Lane 6 Protein pellet with PC+EGTA
Lane 7 Protein pellet with PE+EGTA
Lane 8 Blank
Lane 9 Protein pellet with no lipid+Ca^{2+}
Lane 10 Protein pellet with PS+Ca^{2+}
Lane 11 Protein pellet with PI+Ca^{2+}
Lane 12 Protein pellet with PC+Ca^{2+}
Lane 13 Protein pellet with PE+Ca^{2+}

Figure 4.7b

Lane 1 Molecular weight standards
Lane 2 Blank
Lane 3 Supernatant with no lipid+EGTA
Lane 4 Supernatant with PS+EGTA
Lane 5 Supernatant with PE+EGTA
Lane 6 Supernatant with PC+EGTA
Lane 7 Supernatant with PI+EGTA
Lane 8 Blank
Lane 9 Supernatant with no lipid+Ca^{2+}
Lane 10 Supernatant with PS+Ca^{2+}
Lane 11 Supernatant with PE+Ca^{2+}
Lane 12 Supernatant with PC+Ca^{2+}
Lane 13 Supernatant with PI+Ca^{2+}

4.7a

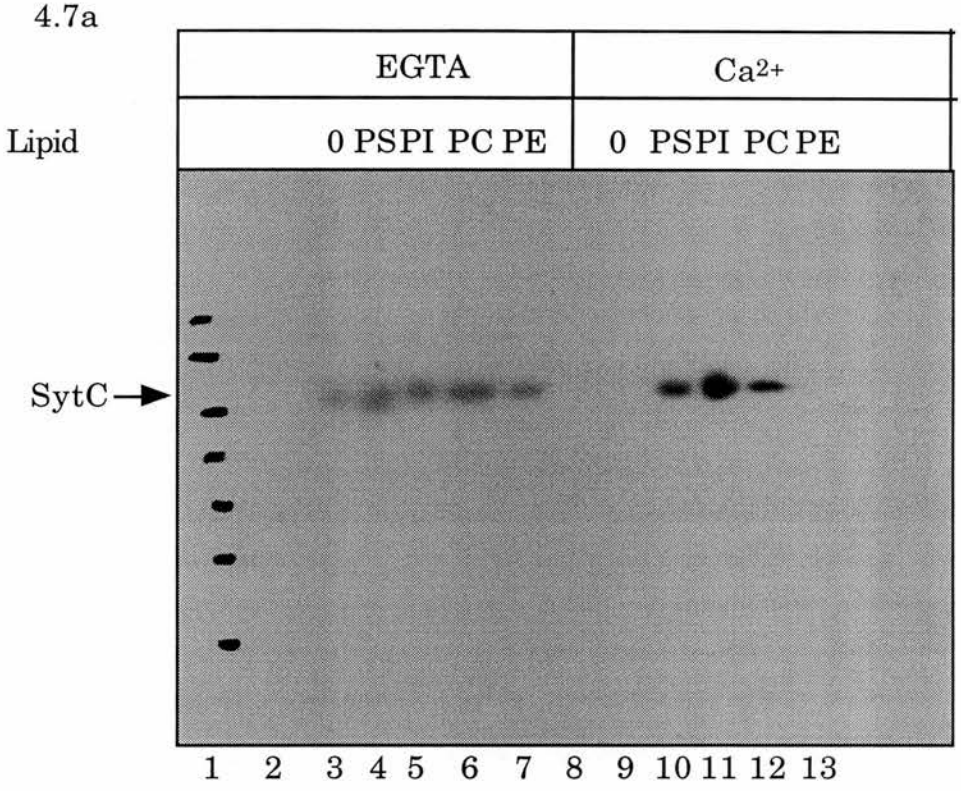
EGTA
Ca2+
Lipid
0 PS PI PC PE
0 PS PI PC PE
SytC
1 2 3 4 5 6 7 8 9 10 11 12 13

4.7b

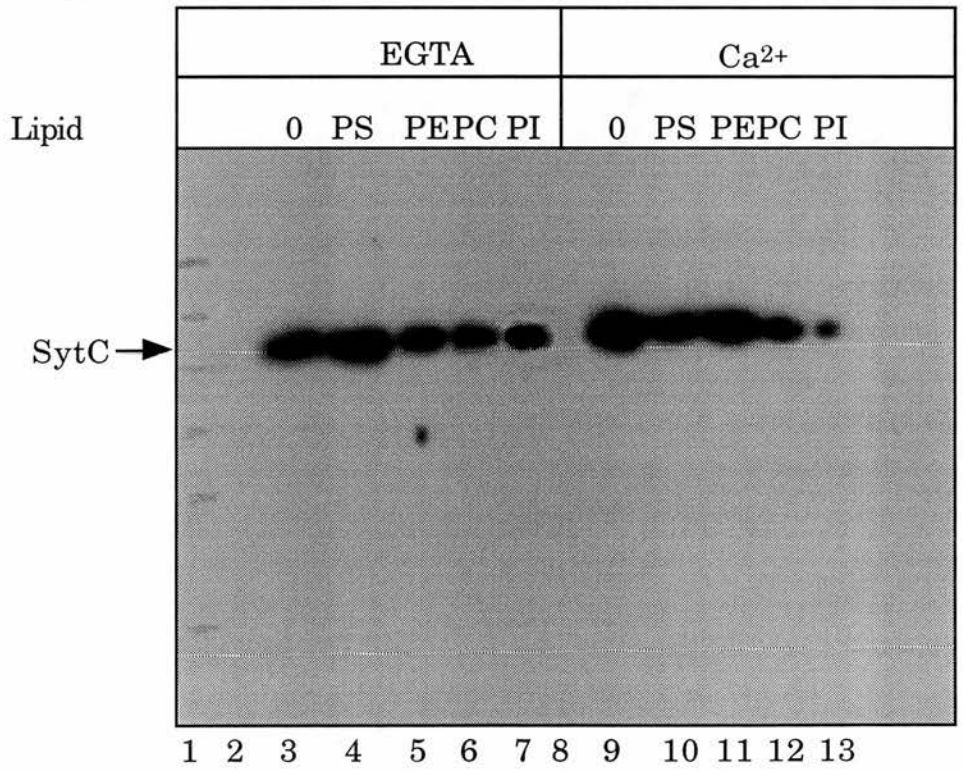
EGTA
Ca2+
Lipid
0 PS PE PC PI
0 PS PE PC PI
SytC
1 2 3 4 5 6 7 8 9 10 11 12 13

Figure 4.8 Binding of SytC to phospholipid vesicles of complex composition

Phospholipid vesicle binding assays were carried out as already outlined using vesicles of 20% (w/v) cholesterol and 40% (w/v) each of two phospholipids. All possible combinations of four lipids were used: PS/PC, PS/PI, PS/PE, PC/PI, PC/PE and PI/PE and lipid vesicles of a mixed composition more typical of biological membranes were also used (25% (w/v) cholesterol, 5% (w/v) PI, 60% (w/v) PC and 10% (w/v) PS. 5 µl of each lipid pellet and the corresponding TCA precipitated supernatant were analysed by SDS-PAGE and Western blotting using cgm67 at a dilution of 1:5 for detection.

All gels were loaded similarly as outlined below

Figure 4.8a	Lipid pellets with EGTA
Figure 4.8b	Supernatants with EGTA
Figure 4.8c	Lipid pellets with Ca^{2+}
Figure 4.8d	Supernatants with Ca^{2+}

Lane 1	No lipid added
Lane 2	PS/PC vesicles
Lane 3	PS/PI vesicles
Lane 4	PS/PE vesicles
Lane 5	PC/PI vesicles
Lane 6	PC/PE vesicles
Lane 7	PI/PE vesicles
Lane 8	PS/PC/PI vesicles

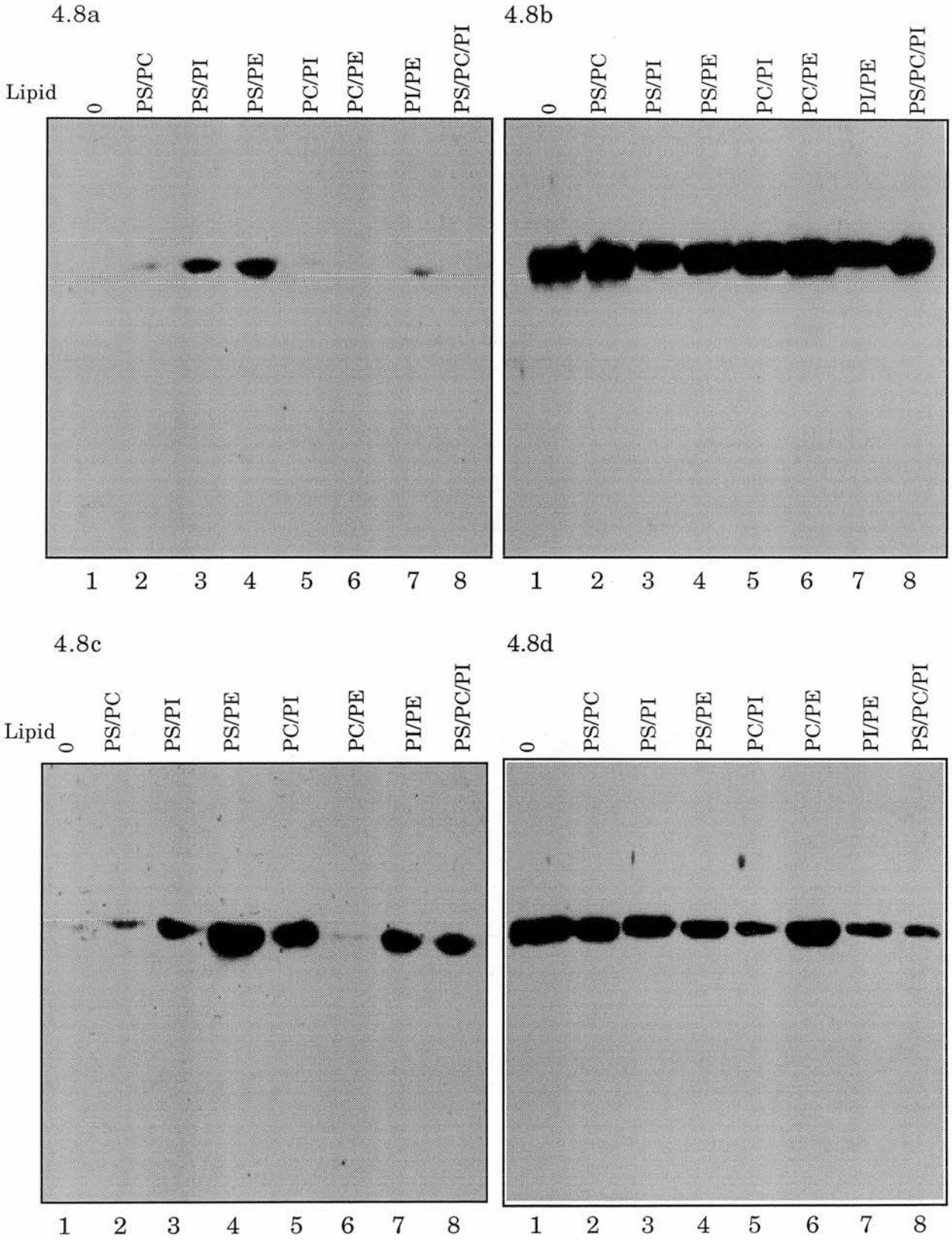
4.8a
4.8b
4.8c
4.8d
Lipid
0
PS/PC
PS/PI
PS/PE
PC/PI
PC/PE
PI/PE
PS/PC/PI
1
2
3
4
5
6
7
8

Figure 4.9 Binding of SytC to immobilised calmodulin

Binding of SytC to immobilised calmodulin was carried out as described in Materials and Methods. The TCA precipitated eluates were resuspended in 50 µl SDS-PAGE sample buffer and neutralised with 2 µl 2 M Tris. 30 µl samples of the starting protein and the protein after binding to the immobilised calmodulin were taken and 10 µl 4x SDS-PAGE sample buffer added. 5 µl of these samples and 10 µl of the eluates were analysed with SDS-PAGE and Western blotting using cgm67 at a dilution of 1:5 for detection.

lane	figure 4.9a	figure 4.9b
1	Starting SytC sample	Starting SytC sample
2	Native synaptotagmin starting sample	Supernatant after binding in EGTA
3	Supernatant after binding in EGTA	Supernatant after binding in Ca2+
4	Supernatant after binding in Ca2+	Supernatant after binding in Ba2+
5	Eluate from Ca2+ binding	Eluate from EGTA binding
6	Eluate from EGTA binding	Calmodulin agarose from EGTA binding
7	Blank	Eluate from Ba2+ binding
8	Blank	Calmodulin agarose from Ba2+ binding
9	Native synaptotagmin after binding in Ca2+	Eluate from Ca2+ binding
10	Eluate of native synaptotagmin in Ca2+	Calmodulin agarose from Ca2+ binding

4.9a

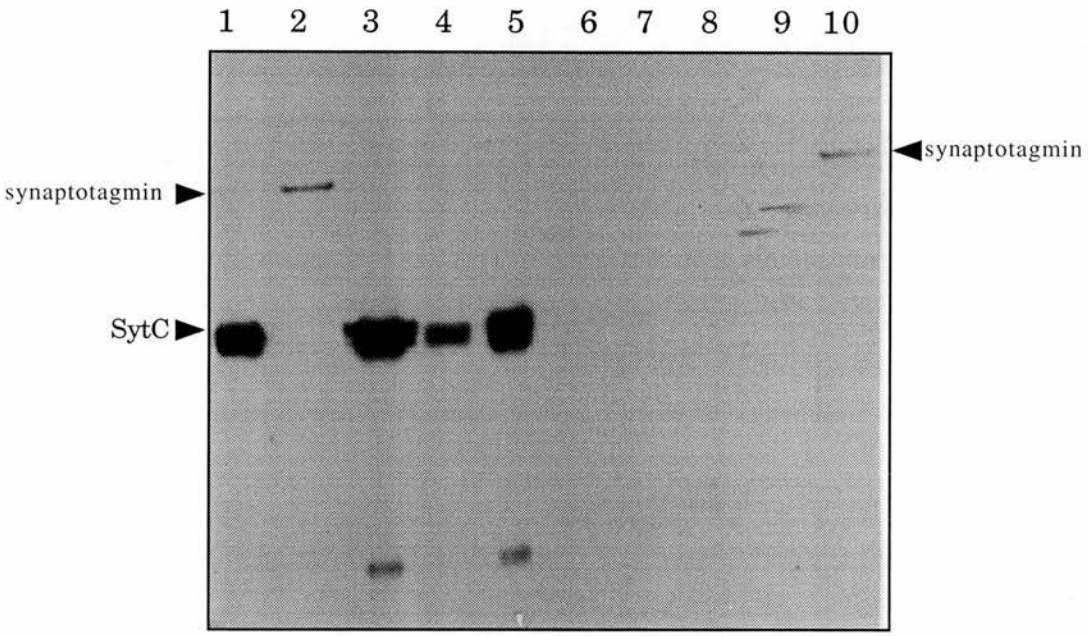
1 2 3 4 5 6 7 8 9 10
synaptotagmin
SytC
synaptotagmin

4.9a

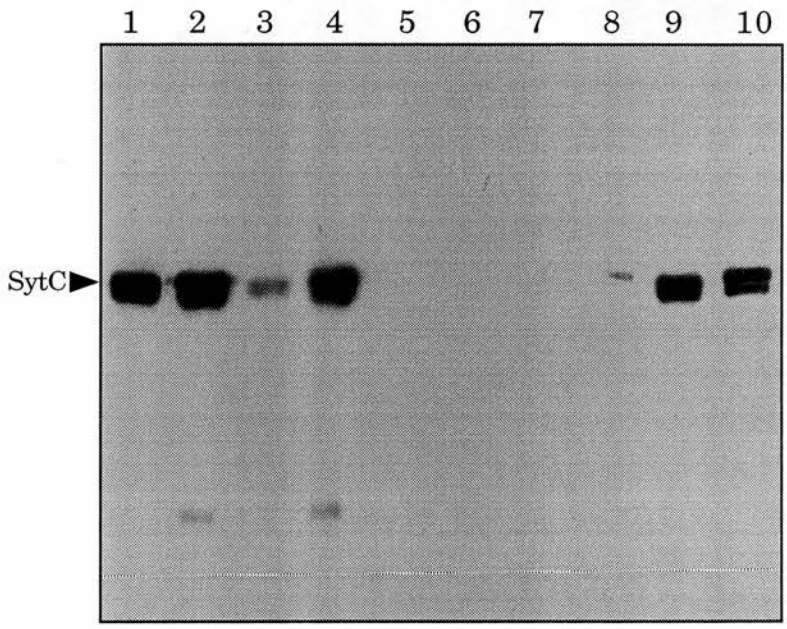
1 2 3 4 5 6 7 8 9 10
SytC

Figure 4.10 Emission spectrum of dansyl calmodulin

A 150 nM solution of dansyl calmodulin was excited at 340 nm and the emission was recorded between 400 and 550 nm.

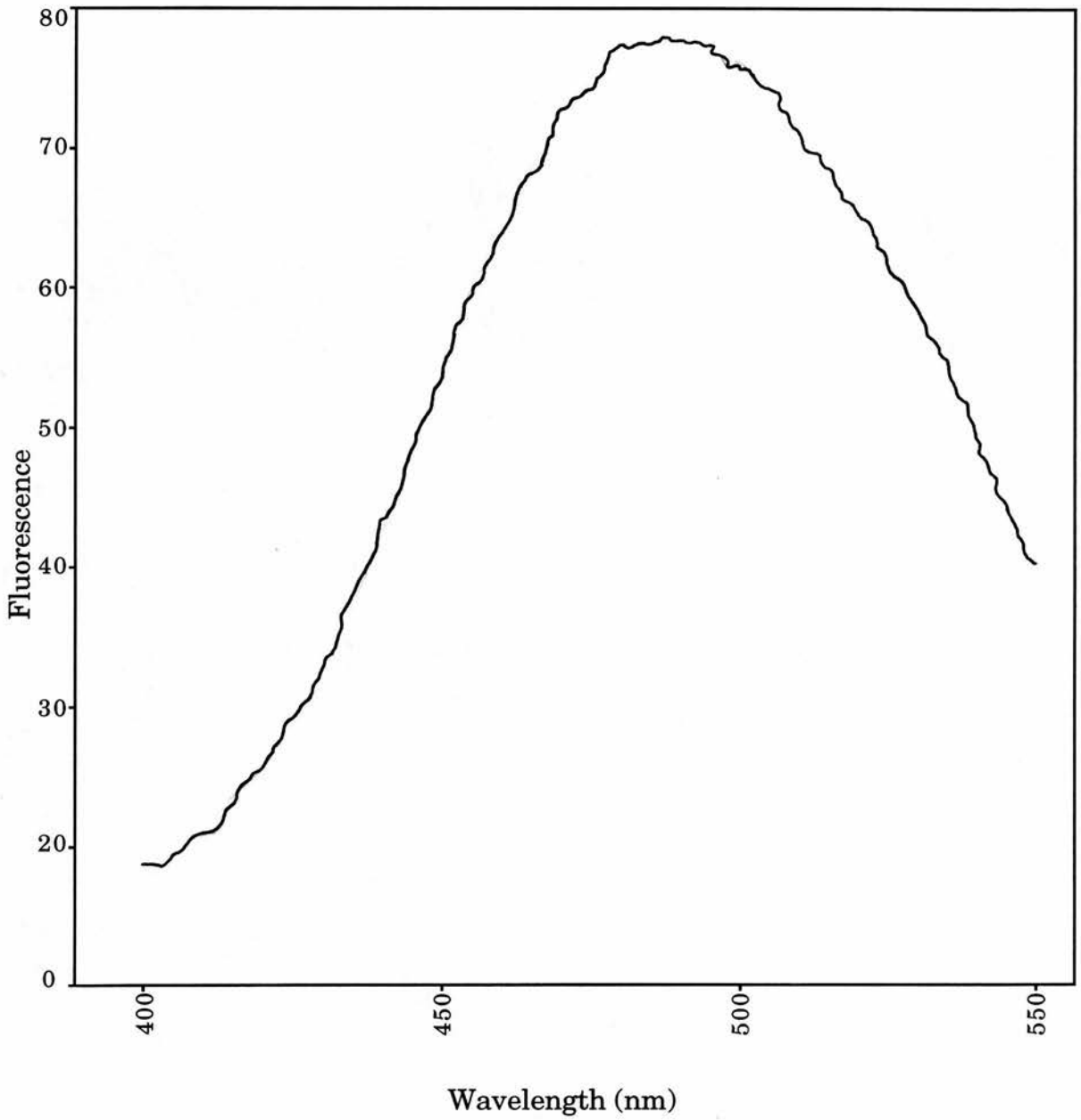
80
70
60
50
40
30
20
0
Fluorescence
400
450
500
550
Wavelength (nm)

Figure 4.11a **Titration of dansyl calmodulin with Ca^{2+}**

A titration with Ca^{2+} was performed as outlined in Materials and Methods using a 150 nM solution of dansyl calmodulin in 50 mM Hepes.NaOH pH 7.4, 1 mM NTA.NaOH pH 7.4. Additions of 100 mM $CaCl_2$ were made so that the free Ca^{2+} concentration would range from 1 - 200 μM.

Line 1	zero Ca^{2+}
Line 2	100 μM Ca^{2+}
Line 3	1 μM Ca^{2+}
Line 4	50 μM Ca^{2+}
Line 5	20 μM Ca^{2+}
Line 6	5 μM Ca^{2+}
Line 7	10 μM Ca^{2+}

Figure 4.11b **Titration of dansyl calmodulin with SytC**

SytC was added to a 150 nM solution of dansyl calmodulin in 50 mM Hepes.NaOH pH 7.4, 1 mM NTA.NaOH pH 7,4 to give SytC:calmodulin ratios of 1:2, 1:1 and 2:1. The solution was excited at 340 nm and the emission spectrum recorded between 400 and 550 nm.

Line 1	SytC:calmodulin 2:1
Line 2	SytC:calmodulin 1:1
Line 3	SytC:calmodulin 1:2
Line 4	dansyl calmodulin only

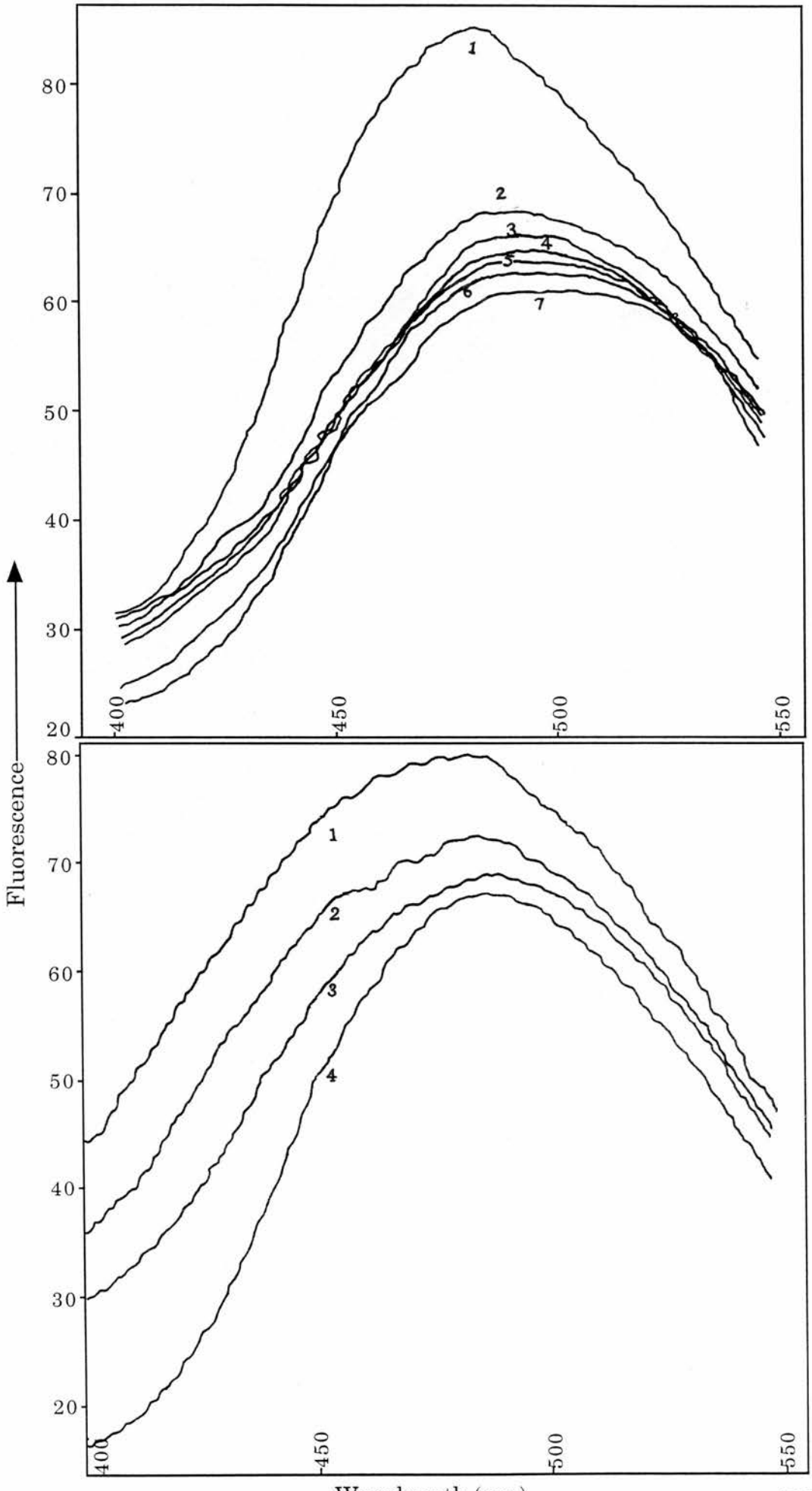
Fluorescence
80
70
60
50
40
30
20
1
2
3
4
5
6
7
400
450
500
550
80
70
60
50
40
30
20
1
2
3
4
400
450
500
550
Wavelength (nm)

Figure 4.12 Fluorescence change on addition of Ca2+

A titration with Ca^{2+} was performed as outlined in Materials and Methods using a 150 nM solution of dansyl calmodulin in 50 mM Hepes.NaOH pH 7.4, 1 mM NTA.NaOH pH 7.4. Additions of 100 mM $CaCl_2$ were made so that the free Ca^{2+} concentration would range from 1 - 200 μM. A similar titration was also carried out using a 300 nM protein solution containing a 1:1 molar ratio of SytC and dansyl calmodulin. Excitation was carried out at 340nm and emissions were recorded at 490 nm after each addition of Ca^{2+}. The fluorescence measurements were then plotted as a function of the free Ca^{2+} concentration in the assay after the figures had been corrected for the difference in starting fluorescence.

Figure 4.12a Fluorescence changes over a wide Ca^{2+} concentration range

Figure 4.12b Fluorescence changes over a narrow Ca^{2+} concentration range

4.12a

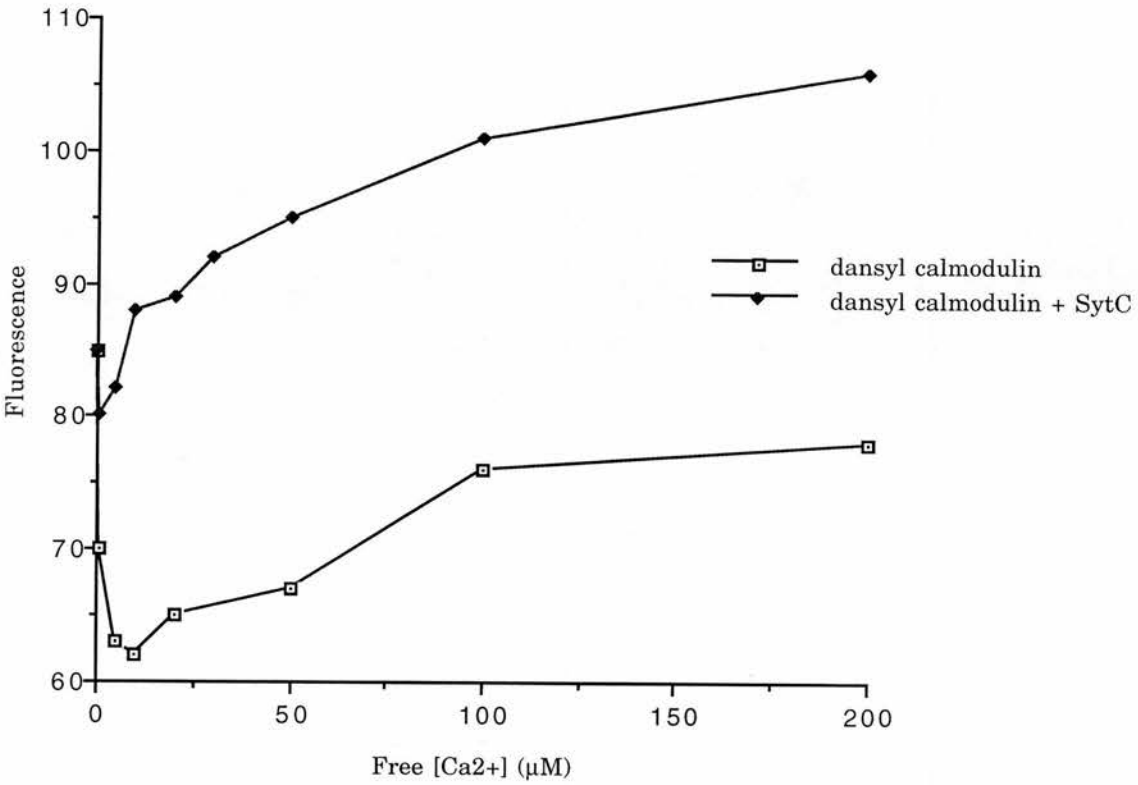
110
100
90
80
70
60
Fluorescence
0
50
100
150
200
Free [Ca2+] (µM)
dansyl calmodulin
dansyl calmodulin + SytC

4.12b

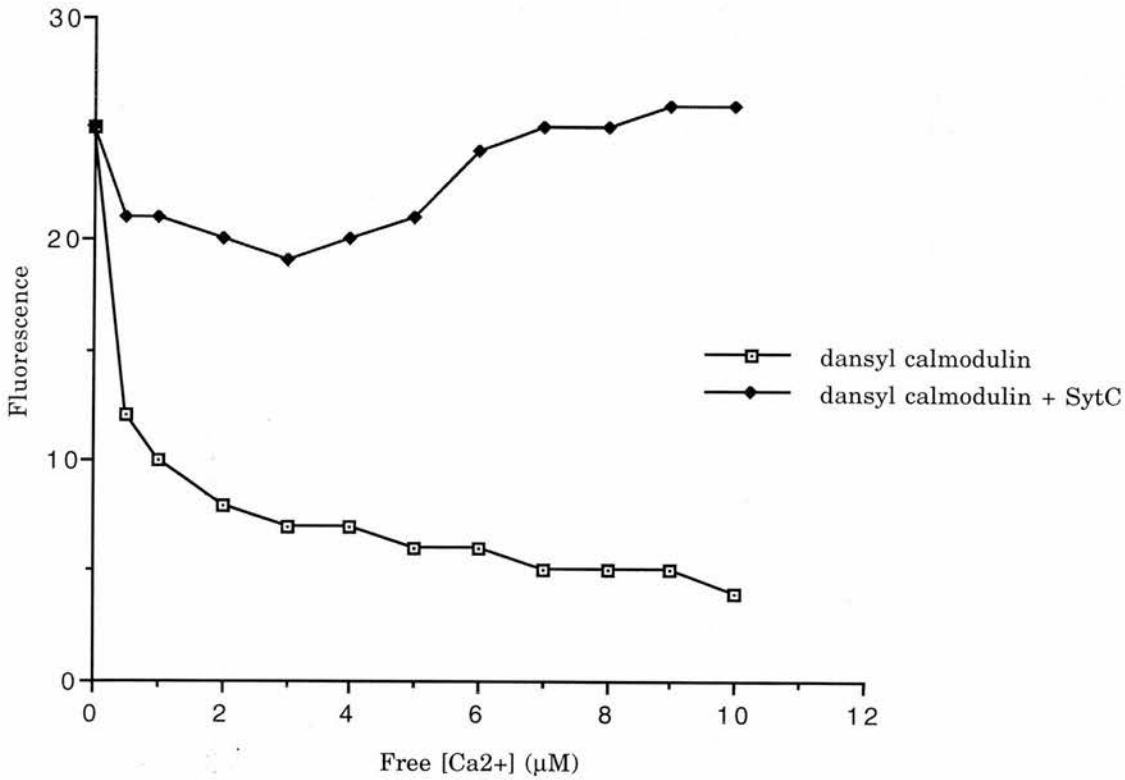
30
20
10
0
Fluorescence
0
2
4
6
8
10
12
Free [Ca2+] (µM)
dansyl calmodulin
dansyl calmodulin + SytC

Chapter 5

Analysis of quaternary structure of recombinant SytC and biophysical analysis of Ca^{2+}-dependent conformational change

5.1 Introduction

Data presented in the previous chapter have suggested that SytC has phospholipid and Ca^{2+}-binding properties as well as interacting with calmodulin. Protection from protease digestion in the presence of Ca^{2+} implies that a Ca^{2+}-dependent conformational change occurs in the protein and this would be one of the likely mechanisms whereby the protein exerts its effect in regulated exocytosis. In addition to this, Tb^{3+} titrations and the study of binding to phospholipid vesicles have shown the protein to be in a state of easily-induceable aggregation which is apparently reversible by the addition of Ca^{2+}.

It was therefore considered important to make a study of the structural properties of the protein and this was done using both gel exclusion chromatography and native gel electrophoresis to look at the quaternary structure of SytC and native bovine synaptotagmin respectively. The biophysical techniques of molecular dynamics and circular dichroism were also used to examine changes in quaternary and secondary structure under different conditions.

5.2 Analysis of the quaternary structure of SytC by gel exclusion chromatography

A Biogel P100 gel exclusion column was used (as in the purification of SytC) to measure the apparent size of SytC when run in buffer containing EGTA or Ca^{2+}. Figure 5.1 shows elution profiles of the protein run under both conditions. As can be seen the major absorbance peak was very similar in both cases giving an apparent size of 50 000 Da in EGTA and 44 000 Da in Ca^{2+} which cannot be classed as a significant difference between the two conditions given the accuracy limits of this technique.

The column had previously been calibrated with standard proteins (chapter 3). This does not rule out the possibility that there are very large aggregates which never enter the column gel but get trapped at the top, so that differences in the solubility in the two conditions are not apparent by this method, or that dissociation of a multimer occurs during filtration, ie that aggregation is a reversible association. It may be significant that in the presence of Ca^{2+}, the protein is more resolved from minor contaminants (peak at fraction 23) and gives a sharper maximum peak at fraction 28 suggesting that the structure is more uniform in Ca^{2+} than in EGTA, where the protein may be more polydisperse. If SytC molecules aggregate or in some way interact with each other then there would probably also be an interaction between SytC and PraSytC (the fusion protein of protein A and SytC). It had previously been noticed during purification by gel exclusion chromatography that a fraction of SytC emerges at a much larger apparent size, approaching the exclusion limit of 100 000 Da, along with traces of PraSytC and other contaminating proteins (fig 5.2a). This was unexpected because purified samples of both SytC and PraSytC alone are resolved well within the elution volume of the column (PraSytC has an apparent size of 68 kDa). It is possible that in the purification mixture, the mixture of contaminating proteins crosslinks a fraction of the SytC by specific or non-specific interactions; the very reason they have remained in the mixture as contaminants. However, the increased elution volume of both SytC and PraSytC and their co-elution can also be detected if the fully-purified proteins are mixed and again separated on the same column. Figure 5.2b shows elution profiles of a mixture of PraSytC and SytC run in the presence of Ca^{2+} and EGTA . Figure 5.2c shows the composition of fractions in the two main peaks of the protein mixture in EGTA. Both conditions gave the same pattern of

protein distribution; two peaks both containing SytC with PraSytC additionally present in the first peak only. The second peak contained the main proportion of total SytC in a purified form. The only difference between the two conditions was that in the presence of Ca^{2+} the first peak emerged just after the void volume and could therefore be estimated to have a size very close to the exclusion limit of 100 kDa whereas the peak in the presence of EGTA emerged exactly at the void volume and may therefore be of any size above 100 kDa or even a large aggregate (markers of both 158 kDa and 670 kDa both eluted in this volume during calibration of the column). Given the narrow difference in elution volume between the two conditions and the possibility that the gel exclusion limit may not be precisely 100 kDa, these data do not constitute strong evidence of a Ca^{2+}-dependent effect on the quaternary structure of SytC but suggested that further study might be valuable. A column with a larger exclusion limit would allow more accurate sizing in this range but it was decided to proceed no further with a column technique because if an equilibrium between multimeric forms of SytC did exist, this technique did not reveal it in either of the purified forms of the protein but only in the mixture, which makes it a possibility that mixing the two forms is producing an artefact by stabilising a transient association or causing an aggregation that would not normally occur. Non invasive biophysical techniques were therefore adopted to probe the quaternary structure in a more dynamic and potentially less disruptive assay.

5.3 Light scattering properties of SytC

The quaternary structure of SytC was further studied by measuring the light scattering properties of the protein molecules in solution and hence estimating their molecular sizes. The Dyna Pro-801 light-scattering

spectrometer fits the data to a single Gaussian distribution measuring the hydrodynamic radii of the molecules and calculating molecular weights from them. If the sample is essentially monodisperse, this unimodal analysis will yield low-error parameters as follows: polydispersity, the standard deviation of the spread of particle sizes about the measured average radius; base line, which represents the completeness and fit of the regression applied during the analysis; and the sum of squares of the deviations between the measured data and the theoretically-calculated data, giving the closeness of fit between the experimental data and an autocorrelation function generated from the analysis results. If the polydispersity measurement is high, bimodal analysis is used to resolve the size distribution more accurately and the same error parameters are calculated for it. Table 5.1 shows examples of raw experimental data illustrating the parameters measured by the light-scattering spectrometer

.

A titration with Ca^{2+} was carried out with a solution of SytC in 20 mM Tris.HCl pH 7.4, 1 mM NTA. Figure 5.3a shows the amplitude of the signal, representative of the proportion of molecules, from different molecular species of various sizes which appear during the addition of Ca^{2+} to the protein solution. All measurements which gave low error readings were included in both monomodal and bimodal analyses. The data show that at zero [Ca^{2+}] SytC exists as a species of between 100-200 Da with a small amount of aggregated protein. Some of the measurements at this stage had high error parameters associated with them indicating that the solution was polydisperse. Both the aggregate and the 100 kDa form of the protein appeared to undergo a transformation at 1 μM Ca^{2+} with the appearance of 80-100 kDa and 200-400 kDa forms. It is possible that this represents a transition through intermediates of disassociation, the

original 100-200 kDa form being converted to a species of 80-100 kDa while the original protein aggregate also disassociated but was observed at an earlier stage of dissociation where a 200-400 kDa species was formed. The error parameters for these size estimates were better than those from the starting solution but still showed polydispersity indicating that the statistical software was not able to resolve only two molecular species. The major change occurred at 5 μM Ca^{2+} when all the forms so far detected were completely converted to a 50-60 kDa species. Here the low error parameters indicated the protein to be monodisperse. The protein remained in this form throughout the subsequent titration except for the appearance of the 200-400 kDa species at 100 μM Ca^{2+}. This was probably not significant since it did not persist at 200 μM Ca^{2+} whereas the 50-60 kDa form remained throughout. The molecular composition of the protein returned to one similar to the starting point upon the addition of EGTA, i.e. mainly the 100-200 kDa form and some aggregated protein. These figures strongly suggest a Ca^{2+}-dependent switch from a multimeric complex or aggregate at low Ca^{2+} to a monomeric form at 1-5 μM Ca^{2+} which is maintained even at super-physiological Ca^{2+} concentrations. From the estimates of molecular weight, the multimer could be a dimer, trimer or tetramer but it was impossible to say exactly because the estimates of the multimer at low [Ca^{2+}] were more variable due to polydispersity. Most of the measurements were in the region of 110 kDa which would point to the existence of a dimer given the monomeric measurement of 55 kDa. No similar changes in the light scattering properties were detected when the titration was performed with Ba^{2+} or Mg^{2+} (data not shown).

The same light scattering experiment was repeated with a 1:1 molecular

mixture of calmodulin and SytC(15μM each protein). The molecular species seen in this mixture are summarised in figure 5.3b. Calmodulin itself is at the limits of detection by this method and when measured alone gave an apparent size of 28 kDa but often gave high error parameters. When mixed with SytC, it was equally difficult to evaluate the data because SytC began as a polydisperse solution and the addition of another protein introduced more noise into the readings. Calmodulin seemed to have a significant effect on the properties of SytC at zero Ca^{2+}. The solution at this point no longer contained large aggregates of high polydispersity but contained a 60-80 kDa species and a 10-20 kDa species which were well resolved by bimodal analysis. Most likely this indicates the existence of a complex between SytC and calmodulin and some free calmodulin since monomeric SytC has an apparent mass of 55 kDa. If calmodulin and SytC are in a 1:1 molecular ratio, there would also be some free SytC if there is free calmodulin. The discrepancy in the result and the logical argument is due to the fact that the analysis package cannot calculate a light scattering distribution for more than two molecules. This means that any mixture likely to be made of more than two molecular species will not be measured accurately and interpreting such results should be done with caution. At low Ca^{2+} concentrations, a 20-30 kDa form appeared which could be calmodulin and the amount of 60-80 kDa molecules is reduced to almost half the previous number suggesting that an initial complex may be separating at 1μM Ca^{2+}. The larger molecule, seen previously, of 100-200 kDa appeared at 5 μM Ca^{2+} but at this Ca^{2+} concentration, calmodulin was calculated to bind much of the Ca^{2+} because its K_d for Ca^{2+} is lower than that of NTA and the concentration of calmodulin in the experiment was high. The [Ca^{2+}] not bound to calmodulin or NTA was calculated to be 0.4 μM. The predominant forms of SytC are

therefore not seen at low [Ca^{2+}]. Presumably, whatever effect calmodulin had on the structure of SytC at zero Ca^{2+} was reduced as soon as calmodulin began to bind Ca^{2+}. Beyond this point in the titration, from 10-200 μM Ca^{2+}, the 20-30 kDa molecule, assumed to be calmodulin, disappeared and the mass estimates varied from 80-50 kDa but the error parameters indicated a monodisperse solution. The polydispersity increased at 100 μM Ca^{2+} but bimodal analysis resolved two components quite well giving a new 10-20 kDa molecule which could be calmodulin.

In summary, these data suggest that a complex exists between SytC and calmodulin at zero Ca^{2+} and at low Ca^{2+} concentrations but since the proteins are necessarily used at high concentrations for light scattering measurements, the calmodulin makes significant changes to the free Ca^{2+} concentrations and so exact changes are difficult to determine. It is clear however that calmodulin does have an effect on the quaternary structure of SytC even in the absence of Ca^{2+} but it is difficult to analyse the data at higher Ca^{2+} concentrations since calmodulin itself is not resolved as a separate species, the size of the molecular species is the same as in the SytC solution alone and the error parameters do not show polydispersity to indicate the presence of other molecular species in the mixture and so there is nothing which suggests the existence of a complex between calmodulin and SytC. On the whole, although this approach is useful for the study of monomer-oligomer transitions and aggregation, it is very difficult to interpret for heterologous interactions, as was required in this study.

5.4 Analysis of the quaternary structure of bovine adrenal synaptotagmin I

The quaternary structure of native bovine synaptotagmin was analysed using Blue Native PAGE, a technique which allows the separation of native proteins according to their molecular size (Schagger, H. 1994). The proteins are mixed with Coomassie blue G which gives the molecules uniform negative charge but does not denature them or disrupt complexes. The proteins solubilised with non ionic detergent if necessary can then be separated on a polyacrylamide gel to visualise the main protein complexes and then further resolved by second dimension electrophoresis in a SDS-polyacrylamide gel, to separate the components of each complex. Chromaffin granule membranes were solubilised with dodecyl maltoside at high ionic strength and the proteins separated in this way. Figure 5.4a shows a Western blot of a first dimension (non denaturing) gel probed with a polyclonal anti-synaptotagmin serum along with the pre-immune serum control. Beef heart mitochondrial respiratory complexes were used as molecular mass markers. The Coomassie G -stained gels of chromaffin granule membranes and beef heart mitochondria are shown in figure 5.4b. The blot showed one main band very close to the 800 kDa marker suggesting that synaptotagmin is part of a large complex. The monoclonal antibody to synaptotagmin, cgm 67, did not recognise any band in a first dimension blot. This is possibly because the epitope for the antibody is masked in the complex. In order to determine whether the 800 kDa species is made up of many proteins or only synaptotagmin, the bands on the first dimension native gel were further separated on a second-dimension SDS gel. Figures 5.5a and b show Western blots of the second dimension with polyclonal and monoclonal antibodies to synaptotagmin and figure 5.5c shows a Coomassie-stained version of the same gel. Both

antibodies decorated a protein of 67 kDa (the expected size of synaptotagmin) but in different places with respect to the first dimension. The polyclonal gives bands at the position of the 800 kDa complex and a wide band at 200-100 kDa whereas the monoclonal shows only a wide band stretching from the position of dopamine β hydroxylase (296 kDa) to a position corresponding to 150 kDa. The monoclonal is probably the more reliable of the two blots since it is cleaner and does not have the curvature which can be seen on the polyclonal blot. It is possible that there is something at 800 kDa which cross-reacts with the polyclonal antibody, possibly the V ATPase subunit A(72 kDA) since V ATPase subunits make up the greatest proportion of proteins at this position (figure 5.5c). There is some evidence of cross reactivity in chromaffin granule membranes on blots of normal Laemmli gels but this has always been assumed to be aggregation in samples. The result obtained with the monoclonal suggests that native synaptotagmin is present in a variety of complexes or multimeric forms and this is supported by the appearance of the wider band on the polyclonal blot. From the stained gel it is difficult to see how many proteins which could be part of a complex are in this region of the gel because the protein concentration is not high enough for clear staining. It may be possible to identify other proteins in a complex with synaptotagmin by using this technique to perform Western blotting with antibodies to other proteins. One experiment of this sort has already been performed in this lab using antibodies to SV2, one of the many proteins which may interact with synaptotagmin, but the two proteins did not appear to comigrate on these gels (data not shown).

5.5 Circular dichroic properties of SytC

Circular dichroic spectroscopy was used to study the changes in the

secondary structure of SytC as [Ca^{2+}] was increased. Figure 5.6 shows the CD spectra of SytC at zero Ca^{2+} and at 200 μM free Ca^{2+}, the extreme points of the Ca^{2+} titration performed. There was no change in the spectrum of SytC at any free Ca^{2+} concentration between 0 and 200 μM but when the measurements were repeated with protein together with phospholipid vesicles (figure 5.7a) there were changes in the peptide backbone mainly occurring at 50 μM free Ca^{2+}. Figure 5.7b shows the 0, 50, and 200 μM Ca^{2+} titration points with the data smoothed. The main changes were occurring in the 200-220 nm region. Unfortunately it was impossible to measure below 200 nm due to noise in the signal. These data suggest that there is a Ca^{2+} - dependent secondary structural change in SytC but that this is also dependent on the presence of phospholipid vesicles.

CD spectroscopy was also used to look for secondary structural changes associated with the interaction between calmodulin and SytC. Mixing the proteins did not produce a spectrum different from the algebraic addition of the spectra of each component and the subsequent addition of Ca^{2+} caused only the spectral change associated with the addition of Ca^{2+} to calmodulin (data not shown).

Originally, SytC was produced also as a His10-SytC fusion but this construct proved difficult to use in many of the experiments described and it was found to be highly aggregated in light-scattering measurements. The protein also seemed to precipitate if the ionic strength was below 300 mM. The CD spectrum of SytC showed the protein to contain 25% α helix and 65% β sheet whereas CD analysis of the His10-SytC protein revealed it to have a totally different structure to that of SytC appearing to be

much more random (figure 5.8). It may well be that the protein conformation is altered by the oligohistidine tag or that it makes the folded conformation less stable.

5.6 Conclusion

Biochemical and biophysical techniques have been described which have been used to investigate the secondary and quaternary structure of SytC. Gel exclusion chromatography, used in the purification of the expressed protein, had suggested that SytC molecules would form complexes or aggregates and light scattering measurements showed that the protein does indeed exist in multimeric and monomeric forms, the interconversions of which are controlled by the Ca^{2+} concentration in the buffer. This technique suggested that calmodulin affects the quaternary structure of SytC in the absence of Ca^{2+} but the results proved too complicated to analyse this and it is probably better to reserve this technique for the study of polydispersity in a solution of a single protein.

Native bovine synaptotagmin also seems to be part of one or different complexes in chromaffin granule membranes although it was impossible to conclude whether the complex is made up of synaptotagmin alone or contains other proteins. Differences in the result obtained with polyclonal and monoclonal antibodies make the data confusing but the monoclonal result seems convincing particularly as there is no other non-specific binding associated with this antibody.

Circular dichroic spectroscopy has shown that SytC has a spectrum consistent with that of a folded protein and calculations indicate a 25% α-helix and 65% β-sheet. The spectrum of His10-SytC was typical of a

protein in random coil. A previously published crystal structure of one C2 domain of synaptotagmin (Sutton *et al* 1995) , approximately half of SytC, indicated a structure composed mainly of β-sheet although no exact figures were given. These data are consistent with the published structure and suggests that the second C2 domain adopts a similar structure to the first in terms of the amount of β-sheet. Circular dichroism has also shown that there is a Ca^{2+} - dependent conformational change at the secondary structural level in SytC which is also dependent on the presence of phospholipid vesicles although there are no conformational changes associated with mixing SytC and calmodulin in the presence or absence of Ca^{2+}.

Figure 5.1 **Elution profile of SytC in buffer containing EGTA or Ca^{2+}**

Purified SytC (15 μg) was loaded onto a Biogel P100 gel exclusion column equilibrated with 20 mM Tris pH 7.4, 100mM NaCl containing either 2 mM EGTA or 1 mM $CaCl_2$. The protein was loaded in 250 μl of this. Fractions of 0.5 ml were collected. The apparent size of the protein was calculated using the calibration curve for the column shown in chapter 3 taking the elution volume corresponding to the fraction with the maximum A_{280}. Where more than one fraction gave a high A_{280} value, the elution volume was taken to be the average of the two fractions taking into account the relative A_{280} of each.

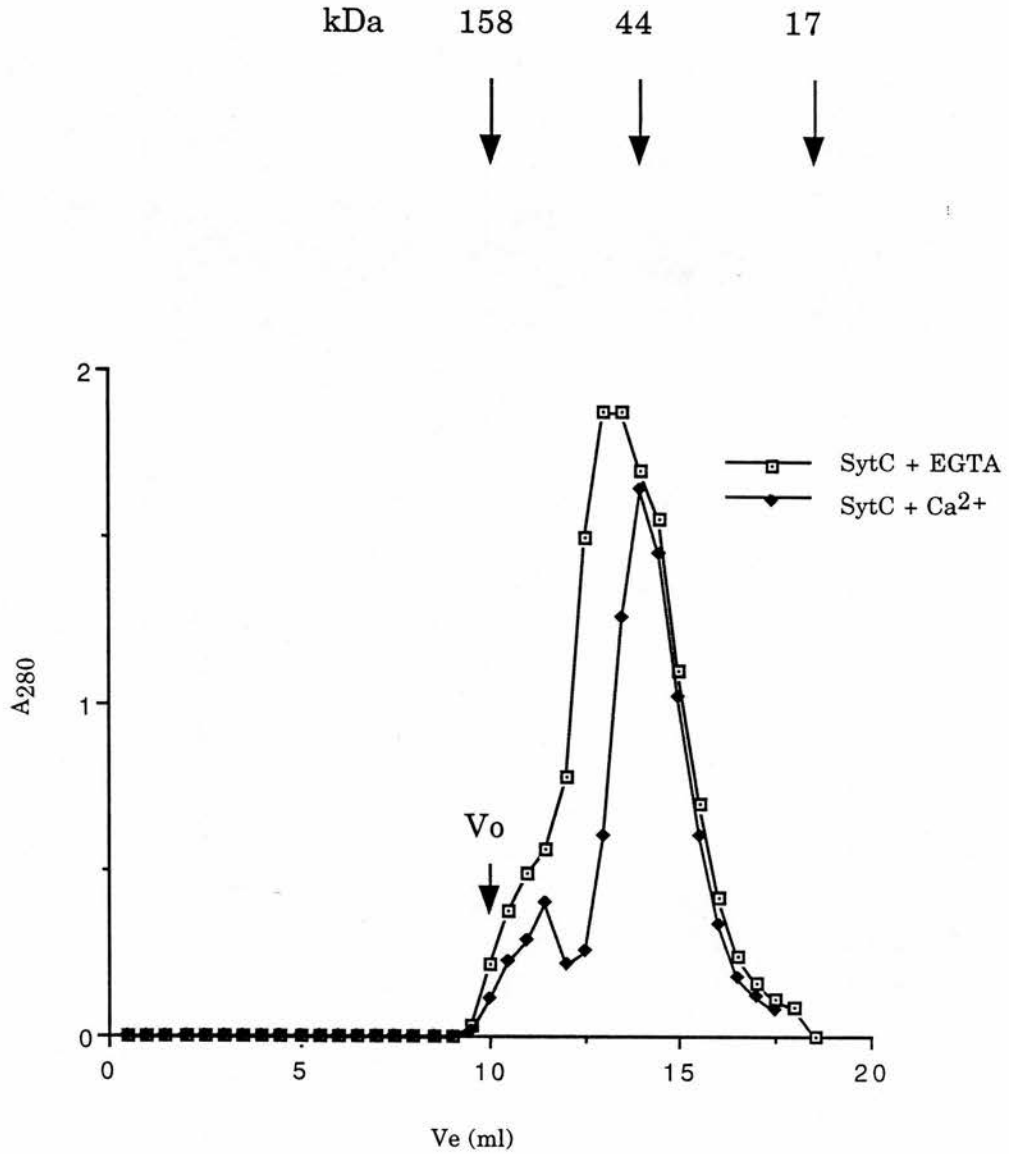
kDa
158
44
17
2
1
0
A280
Vo
0
5
10
15
20
Ve (ml)
SytC + EGTA
SytC + Ca2+

Figure 5.2 **Elution of a mixture of SytC and PraSytC in EGTA or Ca^{2+}**

Purified SytC and PraSytC were mixed in a molar ratio of 4:1 in a 200 µl volume of 20 mM Tris.HCl pH 7.4, 100 mM NaCl containing either 2 mM EGTA or 1 mM $CaCl_2$. The mixture was incubated at 20°C for 15 min and then loaded onto a Biogel P100 gel exclusion column previously equilibrated in the same buffer. Fractions of 0.5 ml were collected in and analysed by measuring the A_{280} and by SDS-PAGE of selected fractions with the peak A_{280} values. Figure 5.2b shows the A_{280} elution profile of the mixture in the two conditions and figure 5.2c shows the composition of the fractions in the two main peaks. Figure 5.2a shows the fractions from routine purification of SytC over the same column.

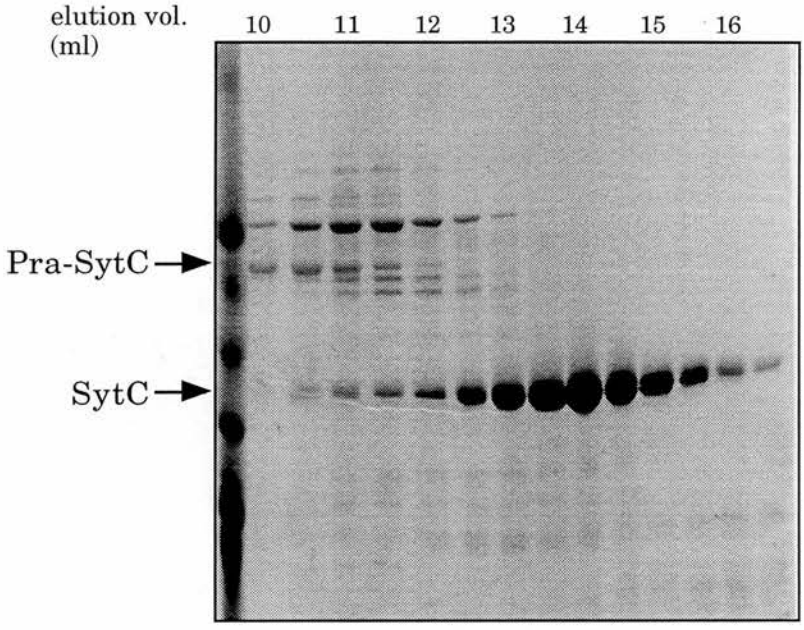
elution vol.
(ml)
10
11
12
13
14
15
16
Pra-SytC
SytC

5.2a

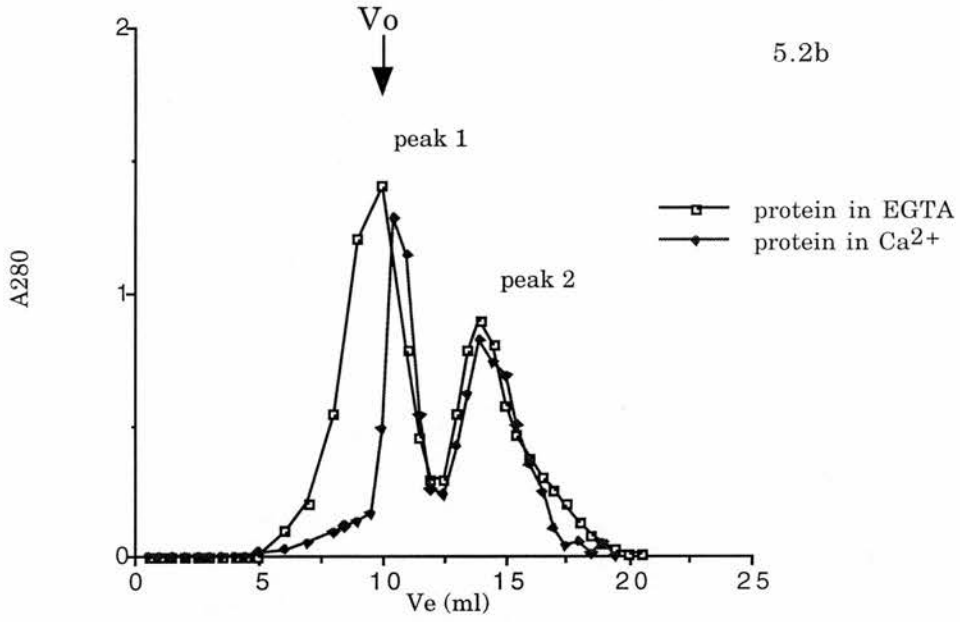
Vo
peak 1
peak 2
protein in EGTA
protein in Ca2+
A280
0
1
2
0
5
10
15
20
25
Ve (ml)

5.2b

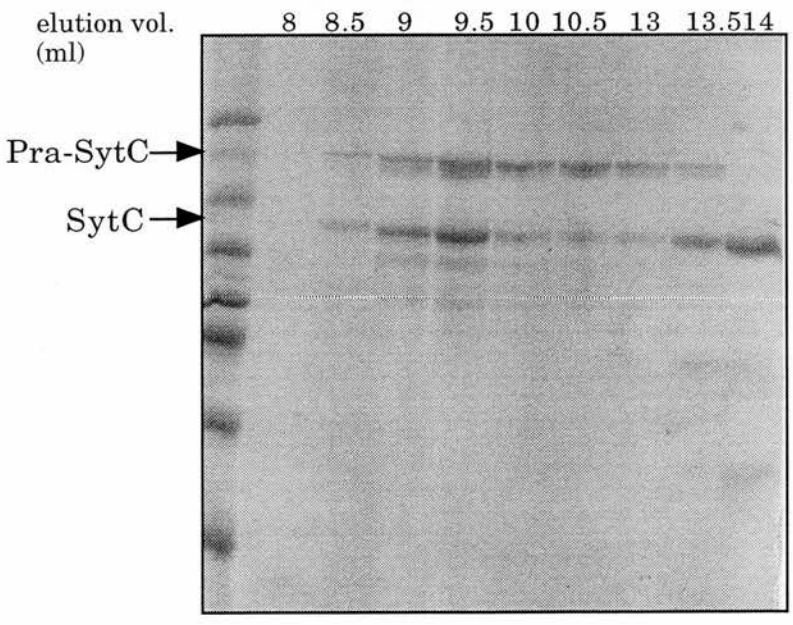
elution vol.
(ml)
8
8.5
9
9.5
10
10.5
13
13.5
14
Pra-SytC
SytC

5.2c

Figure 5.3 Light scattering measurements of SytC

Light scattering measurements were carried out as described in Materials and Methods using SytC solutions of 0.5 mg/ml in 20 mM Tris.HCl pH 7.4. The estimated weights of molecular species appearing during a Ca^{2+} titration are summarised in figure 5.3a. The light scattering amplitude is proportional to the fractional mass of molecules in each category. Measurements with with the lowest error parameters were selected. Figure 5.3b illustrates a similar titration with a protein solution containing SytC and calmodulin in 1:1 molar ratio.

5.3a

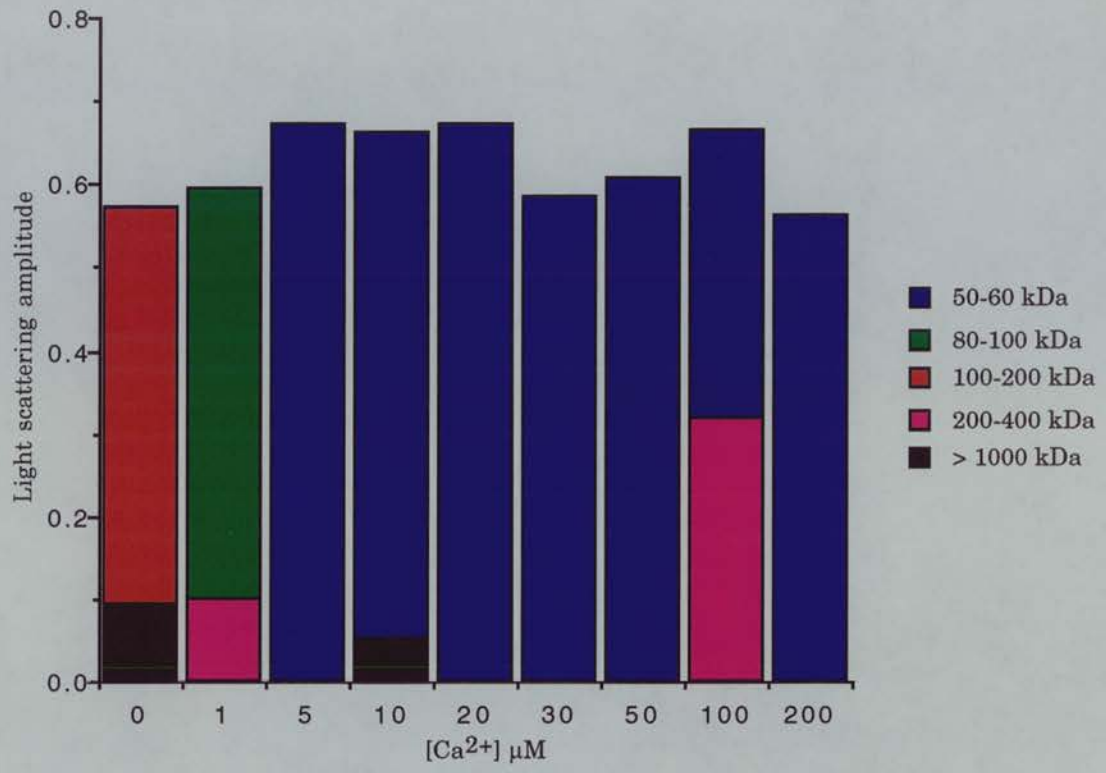
0.8
0.6
0.4
0.2
0.0
Light scattering amplitude
0
1
5
10
20
30
50
100
200
[Ca2+] µM
50-60 kDa
80-100 kDa
100-200 kDa
200-400 kDa
> 1000 kDa

5.3b

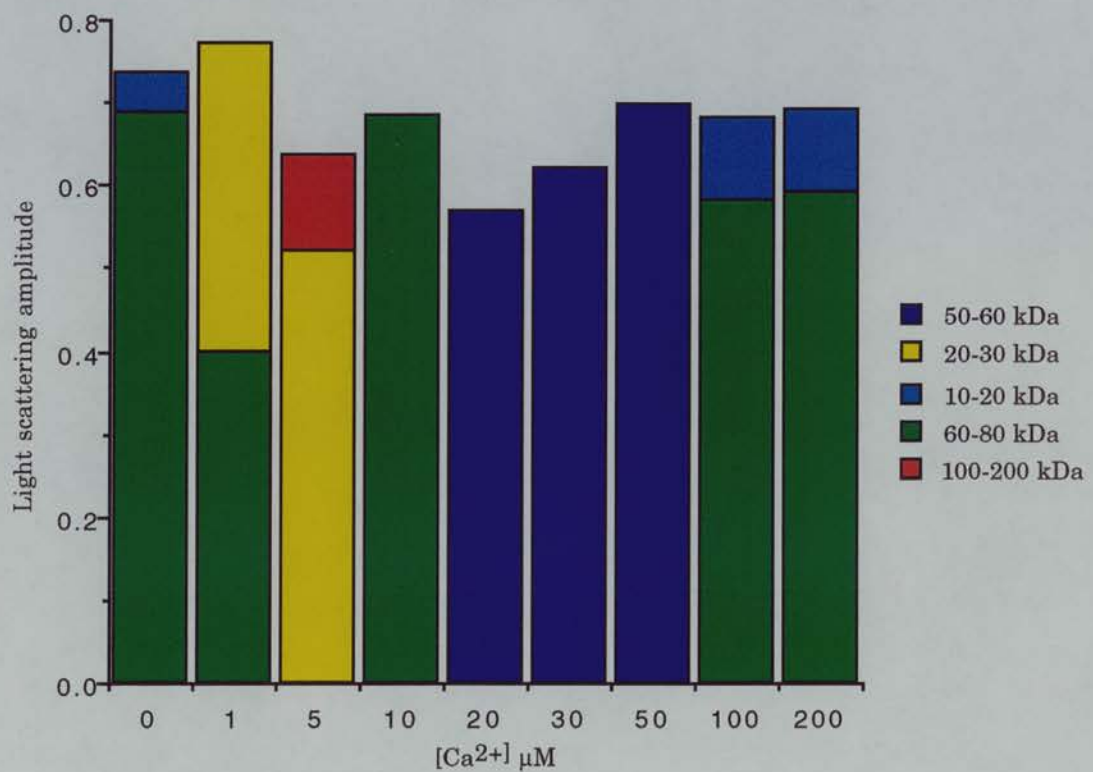
0.8
0.6
0.4
0.2
0.0
Light scattering amplitude
0
1
5
10
20
30
50
100
200
[Ca2+] µM
50-60 kDa
20-30 kDa
10-20 kDa
60-80 kDa
100-200 kDa

Figure 5.4 **Western blot of a first dimension native blue gel of chromaffin granule membranes.**

Chromaffin granule membranes (20 μg of protein per lane of gel) were separated by first dimension native gel electrophoresis and then subjected to standard Western blotting using a polyclonal antibody to synaptotagmin at a dilution of 1:1000 for detection. This is shown on the left (figure 5.4a). A similar Western blot was probed with pre-immune rabbit serum and is shown on the right (figure 5.4b). Figures 5.4c and d show stained native first dimension blue gels of mitochondrial respiratory membranes, used as markers, and chromaffin granule membranes respectively.

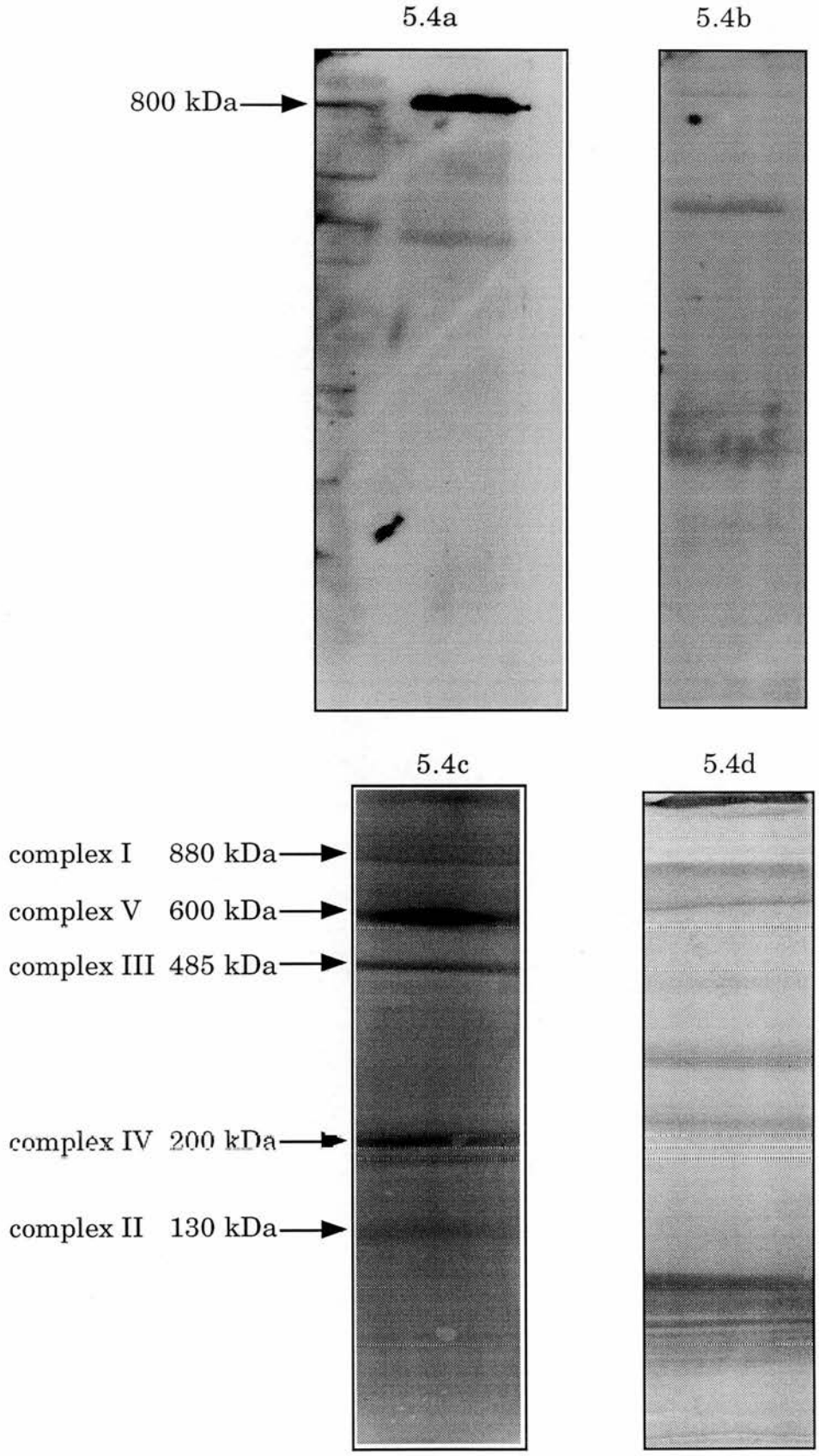
5.4a
5.4b
800 kDa
5.4c
5.4d
complex I 880 kDa
complex V 600 kDa
complex III 485 kDa
complex IV 200 kDa
complex II 130 kDa

Figure 5.5 **Second dimension blue native gel electrophoresis of chromaffin granule membranes**

Chromaffin granule membranes (20 μg of protein per lane of gel) were subjected to first and second dimension blue native electrophoresis. The resulting gel was then subjected to standard Western blotting procedures using either a polyclonal antibody to synaptotagmin at a dilution of 1:1000 for detection (figure 5.5a) or the monoclonal cgm67 at a dilution of 1:5 (figure 5.5b). The second dimension gel was also stained with Coomassie blue G to visualise all the proteins and the molecular weight standards(figure 5.5c)

67 kDa
100 kDa
200 kDa
800 kDa
67 kDa
first dimension
second dimension

100 kDa
200 kDa
67 kDa
first dimension
second dimension

first dimension
second dimension
66 kDa
45 kDa
36 kDa
29 kDa
24 kDa
17 kDa
14 kDa
880 kDa
600 kDa
485 kDa
200 kDa
130 kDa

Figure 5.6 **Circular dichroic spectrum of SytC in two Ca^{2+} concentrations**

A Ca^{2+} titration was performed and the circular dichroism spectrum obtained for a 0.25 mg/ml solution of SytC as described in Materials and Methods. The protein was diluted in 20 mM Tris.H_2SO_4 pH 7.4, 1 mM NTA . Ca^{2+} additions made to give free Ca^{2+} concentrations of 1, 5, 10, 20, 30, 50, 100 and 200 μM and CD spectra measured after each addition. The spectrum at zero Ca^{2+} and the spectrum at the end point of the titration are shown superimposed.

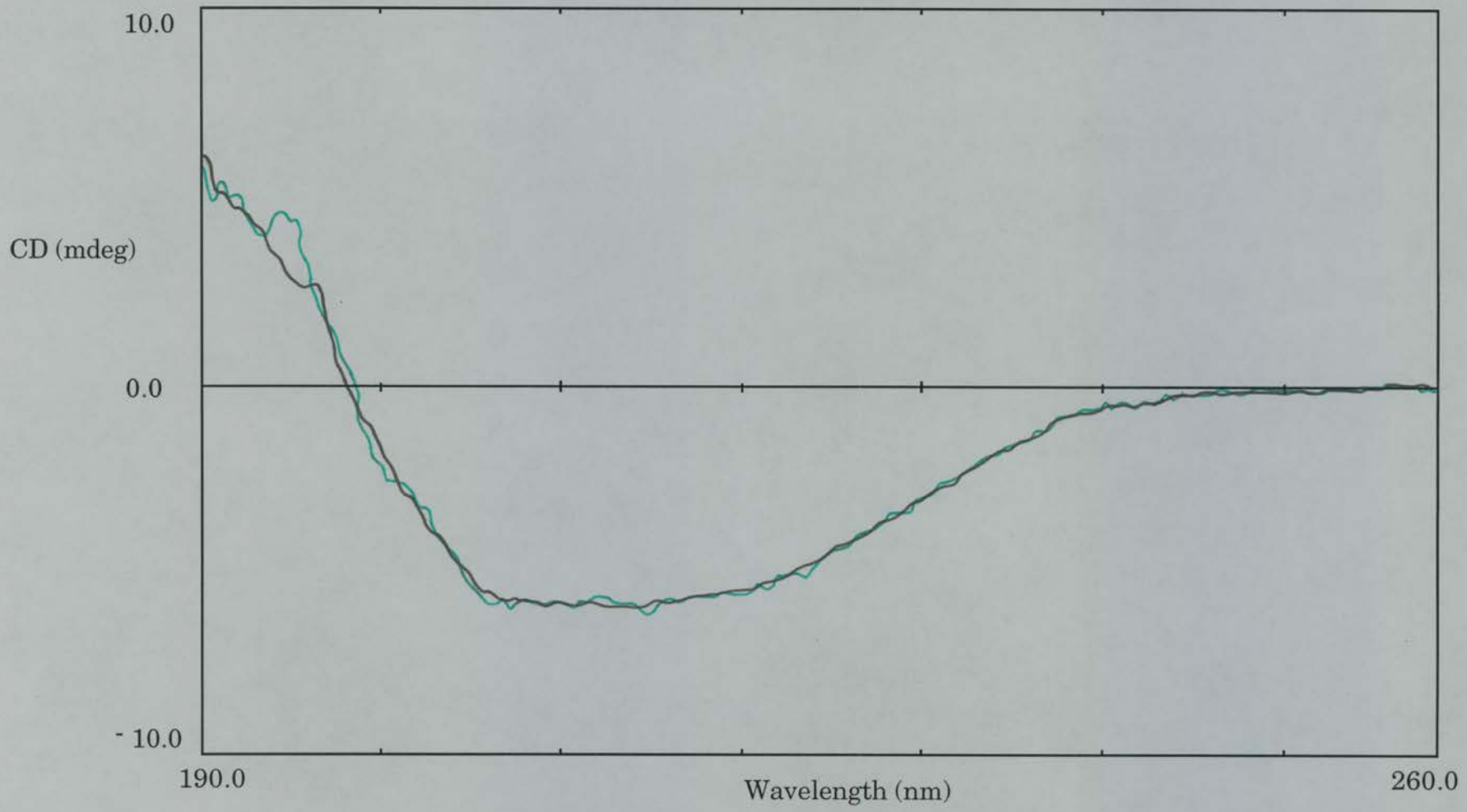
10.0
CD (mdeg)
0.0
- 10.0
190.0
Wavelength (nm)
260.0
0.25 mg/ml SytC with zero Ca2+
0.25 mg/ml SytC with 200 µM Ca2+

Figure 5.7 **Circular dichroic spectra of SytC in different Ca^{2+} concentrations in presence of phospholipid vesicles**

A Ca^{2+} titration was performed as described in the previous figure using a 0.2 mg/ml SytC solution containing 100 μg/ml phospholipid vesicles (20% (w/v) cholesterol, 40% (w/v) PS, 40% (w/v) PC) and the circular dichroism spectrum measured for each concentration. Figure 5.7a shows the data from 200-260 nm for all the titration points. Figure 5.7b shows the three titration points with the data smoothed.

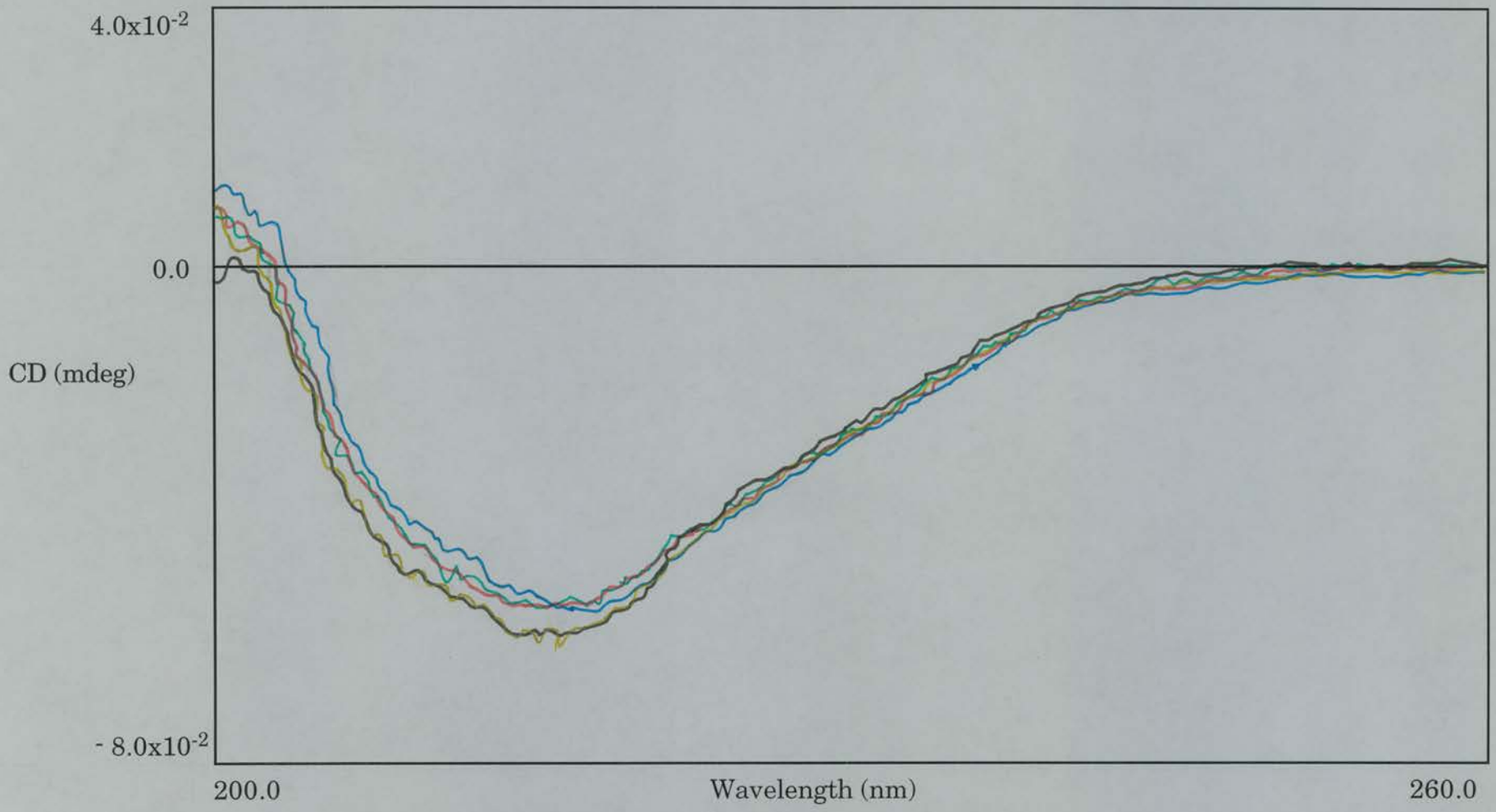
4.0x10-2
0.0
- 8.0x10-2
CD (mdeg)
200.0
Wavelength (nm)
260.0
0.25 mg/ml SytC with zero Ca2+ and with phospholipid
0.25 mg/ml SytC with 10 μM Ca2+ and with phospholipid
0.25 mg/ml SytC with 50 μM Ca2+ and with phospholipid
0.25 mg/ml SytC with 100 μM Ca2+ and with phospholipid
0.25 mg/ml SytC with 200 μM Ca2+ and phospholipid

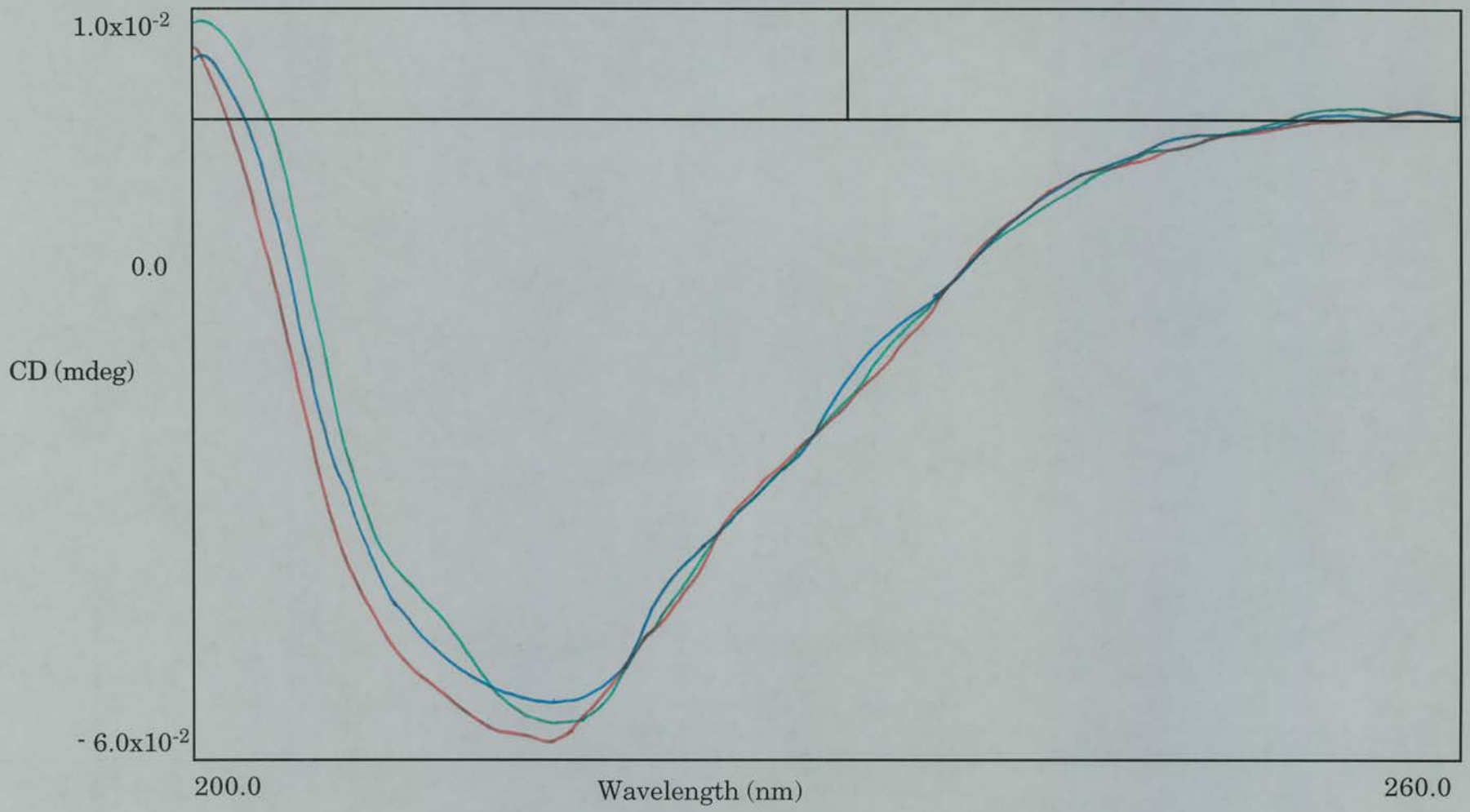
1.0x10-2
0.0
CD (mdeg)
- 6.0x10-2
200.0
Wavelength (nm)
260.0
0.25 mg/ml SytC with zero Ca2+ and no phospholipid
0.25 mg/ml SytC with 50 µM Ca2+ and with phospholipid
0.25 mg/ml SytC with 200 µM Ca2+ and phospholipid

Figure 5.8 **Circular dichroism spectrum for SytC and His10SytC**

The circular dichroism spectra were obtained for SytC and His10SytC and are shown superimposed.

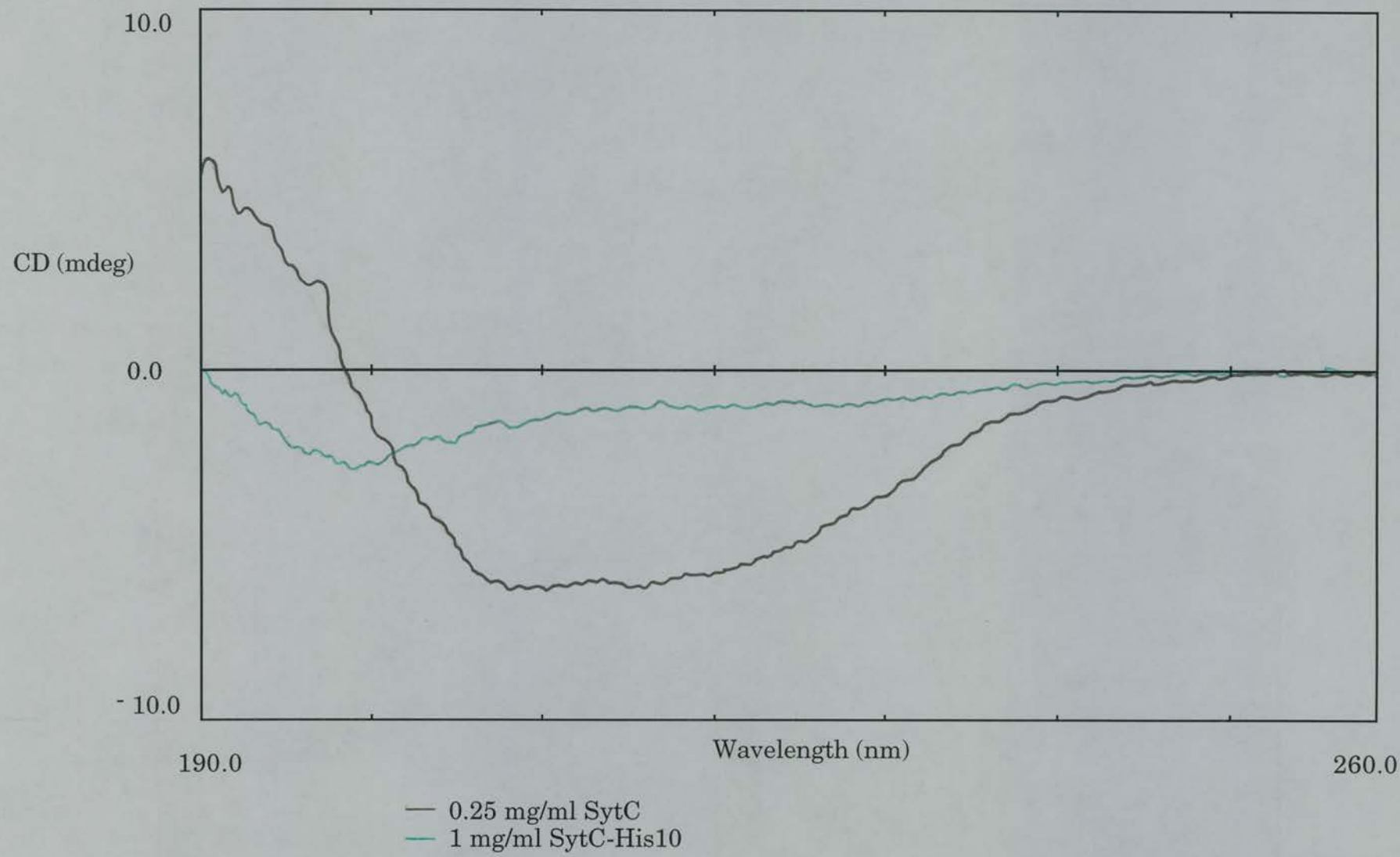
10.0
CD (mdeg)
0.0
- 10.0
190.0
Wavelength (nm)
260.0
0.25 mg/ml SytC
1 mg/ml SytC-His10

Table 5.1 **Raw data from light-scattering measurements of SytC**

The table shows some light-scattering parameters measured for SytC at 0, 1 and 5 μM Ca^{2+} concentrations giving error measurements for both monomodal and, where applicable, bimodal analyses. Base-line readings of 1 or lower, SOS readings of 5 and lower and low polydispersity readings (indicated by a dotted line) show the measurement is representative of a large proportion of the molecules in the solution. If these error readings were high, a bimodal analysis was performed to attempt to resolve signals from the solution into two molecular species rather than one species which is the default analysis performed by the spectrometer.

Data was selected for figure 5.3 if it fitted the base-line and SOS criteria already stated. If the polydispersity was greater than 15% of the average molecular radius measurement given the monomodal default analysis was used. If bimodal analysis was necessary because of high polydispersity the resulting measurements were used instead of the monomodal measurements. If no analysis gave reasonably low error parameters, the monomodal measurements were used but the low reliability of the measurements is discussed.

Ca^{2+} μM	No.	Amp. (nm)	Radius (nm)	Polyd.	Est. MW (kDa)	Base Line	S.O.S. Error
0	1	0.511	8.3	4.635	497	1.065	90.722
	2	0.459	9.3	5.188	654	1.068	100.275
	3	0.553	6.7	3.741	296	1.045	65.330
	4	0.478	4.4	-------	104	1.003	2.025
		0.093	47.5	-------	33763		
1	1	0.582	4.2	2.096	97	1.023	10.562
	2	0.586	4.0	1.574	84	1.017	3.707
	3	0.583	4.9	2.717	136	1.060	15.261
	4	0.494	3.5	-------	65	1.012	1.501
		0.099	7.4	-------	374		
5	1	0.688	3.5	1.215	62	1.002	2.497
	2	0.668	3.2	-------	51	1.000	3.003
	3	0.673	3.5	1.304	60	0.999	4.119
	4	0.078	1.3	-------	5	1.001	2.159
		0.595	3.8	-------	72		

No.4 in each data set is the bimodal analysis

Chapter 6

Summary and Discussion

6 Summary and Discussion

The cytoplasmic domain of synaptotagmin (SytC) was produced by recombinant DNA technology and expression in a bacterial host. Two different cloning and expression strategies were used giving proteins which were tagged either with protein A or oligohistidine to facilitate purification. Purification procedures were developed for both affinity-tagged proteins but the SytC derived from the protein A construct was found to be the more stable and consequently used for most further studies.

The main hypothesis which drove the work was that synaptotagmin effects its function in regulated exocytosis by undergoing a conformational change upon binding of Ca^{2+} which is the stimulus for regulated secretion to occur. Initially, biochemical assays were used to explore the possibility of Ca^{2+}-dependent conformational change and also to look at the interaction of other molecules with the protein with a view to later testing their influence on the protein's conformation. Partial proteolysis of SytC with trypsin in the presence and absence of Ca^{2+} indicated that Ca^{2+} induced a conformational change in the protein which rendered it resistant to proteolytic degradation. Binding assays also showed that SytC interacted with phospholipids in a Ca^{2+}-dependent manner which was subsequently supported by published evidence of these interactions (Davletov and Südhof 1993). Calmodulin was also found to bind the protein in this way, as detected by binding of SytC to immobilised calmodulin and also by fluorimetric analysis using calmodulin with a dansyl reporter group attached. The interaction was shown to be greatest at Ca^{2+} levels between 1-10 μM.

Study of the Ca^{2+}-dependence of SytC would be easier if a simple Ca^{2+}-binding assay was available. An attempt was made to develop a fluorimetric assay for Ca^{2+} binding which would depend on the change in fluorescence from Tb^{3+} used as a competitive probe for Ca^{2+}-binding sites. Unfortunately, Tb^{3+} appeared to cause aggregation of SytC and to bind irreversibly so that Ca^{2+} did not displace it when included in the assay. Direct Ca^{2+} binding measurements were therefore abandoned in favour of techniques which measured the influence of Ca^{2+} on other characteristics of the protein.

The effects of Ca^{2+} on the secondary and quaternary structure of SytC were studied using circular dichroic spectroscopy, gel exclusion chromatography and light scattering. These experiments revealed that SytC may exist as both an oligomer (probably a dimer) and also a monomer depending on the Ca^{2+} concentration in the solution dissociating from a dimer at 1 μM to a monomer at 5 μM free Ca^{2+} and reassociating on removal of the ion. In addition, this effect is not reproduced by Ba^{2+} or Mg^{2+}. The secondary structure, as determined by CD spectroscopy, was primarily composed of β sheet and was not influenced by additions of Ca^{2+} unless phospholipid vesicles were also included, whereupon some shifts in the peptide backbone occurred at a [Ca^{2+}] of 50 μM. Finally, native gel electrophoresis was used to examine the quaternary structure of native synaptotagmin in chromaffin granule membranes. The results again indicate that synaptotagmin exists as a dimer and is possibly a member of a much larger complex of proteins.

The interaction between calmodulin and synaptotagmin was stimulated by low [Ca^{2+}] and the effect was not reproduced using Ba^{2+}. Since calmodulin

shows only a low affinity for Ba^{2+}, this could indicate that the interaction is a result of the binding of Ca^{2+} to calmodulin rather than to synaptotagmin which, in addition to showing some Ba^{2+}-dependent characteristics, has also been shown previously to have a lower affinity for Ca^{2+} than does calmodulin (see introduction). However, there are problems with the interpretation of this experiment. Firstly there is also some evidence in the same experiment of a Ca^{2+}-independent interaction which was not seen using a different technique of binding to immobilised calmodulin and so is potentially an artefact of this technique. Secondly, Ba^{2+} does not seem to mimic the effects of Ca^{2+} on synaptotagmin consistently between different assay types in this thesis and also in the literature (Brose *et al* 1992 found that Ba^{2+} didn't bind synaptotagmin whereas Davletov and Südhof 1993b found that Ba^{2+} had the same effect as Ca^{2+}). It is therefore impossible to be sure that the ineffectiveness of Ba^{2+} in this assay is due to the fact that the interaction is stimulated by Ca^{2+}/calmodulin as it is equally possible that the ion is having no effect on synaptotagmin in this assay. On the whole, more of the literature points to the affinity of synaptotagmin for Ba^{2+} and so it can be tentatively suggested that an interaction exists between calmodulin and synaptotagmin which relies on the effect of Ca^{2+} on calmodulin. The significance of this interaction is, of course, difficult to discuss because of our incomplete understanding of the function of calmodulin in exocytosis. Although it is possible that the interaction does not occur in the cell, some evidence from the literature suggests that calmodulin is involved in the fast step of exocytosis or in endocytosis (Kibble and Burgoyne 1996) and it is possible that the close association of calmodulin with exocytotic proteins is required as a Ca^{2+} buffer to stop 'overshoot' of the Ca^{2+} signal thus maintaining the fidelity of the response. In endocytosis, calmodulin might be needed to remove all traces of Ca^{2+}

before synaptotagmin can be retrieved perhaps in an oligomeric form as discussed below.

The other work presented in this thesis supports the hypothesis that synaptotagmin undergoes a Ca^{2+}-dependent conformational change both in quaternary structure at lower [Ca^{2+}] and secondary structure at higher [Ca^{2+}]. Trypsin digestion indicates quite clearly that there is a structural change upon binding to Ca^{2+} which protects the protein from proteolysis even at high trypsin concentrations and that this protection is also produced by Ba^{2+} which is known to mimic the effects of Ca^{2+} in exocytosis (Terbush and Holz 1992) and has also been found to mimic the effects of Ca^{2+} on synaptotagmin (Davletov and Sudhof 1993b). Further work with light scattering measurements corroborates this. Although it is probable that the recombinant protein shows aggregation which is not a feature of the native protein, the fact that Mg^{2+} does not produce the same effect suggests that it is not simply a result of the increased ionic strength of the solution. The lack of change with Ba^{2+} (which has been found to mimic some effects of Ca^{2+} in this thesis) rules out the possibility that the binding of an ion to the protein will produce the same effect by simple physical or electrostatic disruption of an aggregate. In addition, the fact that the structural change is reversible by removal of Ca^{2+} suggests that there is potential for this change to occur *in vivo* where Ca^{2+} levels rise and fall in a controlled fashion particularly in view of the fact that native synaptotagmin also seems to be a dimer. The changes in secondary structure seem to have the more stringent requirements of a higher [Ca^{2+}] and the presence of phospholipids. Since it was also found that synaptotagmin binds phospholipids in a Ca^{2+}-dependent manner, this effect probably involves the binding of all three molecules which can be easily envisaged given the context of the native protein in the membrane of

secretory vesicles.

The mechanism by which Ca^{2+} induces conformational change is a matter of speculation. However, some clues can be gained from accumulated biochemical and structural information about other proteins which contain a C2 domain such as protein kinase C and phospholipase Cδ. As already discussed in the introduction, the C2 domain is thought to be responsible for the Ca^{2+} - and phospholipid-binding properties of synaptotagmin as it is in protein kinase C. NMR and crystallographic data have shown that metal ion binding to phospholipase Cδ produces a significant conformational change in the C2 domain exposing three lysine residues on the back face of the Ca^{2+} binding site (Grobler *et al* 1996, Essen *et al* 1996) which could bind acidic lipids. This supports biochemical data showing allosteric interactions between Ca^{2+} and lipid binding which is similar to the case of synaptotagmin. In addition, the accepted model of protein kinase C activation also involves conformational change (Bazzi and Nelsestuen 1990, Orr and Newton 1994). In the inactive form, protein kinase C holds part of its own peptide sequence in the active site forming a pseudosubstrate. Binding of phosphatidyl serine to the C2 domain which is allosterically increased by the binding of Ca^{2+} causes a conformational change which removes the pseudosubstrate sequence from the active site, allowing the enzyme to carry out its function. It is therefore a strong possibility that Ca^{2+} functions in the same way for synaptotagmin, causing a conformational change exposing residues which allow the protein to bind phospholipids. The resultant conformational change from the allosteric binding of these two molecules would then cause the 'active site', possibly the point of contact between synaptotagmin and another protein, to become functional.

The secondary and quaternary structural changes measured depended on quite different concentrations of Ca^{2+}. This could be explained simply by the relative sensitivities of the two techniques in which case the two structural changes might actually occur at similar [Ca^{2+}] in the cell. Alternatively, the difference may be a result of the presence of phospholipids in the CD measurements but not in the light scattering experiments. If this is so, then interaction of the phospholipids may 'desensitize' the protein allowing levels of Ca^{2+} to rise higher before exocytosis is triggered. This would be in keeping with the idea that synaptotagmin controls fusion by preventing it and would suggest that synaptotagmin may effect its role by a multi-stage conformational change depending on its position in the cell and the time-point during exocytosis. In such a scheme, the fraction of synaptotagmin molecules associated with the docking complex at the plasma membrane would undergo a fast secondary structural change caused by the relatively high [Ca^{2+}] likely to be present at the plasma membrane near Ca^{2+} channels. Synaptotagmin in vesicles deeper in the cell would experience lower [Ca^{2+}] due to diffusion of the ion inward from the plasma membrane. A quaternary structural change at this point may be a potential contribution to the mobilisation of vesicles to the membrane or the formation of an early complex with SNAP/SNARE proteins. Alternatively, quaternary structural changes could occur at lower Ca^{2+} levels at the very beginning of the inward calcium flow providing a switch from an inactive dimer to an active monomer which can undergo secondary structural shift preceding fusion of the vesicle. Two levels of structural change in this way provide increased control over fusion and provide a mechanism to absorb 'false' signals by giving two energy barriers to be overcome before fusion can take place, thus increasing

fidelity of stimulus-secretion coupling.

Appendix

Appendix 1 **Bacterial strains used in this study**

Strain	Genotype	Source
NM522	*supE thi*-1 Δ(*lac-proAB*) Δ(*mcrB-hsdSM*)5 r_K^- m_K^-) [F ' *proAB lac*I^{q}ZΔM15]	Gough &Murray (1983)
BL21 (DE3)	B F$^-$ *dcm ompT hsdS*(r_B^- m_B^-) *gal* λ(DE3)	Stratagene
BL21 (DE3) pLysS	B F$^-$ *dcm ompT hsdS*(r_B^- m_B^-) *gal* λ(DE3) [pLysS Cam^r]	Stratagene
DH5α	*supE*44 Δ*lacU*169 (Φ80 *lacZ*ΔM15) *hsdR*17 *recA*1 *endA*1 *gyrA*96 *thi*-1 *relA*1	Gibco, BRL

Appendix 2 Plasmids used in this study

Table A2a Plasmids obtained from others

Plasmid	Supplier	Reference
pAX11	A. Boyd	Zueco & Boyd (1992)
pGEM-T	Promega	
pET16b	Novagen	Studier *et al* (1990)

Table A2b Plasmids constructed in this study

Plasmid	Cloning strategy
pGEM100	1 kb PCR product obtained using the two oligonucleotides 5'-ATG AAA GTC GAC TTA CTT CTT GAC GGC GAG CAT GGC & 5'-AAG TTT GAA TTC GGC CCG CGC GGA GGA AAG AAC GCG ATT AAC as primers and bovine adrenal cDNA plasmid library as template. Cloned into pGEM-T linear vector with 5' T extensions (fragment has 3' A extensions added by *Taq* polymerase).
pLC100	1 kb fragment with cohesive ends created following *Eco*RI / *Sal* I digestion of pGEM100 cloned into *Eco*RI / *Sal* I digested pAX11.
pGEM 600	1 kb PCR product using two oligonucleotides 5'-AAG TTT CAT ATG GGA GGA AAG AAC GCG ATT AAC & 5'-ATG AAA GGA TCC TTA CTT CTT GAC GGC GAG CAT as primers and bovine adrenal cDNA plasmid library as template DNA. Cloned into pGEM-T linear vector with 5' T extensions (fragment has 3' A extensions added by *Taq* polymerase).
pLC600	1 kb fragment with cohesive ends created following *Nde*I / *Bam*HI digestion of pGEM600 cloned into *Nde*I / *Bam*HI digested pET16b.

Appendix 3 DNA and aminoacid sequence of synaptotagmin

The DNA sequence cloned and the corresponding aminoacid sequence is underlined. The first six aminoacid residues of the recombinant SytC are in italics and numbered 97-102.

```
   1                                                    GGCGGCGGCGGCAGCACTTGG
  22 CAGCAGCAACTTGAGACTGCACTGGGGCAAGCCCCCAGGGTGGTGCTCCCCGGAGAGCGGGGCTTGG
  89 TGGCCCGGAGGGGTGTGTGTAGGGTGAGGGCGGCCAGCTGGGACCAGCTGGTGGCCCTGGAAAACCT
 156 CCCACACACCCACACCCACACCCCCCTTTTGTGTTGCAGGCTGCCCCTCCAAGAGCAGAGGCAGCGA
 223 AAGGAGTCGTGTGCACCGGTCAGCCCCGGGAAGCTGTAGGGACCGGCGAGCAGGCACCACCTCCTGT
 290 TCCCCGCTCCAGGAAAACCAGGAAAACGAGAACTAGCAAGAGCTTGACAAACACCTGCCTTCAGATT
 357 GGAAGACCAGTCACCTGTCATTCCTGGACTCTGCACTGCAGCTGTCTAAGTCTCAGCTGAACCCACG
     Met Val Ser Glu Ser His His Glu Ala Leu Ala Ala Pro Pro Val Thr Thr    17
 424 ATG GTG AGC GAG AGC CAT CAC GAG GCG CTG GCA GCC CCG CCG GTC ACC ACT
     Val Ala Thr Val Leu Pro His Asn Ala Thr Glu Pro Ala Ser Pro Gly Glu    34
 476 GTG GCG ACG GTC CTG CCA CAC AAC GCC ACA GAG CCA GCC AGT CCC GGG GAA
     Gly Lys Glu Asp Ala Phe Ser Lys Leu Lys Glu Lys Phe Met Asn Glu Leu    51
 527 GGG AAG GAG GAT GCC TTC TCC AAG CTG AAG GAG AAG TTT ATG AAT GAG TTG
     His Lys Ile Pro Leu Pro Pro Trp Ala Leu Ile Ala Ile Ala Ile Val Ala    68
 578 CAT AAA ATT CCA TTG CCA CCA TGG GCC TTA ATT GCC ATA GCC ATA GTT GCG
     Val Leu Leu Val Leu Thr Cys Cys Phe Cys Ile Cys Lys Lys Cys Leu Phe    85
 629 GTC CTT TTA GTC CTG ACC TGC TGC TTT TGT ATC TGT AAG AAA TGC TTA TTC
     Lys Lys Lys Asn Lys Lys Lys Gly Lys Glu Lys Gly Gly Lys Asn Ala Ile   102
 680 AAA AAG AAA AAC AAG AAG AAG GGA AAG GAA AAG GGA GGG AAG AAT GCC ATT
     Asn Met Lys Asp Val Lys Asp Leu Gly Lys Thr Met Lys Asp Gln Ala Leu   119
 731 AAC ATG AAG GAT GTG AAA GAC TTG GGG AAG ACC ATG AAA GAT CAG GCC CTG
     Lys Asp Asp Asp Ala Glu Thr Gly Leu Thr Asp Gly Glu Glu Lys Glu Glu   136
 782 AAG GAT GAT GAT GCT GAA ACC GGA TTG ACT GAT GGT GAA GAG AAA GAA GAA
     Pro Lys Glu Glu Glu Lys Leu Gly Lys Leu Gln Tyr Ser Leu Asp Tyr Asp   153
 833 CCC AAA GAA GAA GAG AAA CTG GGA AAA CTT CAG TAC TCA CTG GAT TAT GAT
     Phe Gln Asn Asn Gln Leu Leu Val Gly Ile Ile Gln Ala Ala Glu Leu Pro   170
 884 TTC CAG AAT AAC CAG CTG CTG GTA GGA ATC ATC CAG GCT GCC GAG TTG CCC
     Ala Leu Asp Met Gly Gly Thr Ser Asp Pro Tyr Val Lys Val Phe Leu Leu   187
 935 GCC TTG GAC ATG GGG GGC ACC TCT GAT CCC TAT GTG AAG GTT TTT CTG CTG
     Pro Asp Lys Lys Lys Lys Phe Glu Thr Lys Val His Arg Lys Thr Leu Asn   204
 986 CCC GAT AAA AAG AAG AAA TTT GAG ACA AAA GTC CAC CGA AAG ACC CTT AAT
     Pro Val Phe Asn Glu Gln Phe Thr Phe Lys Val Pro Tyr Ser Glu Leu Gly   221
1037 CCT GTC TTC AAC GAG CAA TTT ACT TTC AAG GTG CCA TAT TCG GAA TTG GGT
     Gly Lys Thr Leu Val Met Ala Val Tyr Asp Phe Asp Arg Phe Ser Lys His   238
1088 GGC AAA ACT CTG GTG ATG GCC GTC TAT GAT TTT GAT CGC TTC TCA AAG CAT
     Asp Ile Ile Gly Glu Phe Lys Val Pro Met Asn Thr Val Asp Phe Gly His   255
1139 GAC ATC ATT GGG GAA TTT AAA GTC CCC ATG AAC ACG GTG GAT TTC GGT CAC
     Val Thr Glu Glu Trp Arg Asp Leu Gln Ser Ala Glu Lys Glu Glu Gln Glu   272
1190 GTA ACT GAG GAG TGG CGT GAT CTG CAA AGT GCA GAG AAG GAA GAG CAA GAG
     Lys Leu Gly Asp Ile Cys Phe Ser Leu Arg Tyr Val Pro Thr Ala Gly Lys   289
1241 AAA TTG GGT GAT ATC TGC TTC TCC CTT CGC TAT GTA CCT ACT GCT GGC AAG
     Leu Thr Val Val Ile Leu Glu Ala Lys Asn Leu Lys Lys Met Asp Val Gly   306
1292 CTG ACT GTT GTC ATT CTG GAG GCA AAG AAC CTG AAG AAG ATG GAT GTG GGT
     Gly Leu Ser Asp Pro Tyr Val Lys Ile His Leu Met Gln Asn Gly Lys Arg   323
1343 GGC TTG TCT GAT CCT TAT GTG AAG ATT CAT CTG ATG CAG AAT GGC AAG AGG
     Leu Lys Lys Lys Lys Thr Thr Ile Lys Lys Asn Thr Leu Asn Pro Tyr Tyr   340
1394 CTG AAG AAG AAA AAG ACA ACA ATT AAA AAG AAT ACA CTT AAC CCC TAC TAC
     Asn Glu Ser Phe Ser Phe Glu Val Pro Phe Glu Gln Ile Gln Lys Val Gln   357
```

```
1445 AAT GAG TCA TTC AGC TTT GAA GTA CCC TTT GAG CAA ATC CAG AAA GTG CAA
     Val Val Val Thr Val Leu Asp Tyr Asp Lys Ile Gly Lys Asn Asp Ala Ile   374
1496 GTG GTG GTA ACT GTT TTG GAC TAT GAC AAG ATT GGC AAG AAC GAT GCC ATC
     Gly Lys Val Phe Val Gly Tyr Asn Ser Thr Gly Ala Glu Leu Arg His Trp   391
1547 GGC AAA GTG TTC GTG GGC TAC AAC AGC ACC GGG GCG GAG CTG CGA CAC TGG
     Ser Asp Met Leu Ala Asn Pro Arg Arg Pro Ile Ala Gln Trp His Thr Leu   408
1598 TCA GAC ATG CTG GCT AAC CCC CGG CGC CCC ATC GCC CAG TGG CAC ACC CTG
     Gln Val Glu Glu Glu Val Asp Ala Met Leu Ala Val Lys Lys Stop          422
1649 CAG GTA GAG GAG GAG GTT GAC GCC ATG CTG GCA GTC AAG AAG TAA GGGGAGA
1701 AGAAGCCTTTCTGTGTTTGCCCACATAGTGCTCTTTAGCCAGTATCTGTAAATACCTCAGTAATATG
1768 GGTCCTTTCGTTTTTCCAGCCATGCATTCCTAACACAATTCAGTGGTACTTCAAATCCTGTTTTAAT
1835 TTGCACAAATTTAAATGTAGAGAGCCCCAAAGCCCTTCATCATACCACTGCCCTCCAAATCTACTCT
1902 TCTTTTAAGCAATATGATGTGTAGATAGAGCATGACGGAAATTCTTTATTGTATCACACCGTTGTAC
1969 ATATCAGTATGCTAAAGATTTATTTCTAGTTTGTGTATTTGTATGTTGTAAGCGTTTCCTAATCTGT
2036 GTATATCTAGATGTTTTTAATAAGATGTTCTATTTTAAACTATGTAAATTGACTGAGATATAGGAGA
2103 GCTGATAATATATTATACGGTAAATAGAGTATCATCTGCATTCCAGCAATCTCAACTTGTAAGGCAC
2170 TAGTACAGTGAAGCTGACATCTTAAAGGACAACTTAAACCTGAGCTTCTATTGAATCCTATGAGCAC
2237 CAAGATACGCTTGCACCACAGATTTGGTGGGCGAATCCAATTTTGTAGAATTTCTTCACAGGCAAAC
2304 TAGCATGATCTGAGCAGCATCCAGCCTGACCTCCAGGAAGCACAGCCACAAACAGAATAGTATCCGT
2371 CTGTGCATATCTACAGAGCTTAAGTCAGAGCTTAACTCTGACATTCGCAGAAGCAACTGACCAGTGG
2438 TTGATGATTCCATGTTACTGCACATAGAGTAATGACTTGATGGTATTCCGTGTGTGTGTGTGTTTGT
2505 GTGTGTGTGTGTGTGTACACACCCGCATTTGTCTAGGGATGGGAGGGGTGGGAAGAAGCAGAGGAGA
2572 GAAGTCGGCATTTCTAAATGTTGCCTGACTATTCAAGAAGAAAAGTAGCTCT
```

Appendix 4 Sequence analysis of gene encoding His10-SytC

Schematic representation of the gene construct showing three potential initiation codons

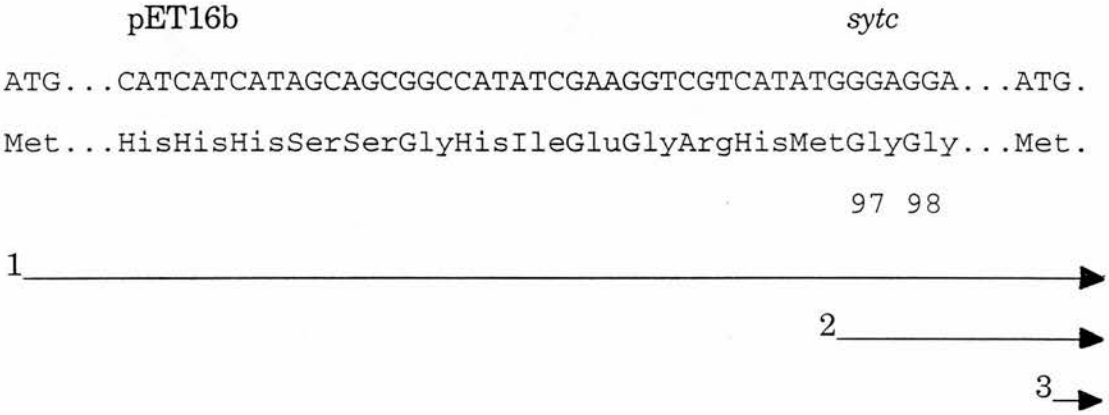

The arrows indicate direction of translation. The sequence shows three potential start codons 1, 2 and 3. Translation from Met1 gives a protein containing both the His10 and SytC portion of the fusion and is therefore easily purified on Ni-NTA agarose. Translation from either Met2 or Met3 gives rise to a protein consisting mainly of SytC. The resulting protein is seen on a Western blot using a SytC specific antibody but cannot be purified with Ni-NTA agarose since it lacks the His10 portion which has affinity for Ni.

References

Alvarez, E., Girones, N. and Davis, R.J. Inhibition of the receptor-mediated endocytosis of diferric transferrin is associated with the covalent modification of the transferrin receptor with palmitic acid. *Journal of Biological Chemistry* 265:16644-16655, 1990.

Anderson, R.G.W. Dissecting clathrin-coated pits. *Trends in Cell Biology* 3:177-179, 1993.

Angaut-Petit, D., Juzans, P., Molgo, J., Faille, L., Seagar, M.J., Takahashi, M. and Shoji-Kasai, Y. mouse motor nerve terminal immunoreactivity to synaptotagmin II during sustained quantal transmitter release. *Brain Research* 681:213-217, 1995.

Artalejo, C.R., Elhamdani, A. and Palfrey, H.C. Calmodulin is the divalent cation receptor for rapid endocytosis, but not exocytosis, in adrenal chromaffin cells. *Neuron.* 16:195-205, 1996.

Augustine, G.J. and Neher, E. Calcium requirements for secretion in bovine chromaffin cells. *Journal of Physiology* 450:247-271, 1992.

Bader, M.F., Hikita, T. and Trifaro, J.M. Calcium-dependent calmodulin binding to chromaffin granule membranes: Presence of a 65-kilodalton calmodulin-binding protein. *Journal of Neurochemistry* 44:526-539, 1985.

Banerjee, A., Barry, V.A., DasGupta, B.R. and Martin, T.F.J. N-ethylmaleimide-sensitive factor acts at a prefusion ATP-dependent step in Ca^{2+}-activated exocytosis. *Journal of Biological Chemistry* 271:20223-20226, 1996.

Bauerfeind, R. and Huttner, W.B. Biogenesis of constitutive secretory vesicles, secretory granules and synaptic vesicles. *Current Opinion in Cell Biology* 5:1106, 1993.

Bauerfeind, R., Jelinek, R. and Huttner, W.B. Synaptotagmin I- and II-deficient PC12 cells exhibit calcium- independent, depolarization-induced neurotransmitter release from synaptic-like microvesicles. *FEBS Letters* 364:328-334, 1995.

Bazzi, M. and Nelsestuen, G.L. Protein kinase C interaction with calcium: A phospholipid-dependent process. *Biochemistry (USA)* 29:7624-7630, 1990.

Bennet, M.K. and Scheller, R.H. The molecular machinery for secretion is conserved from yeast to neurons. *Proceedings of the National Academy of Sciences of the United States of America* 90:2559-2563, 1993.

Birnboim, H.C. and Doly, J. A rapid extraction procedure for screenin recombinant plasmid DNA. *Nucleic Acids Research* 76:1513-1523, 1979.

Bittner, M.A. and Holz, R.W. Phorbol esters enhance exocytosis from chromaffin cells by two mechanisms. *Journal of Neurochemistry* 54:205-210, 1990.

Bittner, M.A. and Holz, R.W. Kinetic analysis of secretion from permeabilized adrenal chromaffin cells reveals distinct components. *Journal of Biological Chemistry* 267:16219-16225, 1992.

Bommert, K., Charlton, M.P., DeBello, W.M., Chin, G.J., Betz, H. and Augustine, G.J. Inhibition of neurotransmitter release by C2-domain peptides implicates synaptotagmin in exocytosis. *Nature* 363:163-165, 1993.

Bordier, C. Phase separation of integral membrane proteins in Triton X-114 solution. *J.Biol.Chem.* 256:1604-1607, 1981.

Broadie, K., Bellen, H.J., DiAntonio, A., Littleton, J.T. and Schwarz, T.L. Absence of synaptotagmin disrupts excitation-secretion coupling during synaptic transmission. *Proceedings of the National Academy of Sciences of the United States of America* 91:10727-10731, 1994.

Broadie, K., Prokop, A., Bellen, H.J., OKane, C.J., Schulze, K.L. and Sweeney, S.T. Syntaxin and synaptobrevin function downstream of vesicle docking in drosophila. *Neuron* 15:663-673, 1995.

Brose, N., Petrenko, A.G., Südhof, T.C. and Jahn, R. Synaptotagmin: A calcium sensor on the synaptic vesicle surface. *Science* 256:1021-1025, 1992.

Burgoyne, R.D. Control of exocytosis in adrenal chromaffin cells. *Biochimica et Biophysica Acta - Reviews on Biomembranes* 1071:174-202, 1991.

Burgoyne, R.D. and Morgan, A. Ca^{2+} and secretory-vesicle dynamics. *Trends in Neurosciences* 18:191-196, 1995.

Burgoyne, R.D., Morgan, A., Barnard, R.J.O., Chamberlain, L.H., Glenn, D.E. and Kibble, A.V. SNAPs and SNAREs in exocytosis in chromaffin cells. *Biochemical Society Transactions* 24:653-657, 1996.

Calakos, N. and Scheller, R.H. Synaptic vesicle biogenesis, docking, and fusion: A molecular description. *Physiol.Rev.* 76:1-29, 1996.

Chamberlain, L.H., Roth, D., Morgan, A. and Burgoyne, R.D. Distinct effects of a-SNAP, 14-3-3 proteins and calmodulin on priming and triggering of regulated exocytosis. *J.Cell Biol.* 130:1063-1070, 1995.

Chapman, E.R., An, S., Edwardson, J.M. and Jahn, R. A novel function for the second C2 domain of synaptotagmin - Ca^{2+}- triggered dimerization. *J.Biol.Chem.* 271:5844-5849, 1996b.

Chapman, E.R., Blasi, J., An, S., Brose, N., Johnston, P.A., Südhof, T.C. and Jahn, R. Fatty acylation of synaptotagmin in PC12 cells and synaptosomes. *Biochemical and Biophysical Research Communications* 225:326-332, 1996a.

Chapman, E.R., Hanson, P.I., An, S. and Jahn, R. Ca^{2+} regulates the interaction between synaptotagmin and syntaxin 1. *Journal of Biological Chemistry* 270:23667-23671, 1995.

Chapman, E.R. and Jahn, R. Calcium-dependent interaction of the cytoplasmic region of synaptotagmin with membranes. Autonomous function of a single C2- homologous domain. *Journal of Biological Chemistry* 269:5735-5741, 1994.

Cooper, R.L., Hampson, D.R. and Atwood, H.L. Synaptotagmin-like expression in the motor nerve terminals of crayfish. *Brain Res.* 703:214-216, 1995.

Damer, C.K. and Creutz, C.E. Synergistic membrane interactions of the two C2 domains of synaptotagmin. *Journal of Biological Chemistry* 269:31115-31123, 1994.

Damer, C.K. and Creutz, C.E. Calcium-dependent self-association of synaptotagmin I. *Journal of Neurochemistry* 67:1661-1668, 1996.

Davletov, B., Sontag, J.M., Hata, Y., Petrenko, A.G., Fykse, E.M., Jahn, R. and Südhof, T.C. Phosphorylation of synaptotagmin I by casein kinase II. *Journal of Biological Chemistry* 268:6816-6822, 1993.

Davletov, B.A., Shamotienko, O.G., Lelianova, V.G., Grishin, E.V. and Ushkaryov, Y.A. Isolation and biochemical characterization of a Ca^{2+}-independent alpha- latrotoxin-binding protein. *Journal of Biological Chemistry* 271:23239-23245, 1996.

Davletov, B.A. and Südhof, T.C. A single C2 domain from synaptotagmin I is sufficient for high affinity Ca^{2+}/phospholipid binding. *Journal of Biological Chemistry* 268:26386-26390, 1993.

Davletov, B.A. and Südhof, T.C. Ca^{2+}-dependent conformational change in synaptotagmin I. *Journal of Biological Chemistry* 269:28547-28550, 1994.

DiAntonio, A., Parfitt, K.D. and Schwarz, T.L. Synaptic transmission persists in synaptotagmin mutants of Drosophila. *Cell* 73:1281-1290, 1993.

Dunbar, B. and Wilson, S.B. A buffer exchange procedure giving enhanced resolution to polyacrylamide gels prerun for protein sequencing. *Analytical Biochemistry* 216:227-228, 1994.

Egger, C., Kirchmair, R., Kapelari, S., FischerColbrie, R., HogueAngeletti, R. and Winkler, H. Bovine posterior pituitary: Presence of p65 (synaptotagmin), PC1, PC2 and secretoneurin in large dense core vesicles. *Neuroendocrinology* 59:169-175, 1994.

El Far, O., MartinMoutot, N., Leveque, C., David, P., Marqueze, B., Lang, B., NewsomDavis, J., Hoshino, T., Takahashi, M. and Seagar, M.J. Synaptotagmin associates with presynaptic calcium channels and is a Lambert-Eaton myasthenic syndrome antigen. *Annals of the New York Academy of Sciences* 707:382-385, 1993.

Elferink, L.A., Peterson, M.R. and Scheller, R.H. A role for synaptotagmin (p65) in regulated exocytosis. *Cell* 72:153-159, 1993.

Essen, L.O., Perisic, O., Cheung, R., Katan, M. and Williams, R.L. Crystal structure of a mammalian phosphoinositide-specific phospholipase Cdelta. *Nature* 380:595-602, 1996.

Feany, M.B. and Buckley, K.M. The synaptic vesicle protein synaptotagmin promotes formation of filopodia in fibroblasts. *Nature* 364:537-540, 1993.

Fesce, R., Grohovaz, F., Valtorta, F. and Meldolesi, J. Neurotransmitter release: Fusion or 'kiss-and-run'? *Trends in Cell Biology* 4:1-4, 1994.

Fournier, S., Novas, M.L. and Trifaro, J.M. Subcellular distribution of 65,000 calmodulin-binding protein (p65) and synaptophysin (p38) in adrenal medulla. *Journal of Neurochemistry* 53:1043-1049, 1989.

Fournier, S. and Trifaro, J.M. A similar calmodulin-binding protein expressed in chromaffin, synaptic, and neurohypophyseal secretory vesicles. *Journal of Neurochemistry* 50:27-37, 1988a.

Fournier, S. and Trifaro, J.M. Calmodulin-binding proteins in chromaffin cell plasma membranes. *Journal of Neurochemistry* 51:1599-1609, 1988b.

Fukuda, M., Kojima, T., Aruga, J., Niinobe, M. and Mikoshiba, K. Functional diversity of C2 domains of synaptotagmin family. Mutational analysis of inositol high polyphosphate binding domain. *Journal of Biological Chemistry* 270:26523-26527, 1995b.

Fukuda, M., Kojima, T. and Mikoshiba, K. Phospholipid composition dependence of Ca^{2+}-dependent phospholipid binding to the C2A domain of synaptotagmin IV. *J.Biol.Chem.* 271:8430-8434, 1996.

Fukuda, M., Kojima, T. and Mikoshiba, K. Regulation by bivalent cations of phospholipid binding to the C2A domain of synaptotagmin III. *Biochemical Journal* 323:421-425, 1997.

Fukuda, M., Moreira, J.E., Lewis, F.M.T., Sugimori, M., Niinobe, M., Mikoshiba, K. and Llinas, R. Role of the C2B domain of synaptotagmin in vesicular release and recycling as determined by specific antibody injection into the squid giant synapse preterminal. *Proceedings of the National Academy of Sciences of the United States of America* 92:10708-10712, 1995a.

Garewal, H.S. A procedure for the estimation of microgram quantities of triton X-100. *Analytical Biochemistry* 54:319-324, 1973.

Geppert, M., Archer BT, I.I.I. and Südhof, T.C. Synaptotagmin II: A novel differentially distributed form of synaptotagmin. *Journal of Biological Chemistry* 266:13548-13552, 1991.

Geppert, M., Goda, Y., Hammer, R.E., Li, C., Rosahl, T.W., Stevens, C.F. and Südhof, T.C. Synaptotagmin I: A major Ca^{2+} sensor for transmitter release at a central synapse. *Cell* 79:717-727, 1994.

Gillis, K.D. and Chow, R.H. Kinetics of exocytosis in adrenal chromaffin cells. *Cell and Developmental Biology* 8:133-140, 1997.

Gillis, K.D., Mossner, R. and Neher, E. Protein kinase C enhances exocytosis from chromaffin cells by increasing the size of the readily releasable pool of secretory granules. *Neuron.* 16:1209-1220, 1996.

Goda, Y. SNARES and regulated vesicle exocytosis. *Proceedings of the National Academy of Sciences of the United States of America* 94:769-772, 1997.

Goda, Y. and Stevens, C.F. Two components of transmitter release at a central synapse. *Proceedings of the National Academy of Sciences of the United States of America* 91:12942-12946, 1994.

Gough, J.A. and Murray, N.E. Sequence diversity among related genes for recognition of specific targets in DNA molecules. *Journal of Molecular Biology* 166:1-19, 1983.

Grobler, J.A., Essen, L.O., Williams, R.L. and Hurley, J.H. C2 domain conformational changes in phospholipase C-delta1. *Nature Structural Biology* 3:788-795, 1996.

Hadad, N., Zable, A.C., Abramson, J.J. and Shoshan-Barmatz, V. Binding sites of the ryanodine receptor/Ca^{2+} release channel of the sarcoplasmic reticulum. *Journal of Biological Chemistry* 269:24864-24889, 1994.

Hajela, R.K. and Atchison, W.D. The proteins synaptotagmin and syntaxin are not general targets of Lambert-Eaton myasthenic syndrome autoantibody. *Journal of Neurochemistry* 64:1245-1251, 1995.

Hata, Y., Davletov, B., Petrenko, A.G., Jahn, R. and Südhof, T.C. Interaction of synaptotagmin with the cytoplasmic domains of neurexins. *Neuron* 10:307-315, 1993.

Hay, J.C., Fisette, P.L., Jenkins, G.H., Fukami, K., Takenawa, T., Anderson, R.A. and Martin, T.F.J. ATP-dependent inositide phosphorylation required for Ca^{2+}-activated secretion. *Nature* 374:173-177, 1995.

Heidelberger, R., Heinemann, C., Neher, E. and Matthews, G. Calcium dependence of the rate of exocytosis in a synaptic terminal. *Nature* 371:513-515, 1994.

Heinemann, C., Chow, R.H., Neher, E. and Zucker, R.S. Kinetics of the secretory response in bovine chromaffin cells following flash photolysis of caged Ca^{2+}. *Biophysical Journal* 67:2546-2557, 1994.

Hens, J.J.H., Oestreicher, A.B., DeWit, M., Marquart, A., Gispen, W.H. and DeGraan, P.N.E. Evidence for a role of calmodulin in calcium-induced noradrenaline release from permeated synaptosomes: Effects of calmodulin antibodies and antagonists. *J.Neurochem.* 66:1933-1942, 1996.

Hikita, T., Bader, M.F. and Trifaro, J.M. Adrenal chromaffin cell calmodulin: its subcellular distribution and binding to chromaffin granule membrane proteins. *J.Neurochem.* 43:1087-1097, 1984.

Holz, R.W., Bittner, M.A., Peppers, S.C., Senter, R.A. and Eberhard, D.A. MgATP-independent and MgATP-dependent exocytosis. Evidence that MgATP primes adrenal chromaffin cells to undergo exocytosis. *Journal of Biological Chemistry* 264:5412-5419, 1989.

Hunt, J.M., Bommert, K., Charlton, M.P., Kistner, A., Habermann, E., Augustine, G.J. and Betz, H. A post-docking role for synaptobrevin in synaptic vesicle fusion. *Neuron* 12:1269-1279, 1994.

Jorgensen, E.M., Hartwieg, E., Schuske, R., Nonet, M.L., Jin, Y. and Horvitz, H.R. Defective recycling of synaptic vesicles in synaptotagmin mutants of Caenorhabditis elegans. *Nature* 378:196-199, 1995.

Kee, Y. and Scheller, R.H. Localization of synaptotagmin-binding domains on syntaxin. *J.Neurosci.* 16:1975-1981, 1996.

Kibble, A.W. and Burgoyne, R.D. Calmodulin increases the initial rate of exocytosis in adrenal chromaffin cells. *Pflugers.Arch.Eur.J.Physiol.* 431:464-466, 1996.

Klee, C.B. Interactions of calmodulin with Ca^{2+} and target proteins. In: *Calmodulin*, edited by Klee, C.B. and Cohen, P. New York: Elsevier, 1988, p. 35-89.

Krasnoperov, V.G., Bittner, M.A., Beavis, R., Kuang, Y., Salnikow, K.V., Chepurny, O.G., Little, A.R., Plotnikov, A.N., Wu, D., Holz, R.W. and Petrenko, A.G. alpha-Latrotoxin stimulates exocytosis by the interaction with a neuronal G-protein-coupled receptor. *Neuron* 18:925-937, 1997.

Krueger, B.K., Ratzlaff, G.R., Strichartz, G.R. and Blaustein, M.P. Saxitoxin binding to synaptosomes, membranes and solubilised binding sites from rat brain. *Journal of Membrane Biology* 50:287-310, 1979.

Laemmli, U.K. Cleavage of structural proteins during the assembly of the head of bacteriophage T4. *Nature* 227:680-685, 1979.

Leveque, C., Hoshino, T., David, P., ShojiKasai, Y., Leys, K., Omori, A., Lang, B., Far, O.E., Sato, K., MartinMoutot, N., NewsomDavis, J., Takahashi, M. and Seagar, M.J. The synaptic vesicle protein synaptotagmin associates with calcium channels and is a putative Lambert-Eaton myasthenic syndrome antigen. *Proceedings of the National Academy of Sciences of the United States of America* 89:3625-3629, 1992.

Li, C., Ullrich, B., Zhang, J.Z., Anderson, R.G.W., Brose, N. and Südhof, T.C. Ca^{2+} -dependent and -independent activities of neural and non-neural synaptotagmins. *Nature* 375:594-599, 1995.

Li, J.Y., Jahn, R. and Dahlstrom, A. Synaptotagmin I is present mainly in autonomic and sensory neurons of the rat peripheral nervous system. *Neuroscience* 63:837-850, 1994.

Lindau, M. and Gomperts, B.D. Techniques and concepts in exocytosis: Focus on mast cells. *Biochimica et Biophysica Acta - Reviews on Biomembranes* 1071:429-471, 1991.

Littleton, J.T., Bellen, H.J. and Perin, M.S. Expression of synaptotagmin in Drosophila reveals transport and localization of synaptic vesicles to the synapse. *Development* 118:1077-1088, 1993a.

Littleton, J.T., Stern, M., Perin, M. and Bellen, H.J. Calcium dependence of neurotransmitter release and rate of spontaneous vesicle fusions are altered in Drosophila synaptotagmin mutants. *Proceedings of the National Academy of Sciences of the United States of America* 91:10888-10892, 1994.

Littleton, J.T., Stern, M., Schulze, K., Perin, M. and Bellen, H.J. Mutational analysis of Drosophila synaptotagmin demonstrates its essential role in Ca^{2+}-activated neurotransmitter release. *Cell* 74:1125-1134, 1993b.

Llinas, R., Sugimori, M., Lang, E.J., Morita, M., Fukuda, M., Niinobe, M. and Mikoshiba, K. The inositol high-polyphosphate series blocks synaptic transmission by preventing vesicular fusion: A squid giant synapse study. *Proceedings of the National Academy of Sciences of the United States of America* 91:12990-12993, 1994.

Lowe, A.W., Madeddu, L. and Kelly, R.B. Endocrine secretory granules and neuronal synaptic vesicles have three integral membrane proteins in common. *Journal of Cell Biology* 106:51-59, 1988.

Lowenadler, B., Nilsson, B., Abrahmsen, L., Moles, T., Ljungqvist, L., Holmgren, E., Paleus, S., Josephson, S., Philipson, L. and Uhlen, M. Production of specific antibodies against protein A fusion proteins. *EMBO J.* 5:2393-2398, 1986.

Lowry, O.H., Rosebrough, N.J., Farr, A.L. and Randall, R.J. Protein measurement with the folin reagent. *J.Biol.Chem.* 193:265-275, 1951.

Martin, T.F.J Stages of regulated exocytosis. *Trends in Cell Biology* 7:271-276, 1997.

Matsudaira, P. Sequence from picomole quantities of proteins electroblotted onto polyvinylidene difluoride membranes. *Journal of Biological Chemistry* 262:10035-10038, 1987.

Matthew, W.D., Tsavaler, L. and Reichardt, L.F. Identification of a synaptic vesicle-specific membrane protein with a wide distribution in neuronal and neurosecretory tissue. *Journal of Cell Biology* 91:257-269, 1981.

Mayer, A., Wickner, W. and Haas, A. Sec18p (NSF)-driven release of Sec17p (alpha-SNAP) can precede docking and fusion of yeast vacuoles. *Cell* 85:83-94, 1996.

Mehta, P.P., Battenberg, E. and Wilson, M.C. SNAP-25 and synaptotagmin involvement in the final Ca^{2+}-dependent triggering of neurotransmitter exocytosis. *Proceedings of the National Academy of Sciences of the United States of America* 93:10471-10476, 1996.

Mikoshiba, K., Fukuda, M., Moreira, J.E., Lewis, F.M.T., Sugimori, M., Niinobe, M. and Llinas, R. Role of the C2A domain of synaptotagmin in transmitter release as determined by specific antibody injection into the squid giant synapse preterminal. *Proceedings of the National Academy of Sciences of the United States of America* 92:10703-10707, 1995.

Mizuta, M., Inagaki, N., Nemoto, Y., Matsukura, S., Takahashi, M. and Seino, S. Synaptotagmin III is a novel isoform of rat synaptotagmin expressed in endocrine and neuronal cells. *Journal of Biological Chemistry* 269:11675-11678, 1994.

Mochida, S., Fukuda, M., Niinobe, M., Kobayashi, H. and Mikoshiba, K. Roles of synaptotagmin C2 domains in neurotransmitter secretion and inositol high-polyphosphate binding at mammalian cholinergic synapses. *Neuroscience* 77:937-943, 1997.

Morgan, A. and Burgoyne, R.D. Is NSF a fusion protein? *Trends in Cell Biology* 5:335-339, 1995.

Morgan, A. and Burgoyne, R.D. Common mechanisms for regulated exocytosis in the chromaffin cell and the synapse. *Seminars in Cell and Developmental Biology* 8:141-149, 1997.

Morimoto, T., Popov, S., Buckley, K.M. and Poo, M.M. Calcium-dependent transmitter secretion from fibroblasts: Modulation by synaptotagmin I. *Neuron* 15:689-696, 1995.

Morris, S.J. and Schober, R. Demonstration of binding sites for divalent and trivalent ions on the outer surface of chromaffin granule membranes. *Eur J Bioch* 75:1-12, 1977.

Neher, E. and Zucker, R.S. Multiple calcium-dependent processes related to secretion in bovine chromaffin cells. *Neuron* 10:21-30, 1993.

Newton, A.C. Protein kinase C: Structure, function, and regulation. *Journal of Biological Chemistry* 270:28495-28498, 1995.

Newton, A.C. Regulation of protein kinase C. *Current Opinion in Cell Biology* 9:161-167, 1997.
Niinobe, M., Yamaguchi, Y., Fukuda, M. and Mikoshiba, K. Synaptotagmin is an inositol polyphosphate binding protein: Isolation and characterization as an Ins 1,3,4,5-P4 binding protein. *Biochemical and Biophysical Research Communications* 205:1036-1042, 1994.

Nishiki, T., Tokuyama, Y., Kamata, Y., Nemoto, Y., Yoshida, A., Sato, K., Sekiguchi, M., Takahashi, M. and Kozaki, S. The high-affinity binding of Clostridium botulinum type B neurotoxin t o synaptotagmin II associated with gangliosides G(T1b)/G(D1a). *FEBS Lett.* 378:253-257, 1996.

Nishiki, T.I., Kamata, Y., Nemoto, Y., Omori, A., Ito, T., Takahashi, M. and Kozaki, S. Identification of protein receptor for Clostridium botulinum type B neurotoxin in rat brain synaptosomes. *Journal of Biological Chemistry* 269:10498-10503, 1994.

Nonet, M.L., Grundahl, K., Meyer, B.J. and Rand, J.B. Synaptic function is impaired but not eliminated in C. elegans mutants lacking synaptotagmin. *Cell* 73:1291-1305, 1993.
O'Connor, V.M., Augustine, G.J. and Betz, H. Synapic vesicle exocytosis: molecules and models. *Cell* 76:785-787, 1994.

O'Connor, V.M., Shamotienko, O., Grishin, E. and Betz, H. On the structure of the 'synaptosecretosome'. Evidence for a neurexin/synaptotagmin/syntaxin/Ca^{2+} channel complex. *FEBS Letters* 326:255-260, 1993.

Orr, J.W. and Newton, A.C. Intrapeptide Regulation of Protein Kinase C. *Journal of Biological Chemistry* 269:8383-8387, 1994.

Parsons, T.D., Coorssen, J.R., Horstmann, H. and Almers, W. Docked granules, the exocytic burst, and the need for ATP hydrolysis in endocrine cells. *Neuron* 15:1085-1096, 1995.

Patzak, A. and Winkler, H. Exocytotic exposure and recycling of membrane antigens of chromaffin granules: Ultrastructural evaluation after immunolabeling. *Journal of Cell Biology* 102:510-515, 1986.

Perin, M.S. The COOH terminus of synaptotagmin mediates interaction with the neurexins. *Journal of Biological Chemistry* 269:8576-8581, 1994.

Perin, M.S. Mirror image motifs mediate the interaction of the COOH terminus of multiple synaptotagmins with the neurexins and calmodulin. *Biochemistry* 35:13808-13816, 1996.

Perin, M.S., Brose, N., Jahn, R. and Südhof, T.C. Domain structure of synaptotagmin (p65). *Journal of Biological Chemistry* 266:623-629, 1991a.

Perin, M.S., Fried, V.A., Mignery, G.A., Jahn, R. and Südhof, T.C. Phospholipid binding by a synaptic vesicle protein homologous to the regulatory region of protein kinase C. *Nature* 345:260-263, 1990.

Perin, M.S., Johnston, P.A., Ozcelik, T., Jahn, R., Francke, U. and Südhof, T.C. Structural and functional conservation of synaptotagmin (p65) in Drosophila and humans. *Journal of Biological Chemistry* 266:615-622, 1991b.

Petrenko, A.G., Perin, M.S., Davletov, B.A., Ushkaryov, Y.A., Geppert, M. and Südhof, T.C. Binding of synaptotagmin to the alpha-latrotoxin receptor implicates both in synaptic vesicle exocytosis. *Nature* 353:65-68, 1991.

Popoli, M. Synaptotagmin is endogenously phosphorylated by Ca^{2+}/calmodulin protein kinase II in synaptic vesicles. *FEBS Letters* 317:85-88, 1993.

Popoli, M., Venegoni, A., Vocaturo, C., Buffa, L., Perez, J., Smeraldi, E. and Racagni, G. Long term blockade of serotonin reuptake affects synaptotagmin phosphorylation in the hippocampus. *Molecular Pharmacology* 51:19-26, 1997.

Redecker, P., Cetin, Y. and Grube, D. Differential distribution of synaptotagmin I and rab3 in the anterior pituitary of four mammalian species. *Neuroendocrinology* 62:101-110, 1995.

Roth, D. and Burgoyne, R.D. Stimulation of catecholamine secretion from adrenal chromaffin cells by 14-3-3 proteins is due to reorganisation of the cortical actin network. *FEBS Letters* 374:77-81, 1995.

Rothman, J.E. Mechanisms of intracellular protein transport. *Nature* 372:55-63, 1994.

Sambrook, J., Fritsch, E.F. and Maniatis, T. *Molecular cloning: A laboratory manual*, New York:Cold Spring Harbour Laboratory Press, 1989. Ed. 2

Sanger, F., Nicklen, S. and Coulson, A.R. DNA sequencing with chain termination inhibitors. *Proc.Natl.Acad.Sci.USA.* 74:5463, 1977.

Schagger, H. Native gel electrophoresis. In: *A practical guide to membrane protein purification*, edited by Von Jagow, G. and Schagger, H. Academic Press, 1994,

Schiavo, G., Gu, Q.M., Prestwich, G.D., Sollner, T.H. and Rothman, J.E. Calcium-dependent switching of the specificity of phosphoinositide binding to synaptotagmin. *Proceedings of the National Academy of Sciences of the United States of America* 93:13327-13332, 1996.

Schiavo, G., Stenbeck, G., Rothman, J.E. and Sollner, T.H. Binding of the synaptic vesicle v-SNARE, synaptotagmin, to the plasma membrane t-SNARE, SNAP-25, can explain docked vesicles at neurotoxin- treated synapses. *Proceedings of the National Academy of Sciences of the United States of America* 94:997-1001, 1997.

Schivell, A.E., Batchelor, R.H. and Bajjalieh, S.M. Isoform-specific, calcium-regulated interaction of the synaptic vesicle proteins SV2 and synaptotagmin. *Journal of Biological Chemistry* 271:27770-27775, 1996.

Shao, X., Li, C., Fernandez, I., Zhang, X., Südhof, T.C. and Rizo, J. Synaptotagmin-syntaxin interaction: The C2 domain as a Ca^{2+}-dependent electrostatic switch. *Neuron* 18:133-142, 1997.

Shao, X.G., Davletov, B.A., Sutton, R.B., Südhof, T.C. and Rizo, J. Bipartite Ca^{2+}-binding motif in C-2 domains of synaptotagmin and protein kinase C. *Science* 273:248-251, 1996.

ShojiKasai, Y., Yoshida, A., Ogura, A., Kuwahara, R., Grasso, A. and Takahashi, M. Synaptotagmin I is essential for Ca^{2+}-independent release of neurotransmitter induced by alpha-latrotoxin. *FEBS Letters* 353:315-318, 1994.

ShojiKasai, Y., Yoshida, A., Sato, K., Hoshino, T., Ogura, A., Kondo, S., Fujimoto, Y., Kuwahara, R., Kato, R. and Takahashi, M. Neurotransmitter release from synaptotagmin-deficient clonal variants of PC12 cells. *Science* 256:1820-1823, 1992.

Smith, D.O., Conklin, M.W., Jenson, P.J. and Atchison, W.D. Decreased calcium current in motor nerve terminals of mice with Lambert-Eaton myasthenic syndrome. *Journal of Physiology* 487:115-123, 1995.

Sollner, T., Bennett, M.K., Whiteheart, S.W., Scheller, R.H. and Rothman, J.E. A protein assembly-disassembly pathway in vitro that may correspond to sequential steps of synaptic vesicle docking, activation, and fusion. *Cell* 75:409-418, 1993b.

Sollner, T., Whiteheart, S.W., Brunner, M., ErdjumentBromage, H., Geromanos, S., Tempst, P. and Rothman, J.E. SNAP receptors implicated in vesicle targeting and fusion. *Nature* 362:318-324, 1993a.

Studier, F.W., Rosenberg, A.H., Dunn, J.J. and Dubendorff, J.W. Use of T7 RNA polymerase to direct expression of cloned genes. *Methods in Enzymology* 185:60-89, 1990.

Sugita, S., Hata, Y. and Südhof, T.C. Distinct Ca^{2+}-dependent properties of the first and second C-2-domains of synaptotagmin I. *J.Biol.Chem.* 271:1262-1265, 1996.

Sutton, R.B., Davletov, B.A., Berghuis, A.M., Südhof, T.C. and Sprang, S.R. Structure of the first C2 domain of synaptotagmin I: A novel Ca^{2+}/phospholipid-binding fold. *Cell* 80:929-938, 1995.

Takamori, M., Hamada, T., Komai, K., Takahashi, M. and Yoshida, A. Synaptotagmin can cause an immune-mediated model of Lambert-Eaton myasthenic syndrome in rats. *Annals of Neurology* 35:74-80, 1994.

TerBush, D.R. and Holz, R.W. Barium and calcium stimulate secretion from digitonin-permeabilized bovine adrenal chromaffin cells by similar pathways. *Journal of Neurochemistry* 58:680-687, 1992.

Tocco, G., Bi, X.N., Vician, L., Lim, I.K., Herschman, H. and Baudry, M. Two synaptotagmin genes, Syt1 and Syt4, are differentially regulated in adult brain and during postnatal development following kainic acid- induced seizures. *Mol.Brain Res.* 40:229-239, 1996.

Trifaro, J.M. and Vitale, M.L. Cytoskeleton dynamics during neurotransmitter release. *Trends in Neurosciences* 16:466-472, 1993.

Tugal, H.B., Van Leeuwen, F., Apps, D.K., Haywood, J. and Phillips, J.H. Glycosylation and transmembrane topography of bovine chromaffin granule p65. *Biochemical Journal* 279:699-703, 1991.

Ullrich, B., Li, C., Zhang, J.Z., McMahon, H., Anderson, R.G.W., Geppert, M. and Südhof, T.C. Functional properties of multiple synaptotagmins in brain. *Neuron* 13:1281-1291, 1994.

Ullrich, B. and Südhof, T.C. Differential distributions of novel synaptotagmins: Comparison to synapsins. *Neuropharmacology* 34:1371-1377, 1995.

Valtorta, F., Benfenati, F. and Greengard, P. Structure and function of the synapsins. *Journal of Biological Chemistry* 267:7195-7198, 1992.

Vician, L., In Kyoung Lim;, , Ferguson, G., Tocco, G., Baudry, M. and Herschman, H.R. Synaptotagmin IV is an immediate early gene induced by depolarization in PC12 cells and in brain. *Proceedings of the National Academy of Sciences of the United States of America* 92:2164-2168, 1995.

Vitale, M.L., Seward, E.P. and Trifaro, J.M. Chromaffin cell cortical actin network dynamics control the size of the release-ready vesicle pool and the initial rate of exocytosis. *Neuron* 14:353-363, 1995.

Von Ruden, L. and Neher, E. A Ca-dependent early step in the release of catecholamines from adrenal chromaffin cells. *Science* 262:1061-1064, 1993.

Vorherr, T., James, P., Krebs, J., Enyedi, A., McCormic, D.J., Penniston, J.T. and Carafoli, E. Interaction of calmodulin with the calmodulin binding domain of the plasma membrane Ca^{2+} pump. *Biochemistry* 29:355-365, 1990.

Walch-Solimena, C., Blasi, J., Edelmann, L., Chapman, E.R., Von Mollard, G.F. and Jahn, R. The t-SNAREs syntaxin 1 and SNAP-25 are present on organelles that participate in synaptic vesicle recycling. *Journal of Cell Biology* 128:637-645, 1995.

Wendland, B. and Scheller, R.H. Secretion in AtT-20 cells stably transfected with soluble synaptotagmins. *Molecular Endocrinology* 8:1070-1082, 1994.

Wiedemann, C., Schafer, T. and Burger, M.M. Chromaffin granule-associated phosphatidylinositol 4-kinase activity is required for stimulated secretion. *EMBO Journal* 15:2094-2101, 1996.

Wiser, O., Tobi, D., Trus, R. and Atlas, D. Synaptotagmin restores kinetic properties of a syntaxin-associated N- type voltage sensitive calcium channel. *FEBS Letters* 404:203-207, 1997.

Wray, W., Boulikas, T., Wray, V.P. and Hancock, R. Silver staining of proteins in polyacrylamide gels. *Analytical Biochemistry* 118:197-203, 1981.

Zhang, J.Z., Davletov, B.A., Südhof, T.C. and Anderson, R.G.W. Synaptotagmin I is a high affinity receptor for clathrin AP-2: Implications for membrane recycling. *Cell* 78:751-760, 1994.

Zhang, Y., Li, W., Hao, Q., Yu, G., Li, Q. and Yao, Q. Tb(III) and Eu(III) as fluorescent probes to investigate the metal binding sites of trichosanthin. *Biochem.Biophys.Res.Commun.* 197:407-414, 1993.

Zueco, J. and Boyd, A. Protein A fusion vectors for use in combination with pEX vectors in the production and affinity purification of specific antibodies. *Gene* 121:181-182, 1992.